INFORMATION TO USERS

This manuscript has been reproduced from the microfilm master. UMI films the text directly from the original or copy submitted. Thus, some thesis and dissertation copies are in typewriter face, while others may be from any type of computer printer.

The quality of this reproduction is dependent upon the quality of the copy submitted. Broken or indistinct print, colored or poor quality illustrations and photographs, print bleedthrough, substandard margins, and improper alignment can adversely affect reproduction.

In the unlikely event that the author did not send UMI a complete manuscript and there are missing pages, these will be noted. Also, if unauthorized copyright material had to be removed, a note will indicate the deletion.

Oversize materials (e.g., maps, drawings, charts) are reproduced by sectioning the original, beginning at the upper left-hand corner and continuing from left to right in equal sections with small overlaps.

Photographs included in the original manuscript have been reproduced xerographically in this copy. Higher quality 6" x 9" black and white photographic prints are available for any photographs or illustrations appearing in this copy for an additional charge. Contact UMI directly to order.

ProQuest Information and Learning
300 North Zeeb Road, Ann Arbor, MI 48106-1346 USA
800-521-0600

EFFECT OF DRILLING FLUID PARTICLE SIZES ON FORMATION DAMAGE: APPLICATION TO HORIZONTAL WELL

BY

AMAN HASSEN MOHAMMED

A Thesis Presented to the

DEANSHIP OF GRADUATE STUDIES

KING FAHD UNIVERSITY OF PETROLEUM & MINERALS

DHAHRAN, SAUDI ARABIA

In Partial Fulfillment of the
Requirements for the Degree of

MASTER OF SCIENCE

In

PETROLEUM ENGINEERING

November 2001

KING FAHD UNIVERSITY OF PETROLEUM & MINERALS
DHAHRAN, SAUDI ARABIA

DEANSHIP OF GRADUATE STUDIES

This thesis, written by Mr. Aman Hassen Mohammed under the direction of his Thesis Advisor and approved by his Thesis Committee, has been presented to and accepted by the Dean of Graduate Studies, in partial fulfillment of the requirements for the degree of **MASTER OF SCIENCE** in **Petroleum Engineering.**

Thesis Committee:

a. a. almajed

Dr. Abdulaziz A. Al-Majed
Chairman

Habib Menouar

Dr. Habib Menouar
Co-Chairman

Dr. Mohammad Aslam Khan
Member

M. A. Aggour

Dr. Mohammad Ahmad Aggour
Member

a. a. almajed

Dr. Abdulaziz A. Al-Majed
Department Chairman

1/12/2004

Prof. Osama A. Jannadi
Dean of Graduate Studies

عمادة الدراسات العليا
DEANSHIP OF GRADUATE STUDIES

DEDICATION

This work is dedicated to my mother, Shewbeza Siraj

ACKNOWLEDGMENT

All praise is to Almighty Allah, the creator and sustainer of the universe, and peace and blessing of Allah be upon his prophet Mohammed. Acknowledgement is due to King Fahd University of Petroleum and Minerals for the support given through the Petroleum Engineering Department to the accomplishment of this thesis.

My sincere and deep gratitude is due to Dr. Abdulaziz Al-Majed, the Chairman of my thesis committee, for his invaluable help and guidance throughout the course of this work. I am greatly indebted to Dr. Habib Menouar, the Co-Chairman of my thesis committee, for the interest he showed, his input and suggestion to this work. My gratitude also goes to Dr. Mohammad Aslam Khan and Dr. Mohammad Aggour, members of the thesis committee, for their help in many respects that made this work a success.

My appreciation is extended to all other faculty and staff of the Petroleum Engineering Department for their contribution to this work. I am especially indebted to the following laboratory staff and technicians: Mr. Mansour Al-Dhafeer (Lab. Supervisor),Mr. Mousa Ali Mousa, Mr. Abdul Samad Iddrisu, Mr. Ahmad Al-Shuwaikat, Mr. Abdulrahman Mohammadain and Mr. Idris Abukari.

Finally, I am thankful to all my colleagues and friends who made my stay at the university memorable and source of valuable experience.

TABLE OF CONTENTS

LIST OF TABLES

LIST OF FIGURES

THESIS ABSTRACT

NAME OF STUDENT: Aman Hassen Mohammed

TITLE OF STUDY : Effect of Drilling Fluid Particle Sizes on Formation Damage: Application to Horizontal Well

MAJOR FIELD : Petroleum Engineering

Date of Degree : November 2001

Four XC-Polymeric water based mud systems with different median particle sizes of the bridging additives were used to study the effect of particle size distribution and flooding time on formation damage. The experiment was conducted using Leak-Off experimental setup. An Ultrasonic technique, a non-destructive method was implemented to measure depth of invasion by the drilling fluid filtrates and particles on a Berea core samples. The results of this experimental work proved that an increase in the median particle size of the bridging additive would decrease the invasion depth and increase the return permeability. It is also observed that as flooding time increases, permeability impairment and invasion depth increased, which resulted in an increase of the skin factor. For all of the drilling fluid types studied, the largest invasion depth was observed in the first four hours flooding time. This is due to the absence of well-established, low permeable filter cake to protect the formation from invasion by drilling fluid filtrates and drilling fluid particulates down to colloidal sizes. In sizing particles in the drilling fluid system, it is important to consider not only the invasion of particles, but also the invasion of particulates down to colloidal sizes like the polymers. It is possible to achieve minimum formation impairment by properly sizing the particles, not only to minimize the invasion depth into the formation, but also to effectively filter out the smaller polymers and other colloidal particulates in the drilling fluid system. An example is presented at the end to show how this experimental work can be applied to horizontal well.

MASTER OF SCIENCE DEGREE
KING FAHD UNIVERSITY OF PETROLEUM & MINERALS
Dhahran, Saudi Arabia

ملخص البحث

اسم الطالب : أمان حسن محمد

عنوان الدراسة : تأثير حجم جسيمات طين الحفر على إتلاف الطبقات وتطبيقها على الآبار الأفقية

مجال التخصص : هندسة البترول

تاريخ التخرج : نوفمبر ٢٠٠١

في هذه الدراسة استخدمت أربع عينات من طين الحفر المائي البليمري المضاف إليه مواد مجسّرة تتكون من جسيمات متعددة الأحجام لدراسة تأثير حجم الجسيم وطول مدة الغمر على إتلاف الطبقات. وأجريت التجارب باستخدام جهاز مانع للتسرّب كما استخدمت موجات فوق الصوتية في قياس أعماق تسرّب مرشحات طين الحفر والجسيمات داخل العينات اللبية. ولقد أظهرت النتائج أنه كلما كبر حجم الجسيمات كلما قل عمق تسرّب المرشحات وكلما زاد قيمة النفاذية المسترجعة. كما لوحظ أن طول مدة الغمر يتلف النفاذية ويزيد من عمق التسرّب مما يؤدي إلى زيادة معامل القشرة. ولوحظ أيضا في كل التجارب بلوغ أقصى عمق للتسرّب بعد مرور أربع ساعات من بداية الغمر و يعزى ذلك لعدم وجود طبقة مرشّحة تمنع موائع طين الحفر والجسيمات من التسرّب. ولتحقيق أقل تلف أو ضرر للطبقات يتوجب اختيار أحجام مناسبة للجسيمات المضافة ليس فقط لتقليل أعماق التسرّب ولكن أيضا لترشيح الجسيمات الغروية الدقيقة مثل البليمر. كما تستعرض الدراسة مثالا عن كيفية تطبيق نتائج هذا البحث في حفر الآبار الأفقية.

درجة الماجستير في علوم هندسة البترول

جامعة الملك فهد للبترول والمعادن

الظهران- المملكة العربية السعودية

CHAPTER 1

INTRODUCTION

Recently, the demand for horizontal wells has considerably increased due to the advantage brought by this kind of well for improved reservoir drainage and productivity. Some of these advantages being; maximizing reservoir exposure, targeting multiple reservoir from a single platform, reducing drawdown to minimize water and gas conning problems and exploiting thin pay zones.

Horizontal wells are usually completed by, either setting a predrilled or slotted uncemented liner, or leaving the horizontal section as an open hole. In both cases the production interval is not perforated. The reduction of productivity of a well through contamination by drilling fluid and treating fluid is defined as formation damage. All wells are susceptible to formation damage to some degree. Formation damage causes substantial reductions in oil and gas wells productivity. Due to the mechanics of flow into horizontal wells and the fact that most horizontal wells remain as open hole completions, damage effects can be much more severe in horizontal wells than in vertical one. Damage can be caused by mechanical effect (fines mobilization, solids invasion, emulsion

formation, water blocking), chemical effect, and action of bacteria or extreme temperature associated with thermal recovery processes. Mechanism and basic backgrounds of formation damage are briefly discussed in appendix A.

Very often for horizontal well; the water-base polymer type mud systems are used as drilling fluid.[1] By their natures, polymers contained in the filter cake are tough and not easily degradable. The introduction of both the mud solids and polymers into the formation, the changed values of fluids saturation in the pore spaces, and the reaction between the filtrates and the pore contents and/or the matrix materials result in a reduction of the formation's original permeability.

Since most horizontal wells are completed in an open-hole fashion, even relatively shallow near well bore damage may substantially impede flow because produced reservoir fluids must pass through zones of damage. Laboratory and field studies indicate that almost every operation in the field: drilling, completion, workover, production and stimulation are potential sources of damage to well productivity.

Horizontal wells produce at very small pressure drawdown as compared to an inclined or a vertical well which provides insufficient pressure drop to dislodge fines and/or mud cake during well flow back for clean up.

The economic impact of poor productivity of open-hole wells has necessitated in the recent years improvement of laboratory test methods for assessing drilling and

completion-induced formation damage. These laboratory tests must be carried out under conditions that closely simulate the actual borehole conditions.

The objective of this research, therefore, is to study the effect of polymeric water based mud system on formation damage. Specific attention was given to the effect of particle size distribution of the bridging additives and flooding time on the return permeability and invasion depth. An attempt was made to apply these experimental results to a horizontal well under some specific condition.

CHAPTER 2

LITERATURE REVIEW

In recent years extensive work has been conducted to understand formation damage in horizontal wells. Various laboratory and field work have been performed to eliminate/reduce drilling mud induced formation damage especially in a horizontal well where this problem is severe and causes significant reduction in productivity.

Slusser and Glenn (1957)[2] studied the effect of injected mud particles size distribution on formation damage. They performed a static filtration test on alundum core samples of two permeability ranges. The base mud used in this experiment was a 3.2 weight percent bentonite mud, which was centrifuged to remove particles larger than 1micron. Three different sizes of alundum powders (aluminum oxide) were used as bridging additives to the base mud. Their result showed that a certain particle size distribution in the mud is required for a given pore size distribution for minimum permeability impairment. The experimental result also shows less damage in the cores of low permeability; with damage increasing with core permeability.

Abram (1977)[3] performed a laboratory tests on two different types of rock systems: radial, high-permeable, unconsolidated sand, and linear, low permeable dolomite. He emphasized the addition of bridging material to the drilling mud to minimize solids invasion and formation impairment. He defined two rules for the selection of the size and concentration of the bridging additives: 1) the median particle size of the bridging additives should be equal to or slightly greater than $1/3^{rd}$ the median pore size of the formation, 2) the concentration of the bridging solids must be at least 5% by volume of the solids in the final mud mixture. Experimental results with competent muds showed that impairment caused by invasion of mud particles occurred to the depth of less than 1-inch.

Gruesbeck & Collin (1982)[4] presented an experimental study performed to determine the factors affecting entrainment and re-deposition of naturally occurring fine particles in porous media, leading to an abnormal decline in the productivity of producing wells. They proposed a phenomenological theory of entrainment. The central concept of this theory was representation of both particle and pore size distribution by partitioning the porous medium at any cross section into parallel plugging and non-plugging pathways. Their result concluded that a minimum interstitial fluid velocity for fine entrainment is required, which depends on properties of the porous medium and contained fluids.

Marx & Rehman (1987)[5] introduced a new evaluation method for formation damage caused by drilling fluid, which is specially designed for reservoir having pressure

lower than hydrostatic pressure with special interest in enhanced oil recovery (EOR) and underground gas storage projects. Two sandstones of different permeabilities were used to evaluate the formation damage caused by a KCl/chalk drilling fluid. The main influential parameters- differential pressure, temperature, annular velocity and period of contamination were varied over a wide range. They found out that differential pressure doesn't lead to severe formation damage, but only in the first 2-inch of the core section due to invasion by mud particles (at T= 70°c, Vi= 0.8 m/s, t= 1hour). They also observed that above 158 °c, temperature is very influential in formation damage and damage ratio decreases sharply much more in low permeability formation, probably due to degradation of polymers in the mud. The higher the annular velocity, more filtrate would get into formation and more formation damage. Especially for lower permeability formation, contamination period is highly influential.

Joshi (1987)[6] presented a review of the state-of-art of horizontal well technology and provided guideline for the initial evaluation of horizontal well and drainhole drilling prospect. He observed that for a given length of horizontal well, relative productivity impairment over an unstimulated vertical well is higher in a thin reservoir than in a thick reservoir. The influence of well eccentricity on well productivity is very small. He also concluded that the technology to drill and complete horizontal well is available. Methods to forecast oil production from horizontal wells and drainholes have been developed.

Joshi (1988)[7] summarized production-forecasting methods with the help of analytical solution and correlation of numerical models. He suggested methods for the

performance analysis of thin reservoirs (up to 50meters thickness) and single phase flow, solution gas drive, naturally fractured and bottom water drive reservoirs. His study included comparison of productivity for vertical stimulated wells and horizontal wells. His study concluded that horizontal wells are effective in thin reservoir with high vertical permeability. Horizontal well takes longer time for water to breakthrough than vertical well and cumulative oil production from horizontal well is higher than from a vertical well.

Renard and Dupuy (1991)[8] provided a basis for comparing the flow efficiencies of vertical and horizontal wells. Analytical expression was derived assuming steady-state flow of an incompressible fluid in a homogenous anisotropy medium and both the top and bottom horizontal boundaries of the reservoir had no flow condition. The comparison considered an altered zone of the same radius and reduced permeability around the vertical and horizontal wellbores. They concluded that loss of production in horizontal wells is more than vertical wells but flow efficiency is always greater for horizontal wells. They also observed that anisotropy ratio magnifies the influence of the skin damage of horizontal wells and increasing the length slightly reduced the influence of skin on flow efficiency.

Rahman and Marx (1991)[9] conducted a laboratory investigation to study the effect of formation damage due to drilling fluid and cement slurry. Investigation was performed on two different sandstone core samples typical for gas and oil reservoir in Germany. Damage caused by drilling fluids was evaluated by means of damage ratio and

sectional damage ratio (SDR). The value of SDR was used to determine the depth of permeability impairment. Experimental setup consisted of a dynamic flow loop, which contained a core holder that could toke 25cm long and 2.5cm diameter cores. The differential pressure of 35 bars, temperature of 70°C and annular velocity of 0.8m/s were maintained during all experiments. Two types of core samples of 5-15 md and 1500-2500 md permeability and 17-20% and 20-24% porosity respectively were used in the study. Scanning Electron Micrograph study along the axis of the segmented core was made to determine the depth of invasion of solid particles and polymer molecules. The results have shown that the current practice of using low-solid drilling fluid weighted by ground calcium carbonate can cause about 40% reduction in permeability of the core samples extending over 20 cm. The permeability damage of the core samples caused by bentonite polymer drilling fluid was observed to be about 75%.

Ghofrani et. al (1992)[10] studied the role of K^+, Mg^{++} ,or Ca^{++} , clay, solid bridging material (chalk), dynamic filtration characteristics and rheological properties of the drilling fluid and effect of increasing the temperature and differential pressure on formation damage. The experimental setup consisted of a closed loop circulation system. Hassler cell was used as a core holder that could accommodate 1-inch diameter and 10-inch long core. They concluded that the presence of clay and pore bridging materials are the main factors influencing the extent and value of damage in high permeability sandstone. In low permeability sandstone, polymer molecules blocking the comparatively narrow pore channels mainly caused the damage.

Ismail et. al. (1994)[11] conducted an experimental study to investigate the effect of solids concentration and filter media on fluid loss and permeability recovery of the cores. They used KCl-polymer muds of different barite concentrations and different types of core. Filtration tests showed that fluid loss increased as solids concentration in the mud increased. Increasing the solids concentration in the mud appears to improve the permeability recovery when the cores were back flushed. However, high spurt loss and poor permeability recovery were observed if muds containing polymer materials were used without the addition of solid particles. It was observed that with the exception of mud that has no barite content, the results show that the total fluid loss increased as barite content in the mud increases. The highest fluid loss observed for the mud, which doesn't have barite content.

Jose et. al. (1994)[12] conducted an experimental study to investigate the mud solids and filtrate invasion in various rock while using drilling muds. The objective of their study was to evaluate the performance of various rocks, to select the most compatible drilling fluids and to delineate the pore blocking mechanism that causes formation damage. They used core plugs of Berea sandstone, dolomite and limestone to examine permeability reduction during mud circulation by petrographic method. Both water base and oil base muds that are typically used in the field studies were tested for their performance. The main conclusion from their work is that an average reduction of 50-80% of oil mobilities was found in cores of Berea sandstones when exposed to various muds.

Gruber and Adair (1995)[13] developed a more comprehensive test procedure for mud leakoff and regain permeability testing, whereby the regain permeability was measured at incrementally increasing pressure differentials across the core. The cores were mounted in a hydrostatic core holder to simulate reservoir overburden pressure, and located in a constant- temperature air bath set at reservoir temperature of 46.0°c. They also developed a finite-difference wellbore simulator in order to incorporate the dynamic cleanup effect and model early-time transient productivity in a horizontal well. Application of the new test procedure with different drilling fluids on several core plugs of varying permeability indicates that fluid inflow will not occur until a minimum "threshold pressure" is achieved. The model developed predicted significantly poorer flow-contribution profile than might be expected from the flow-capacity (kh) profile. The model also demonstrates how uneven wellbore cleanup is more likely to result in shorter effective well lengths in low-viscosity, high-permeability (high flow-capacity) reservoirs.

Longeron et. al. (1995)[14] presented an experimental approach to study the formation damage induced by drilling muds in oil bearing formations. The objective of their study was to develop an integrated experimental approach to study the mechanisms of mud cake formation and mud filtrate in oil-bearing formations under laboratory conditions that simulates bottom hole conditions. They conducted a series of seven water-based mud invasion experiments on high permeability clayey sandstone. Their result shows that global oil return permeabilities vary from 44% to 90% of initial permeability depending on oil viscosity and overbalance pressure. They concluded that local saturation and pressure measurements are a key point to identify and to quantify the extent and the

amount of damage. Spurt losses and cumulative volumes of filtrate strongly depend on oil viscosity and overbalance pressure.

Yidan et. al (1995)[15] performed static and dynamic filtration experiment both on filter paper and through rock slices under a pressure drop of 7 bars. Their objective was to correlate filtration behavior of water based muds with the structural properties of the cake. The drilling fluid used contains a suspension of bentonite. Experimental setup consists of API static and dynamic filtration apparatus. Their experimental result proved that the addition of salt, NaCl lead to an increase of filtrate volume due to screening of the electrostatic repulsion between the clay sheets with NaCl that induces some aggregate of the clay particles, and lead to a more permeable cake. Conversely, the presence of polyanaonic cellulosic polymer (STP), filtrate volumes are much smaller due to buildup of less permeable cake. They also concluded that polymer chains invade the rock deeper than clay particles.

Lynn (1995)[16] discussed a test apparatus and procedure to evaluate the permeability damage caused by drilling fluids in the near-well bore region of the reservoir. His system can be modified to allow for the examination of the combined effects of various drilling, completion and stimulation fluids used during drilling and production operations. A series of five formulations of drilling fluids was investigated, ranging from a standard bentonite based fresh water mud, to oil based drilling fluid. The main conclusions from his works are: the device proved to be effective for the evaluation of drilling, clean-up, and completion fluids in a laboratory environment; and the device

can reproduce several damage effects common to field operations, including solids invasion and fines mobilization through excessive production rates.

Ghofrani et. al. (1996)[17] used a new defined damage ratio (DR) to evaluate the core damage using different drilling fluids. Their experimental setup consists of closed loop circulating system. A core, saturated with KCl or NaCl solution, with a length up to 25cm, was placed into rubber sleeve in a Hassler type cell. A sleeve pressure of 5Mpa was applied to avoid filtrate flow through a micro annulus between the rubber sleeve and the core. Three different water-based drilling fluids were used to damage the tested core samples. The main conclusion from their work was that an electrolyte treatment and/or temperature aging of the tested fluids result in a more or less considerable increase of the API-fluid-loss. This is firstly because of the higher amount of the available free water in the mud due to the degradation of the hydration layers of the polymers and the clays, and secondly because of the formation of a porous and higher permeable filter cake.

Burnett and Hodge (1996)[18] conducted a laboratory study to identify the effect of drill solids contained in drill-in fluids on formation damage and well screen plugging and to emphasize the importance of minimizing solids, not only to maintain the desired drill fluid rheology, but also to effect better filtercake cleanup. Formation damage tests with drill solids were performed for both water based and synthetic based drill-in fluids. Results of these tests with laboratory –prepared fluids were compared against the performance of the field fluids and correlated with field well performance. Their work concluded that drill solids in the filtercake of drilling fluids adversely affects cleanup.

And damage occurs not from particulate invasion of the formation, but rather from surface damage at the formation face.

Yan et.al. (1997)[19] established a method for quantitative evaluation of the formation damage caused by drilling and completion fluids in horizontal wells. They also investigated the invasion depths of different core samples (taken from Dagang field, China) damaged by several kinds of drilling and completion fluids under various temperature and pressure conditions. Their results and other relevant parameters were used to establish the model for the calculation of invasion depth of drilling and completion fluids through regression analysis. Their work concluded that the effect of formation damage on the flow efficiencies of horizontal wells was generally less than that of vertical wells when β (anisotropy ratio)<3.50, but this was not the case when β was relatively large.

Toulekima and Wattenbarger (1997)[20] performed a three-dimensional reservoir simulation study based on the production performance of an actual horizontal well completed on an oil rim reservoir in West Africa. The study quantified the detrimental effect of formation damage and low vertical/horizontal permeability ratio on the productivity of a horizontal well, which may be improved by increasing the length of the producing interval. A commercial simulator, VIP-EXECUTIVE (1992), by Western Atlas software, was used to model the immiscible flow of gas, oil and water in the reservoir. The results indicated that formation damage, even for a skin factor of < 20, can significantly impair the productivity of a horizontal well. Further, the increment effect of

the skin damage on oil recovery is more significant for lower skin factors than higher values. For the same wall constraints of maximum oil production rate and minimum flowing bottom-hole pressure, the productivity of a horizontal well is more impaired if formation at the toe-end is only damaged than if formation at the heel-end is only damage.

Saleh et. al. (1997)[21] presented an innovative and unique horizontal wellbore model which is designed to simulate realistic radial flow conditions for horizontal wells. The main component of the model is a core holder of 4-ft long 3-inch ID stainless steel pipe, which is specifically designed to accommodate a cylindrical core of Berea sandstone with a horizontal wellbore in its center. The model simulates radial and open-hole flow conditions for horizontal well completion and production. The experimental program evaluated the pre- and post- mud damage well productivity and injectivity. Their work concluded that longer mud circulation creates greater damage in Berea core. A permeability profile showed that pressure drawdown required for initiating well cleanup is in the range of 5-20psi.

Lynn (1998)[22] conducted a research on the performance of five different water-base drilling fluids. The objective of his study was to determine the residual skin factor (retained permeability) after treatment with water-base drilling fluid samples, and to verify the claims of low filtrate loss, with minimum filter cake thickness, after pre-completion well clean-up. The fluids contain sized metamorphic carbonates (marble) to limit the amount of solids and filtrates loss to formation during drilling operation. The

drilling mud damage studies was conducted using a dynamic mud flow loop at an overbalance pressure of up to 400 psig and particle size of up to 2000 μm can be circulated without damaging the system. His result concluded that drilling fluids with high percentage XC-Polymer and sized metamorphic carbonate give the best return permeability.

Azizi et.al. (1998)[23] investigated the mud caking characteristics of four drilling muds: easter mud, high temperature clay inhibitive (HTCI) mud and modified version of HTCI muds on a tight gas sandstone formation. The mud caking performance of these four muds were assessed based on the API filtrate loss, mud spurt loss, dynamic filtrate loss and loss of permeability (permeability impairment) of the formation after dynamic filtration test. Their work concluded that the easter mud resulted in the lowest return permeability of the front section of composite core tested, indicating that it has the ability to form the tightest internal cake among the four muds tested.

Longeron et.al. (1998)[24] in a three year joint industrial project studied the impact of various parameters on formation damage (permeability impairment) such as initial core permeability, fluid saturation (oil or gas), temperature and shear rate during overbalanced drilling and completion operations. Eight typical drilling fluid formulations, including water-based and invert synthetic oil-based muds have been used to perform static and dynamic filtration tests on outcrops sandstone core samples. Their result showed that the water-based mud gave higher spurt losses and filtration rate than the

synthetic oil-based mud. And the formation damage is not seen to be strongly dependent on permeability and shear rate and sensitivity varies with mud compositions.

Lynn and Nasr (1999)[25] introduced a new laboratory core test procedure and a novel interpretation of scale-up equations for formation damage associated with XC-Polymeric water based mud with sized $CaCO_3$ particles used as bridging additives. Their result were compared with field result and showed that the test procedure accurately simulates the damage seen in the formation. During clean up by acidization, the acid penetration and warm-hole wandering can be controlled by monitoring acid injection rate and volume.

Longeron et.al.(2000)[26] conducted a laboratory study to evaluate: i) near wellbore invasion and related damage due to two typical drilling fluids, water and oil based muds. ii) performance of various cleanup procedures using specific breakers. Values of flow initiation pressure (FIP) and return permeabilities measured on rock samples damaged by oil-based mud (OBM) and water-based mud (WBM) were compared to evaluate the self cleaning properties of sandstone core samples having a large permeability contrast. The laboratory flow rates used to generate initial and ultimate return permeabilities were chosen to generate an average velocity of 1.7-1.8m/day. An ultra-low flow rate (0.1ml/min) was used to evaluate the flow initiation pressure (FIP) prior to return permeability measurements. Their results showed that the permeability damage increases with jamming ratio (JR), the ratio of the mean pore throat to mean

solids diameter for both OBM and WBM. However, the damage is more sever in water-based mud than oil-based mud.

Mike et.al.(2000)[27] presented a new drilling and completion techniques for horizontal well development in the subsea West Africa Field. They performed large and small-scale laboratory formation damage and fluid compatibility testing with the oil-based mud system. The drill-in fluids used in this study contained sized $CaCO_3$. The role of this $CaCO_3$ was to provide enhanced bridging of the pore throats to minimize barite invasion. Their result concluded that oil-based drilling fluid allows improved drilling in the offshore Africa channel sands that contain reactive shale stringers. And very low pressures are required to lift-off an oil-based mud filter cake.

Helio and Queiroz (2000)[28] conducted a series of return permeability tests with foam to evaluate the potential for formation damage while drilling underbalanced (UBD). The tests were conducted with overbalanced pressure, simulating the conditions when killing the well is necessary to perform some operations while drilling. The system for pressure measurement consisted of a triplex piston pump, which has a capacity of pumping 132ml/min at 3000psi overbalance. The core holder is similar to a standard Hassler sleeve core holder but with some important differences. It can accommodate 4 to 5 cm long and 2.54 cm diameter plugs. A hydraulic hand pump containing hydraulic oil was used to apply the desired confining pressure. Their results concluded that it is extremely important to pay attention to the period during which the formation is exposed to an overbalanced condition, and try to avoid them as much as possible.

Byrne et.al.(2000)[29] conducted a laboratory core flooding tests to determine the cleanup efficiency of a pseudo-oil based mud at two different overbalance pressures. The test was designed to simulate, as closely as possible, the conditions occurring in the reservoir during the drilling operation. They also performed geological techniques which included dry and cryogenic SEM and thin section analysis to determine the nature of the formation damage mechanisms. Their work concluded that all samples tested showed significant decrease in the return permeability after the core flooding. The higher overbalance produced more damage.

Ajay and Sharma (2001)[30] presented a model that estimates the depth and degree of formation damage caused by solids of widely different sizes that are present in the drilling or completion fluids. They also performed an experimental work to study the effect of the particle size distribution in the drilling fluid, particles concentration and overbalance pressure on the formation impairment. Their experimental results proved that the primary damaging mechanism in the sized $CaCO_3$ fluids is not damage induced by the particles (which did not invade the rock) but by the invasion of polymers and drill solids. Comparison of their model with the experimental result showed a reasonable agreement. They also concluded that using too small a particle size leads to solids invasion and low return permeability recovery; and too large a particle size also results in low return permeability.

Khan et al (2001)[31] reported for the first time the applicability of an ultrasonic method for non-destructive mapping of formation damage. They used a leak-off experimental setup to simulate drilling fluid circulation across the formation under bottom hole conditions. A Hassler type core holder was used that can accommodate a core sample up to 1ft. long and 2-inch diameter. Their result concluded that a minimum invasion depth observed around a critical overbalance pressure of 300psi ($2.07X10^3$kPa). This was explained to be due to entrainment of particles.

CHAPTER 3

STATEMENT OF THE PROBLEM AND OBJECTIVE OF THE STUDY

3-1 STATEMENT OF THE PROBLEM

The advantages of Horizontal wells; such as productivity increment, recovery improvement and minimum gas and oil coning problem could be jeopardized by formation damage due to drilling, completion and/or workover operation. The most common and most severe damage, however, occur during drilling operations.

Drilling-induced damage is affected by several drilling fluid and operation-related parameters. From the literature survey presented in the previous chapter, some work has been done to understand the impact of drilling fluid composition, overbalance pressure and flooding time on the formation damage. Little has been done however, to experimentally determine the significance of particle sizing in the drilling fluid formulation in relation to the formation permeability.

3-2 OBJECTIVE OF THE STUDY

The general objective of this study is, therefore, to investigate the effect of particle size distribution in the drilling fluid system on the formation permeability. It is important to note that both solids and filtrates can cause damage on their own, and in relation to each other.

Specifically, the objectives of present study are:

1. To investigate the effect of particle size & flooding time on damaged zone permeability using a leak-off experimental setup, and an ultrasonic technique for the measurement of mud invasion depth.
2. To use the experimental results to attempt evaluation of the skin distribution along a horizontal well under specific conditions.

CHAPTER 4

EXPERIMENTAL SETUP & PROCEDURE

4-1 LEAK-OFF EXPERIMENTAL SETUP

A schematic of the experimental setup used in the leak-off test is shown in Figure 4-1. The test utilizes fluid flow and displacement in two directions, production and flooding. Any operation that results in drilling fluids being forced into the core is said to be proceeding in the flooding direction. The core will be put into production mode by injecting crude oil in the opposite direction.

The core sample is encased in a rubber sleeve. The ductility of the rubber sleeve allows a confining overburden pressure to be transferred to the core to simulate the reservoir conditions. The core mounted inside the rubber sleeve is placed inside a core holder, which is capable of withholding reservoir pressures up to 10,000psi. This pressure is applied by filling the annular space between the rubber sleeve and the core holder with hydraulic oil and then compressing it with a hand pump to obtain the desired overburden pressure.

Pressure differential is monitored using a pressure transducer. The transducer is mounted directly across the core and measures the pressure differential between the injection and production ends. The signal from the pressure transducer is directly connected to the strip chart recorder, which provides a continuous pressure profile of the test. A validyne type display is also attached to the pressure transducer in order to take the readings as a backup.

A positive displacement pump is used to inject fluids into the core. The pump is capable of injecting at rates from 1 to 10 cc/min. The pump is filled with filtered light silicon oil, mixed with kerosene that displaces either brine\oil or mud from the transfer cell to the core at the specified flow rates.

Both the core holder and the transfer cell are contained in a temperature-controlled oven, which duplicates the reservoir conditions of temperature and eliminates complication of data analysis due to fluctuations in the external ambient temperature. The use of the correct reservoir temperature also ensures that the correct fluid viscosities, which will occur in the reservoir, are properly simulated.

4-1.1 Apparatus

A) Core Holder

A Hassler type core holder, as shown in figure 4-2 is used in this experiment. This core holder is made of stainless steel that can accommodate up to 1-ft long and 2-inch diameter core. The core sample is placed in a flexible rubber sleeve. One end piece of the core holder is fabricated to have two ports. These ports are used to circulate the drilling fluids across the face of the core. A spacer of 10mm in height is placed between the core and the head to provide an annular space for mud cake buildup. The second end piece has only one port to collect the filtrate/oil/brine.

B) Piston Pump

Is a positive displacement pump, connected to the transfer cell to deliver the fluids (mud/oil/brine) at the desired flow rate and pressure. Hydraulic oil, which is a mixture of kerosene and silicon oil, is used as a transferring fluid in the pump. The pump can deliver up to 10cc/min and a pressure of up to 10,000psi.

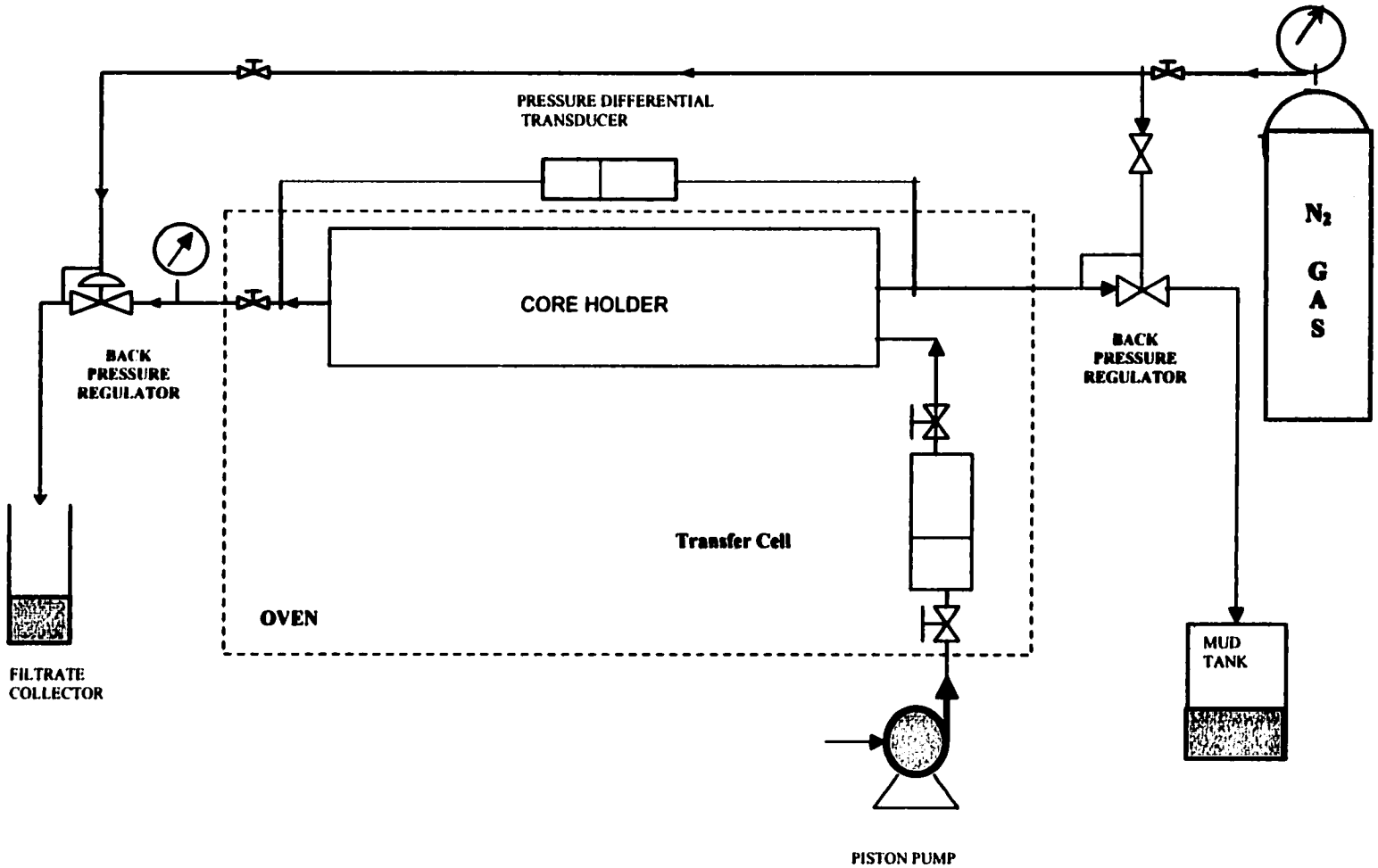

Figure 4-1: Schematics of Leakoff Experimental Setup

C) Transfer Cell

Transfer cell is employed to deliver mud/oil/brine to the core holder at a specific flow rate and pressure. A positive displacement pump dictates these flow-rates and pressures.

D) Differential Pressure Transducer

A differential pressure transducer (Validyne DP303) is connected to the two ends of the core holder in order to measure the differential pressure across the core. These differential pressures are displayed on analogical digitor. The transducers are connected directly to a chart recorder that provides a continuous pressure profile.

E) Fraction Collector

An ISCO fraction collector is used to collect the producing fluids (brine/oil/filtrate) in a 10cc test tube. This fraction collector can be set to move according to a certain time. From the volume collected in the test tube at the specified time, the flow rate across the core will be calculated.

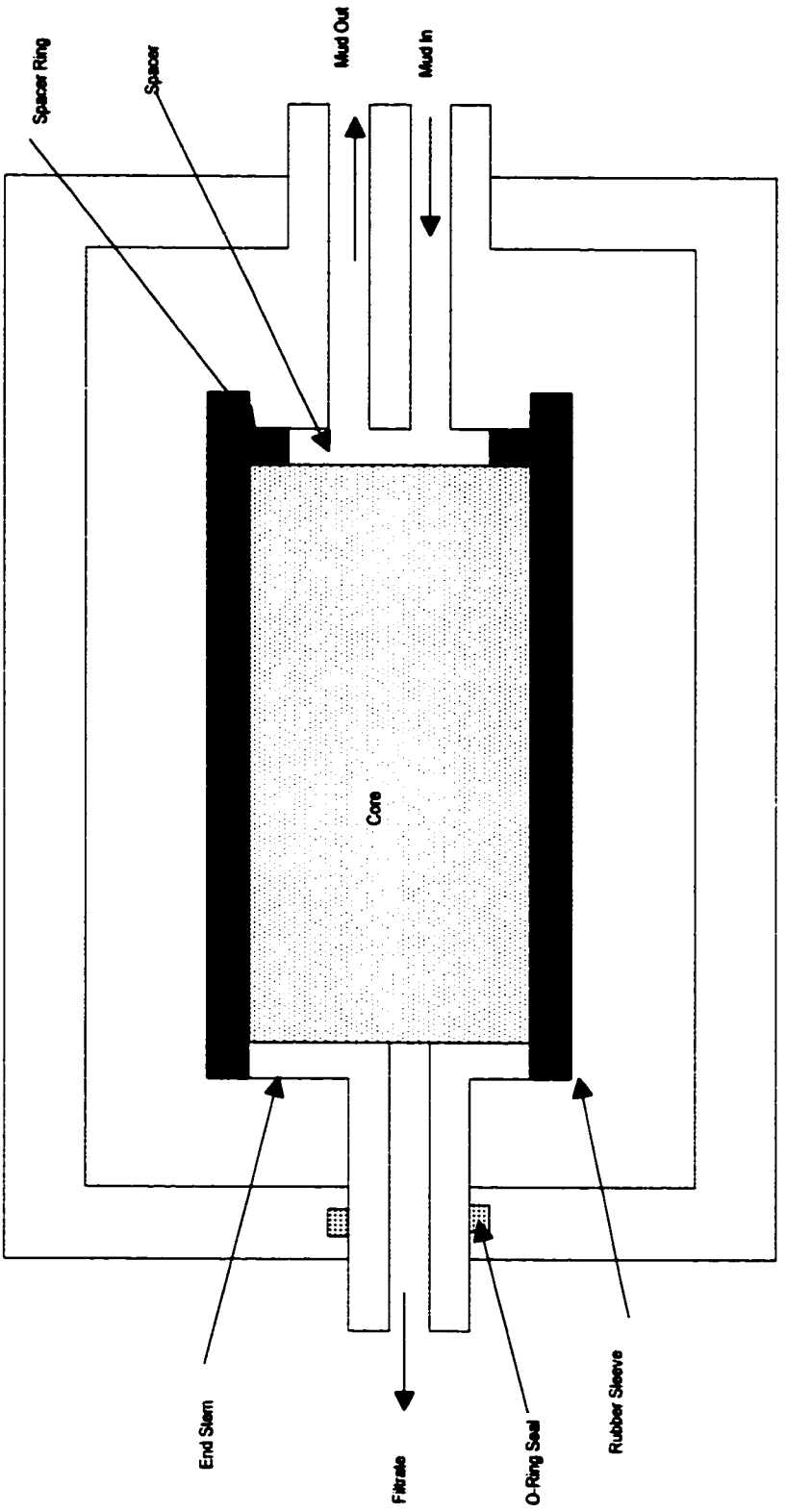

Figure 4-2: A Hassler Type Core Holder

F) Oven

Both transfer cell and the core holder are housed inside an oven where the fluids and core samples can be heated to the required reservoir temperature.

G) Miscellaneous Items

A high-pressure stainless steel tubing's, fittings, shut-off valves, pressure gauges, viscometers, hydrometers, flask, bicker, test tubes, pressure multiplier, verneir calipers, etc.

4-1.2 Experimental Fluid Preparation

A) Oil

A Medium Arabian oil of 33.5°API (sp.gr=0.863 at room temperature) is used during the experiment to measure effective permeability before and after damage. Solids and paraffin components from this oil are removed by means of filter of size one micron before use.

B) Brine

3.5% KCl (~35,000ppm) brine is prepared to saturate cores. The reason for using a 3.5% concentration KCl is to avoid any chance of clay swelling and clay migration. The brine is prepared by dissolving 35gm of KCl in distilled water to make one liter of solution. The brine is filtered by No. 50 API filter paper and then evacuated in desiccators to remove air bubbles.

C) Drilling Fluids

Four different Polymeric water based mud with different sized calcium carbonate as a bridging additive were prepared in the laboratory. The composition and properties of these drilling fluids are given in table 4-1 through 4-6.

TABLE 4-1: COMPOSITION OF WBM-1

COMPONENT	COMPOSITION	MIXING TIME(min)
FRESH WATER,cc	500	-
KCl,gm	66.5	5
XC-POLYMER,gm	2.5	15
DRISPAC,gm	0.85	15
DEXTRID,gm	10	15
KOH, gm	0.5	5
$CaCO_3$ (Fine),gm	8.4	15
$CaCO_3$(Medium-),gm	0	-

TABLE 4-2: COMPOSITION OF WBM-2

COMPONENT	COMPOSITION	MIXING TIME(min)
FRESH WATER, cc	500	-
KCl,gm	66.5	5
XC-POLYMER,gm	2.5	15
DRISPAC,gm	0.85	15
DEXTRID,gm	10	15
KOH, gm	0.5	5
$CaCO_3$(Fine),gm	8.4	15
$CaCO_3$(Medium-12micron),gm	5.7	15

TABLE 4-3: COMPOSITION OF WBM-3

COMPONENT	COMPOSITION	MIXING TIME(min)
FRESH WATER, cc	500	-
KCl,gm	66.5	5
XC-POLYMER, gm	2.5	15
DRISPAC, gm	0.85	15
DEXTRID, gm	10	15
KOH, gm	0.5	5
$CaCO_3$(Fine), gm	8.4	15
$CaCO_3$(Medium-21micron),gm	5.7	15

TABLE 4-4: COMPOSITION OF WBM-4

COMPONENT	COMPOSITION	MIXING TIME(min)
FRESH WATER, gm	500	-
KCl, gm	66.5	5
XC-POLYMER, gm	2.5	15
DRISPAC, gm	0.85	15
DEXTRID, gm	10	15
KOH, gm	0.5	5
$CaCO_3$(Fine), gm	8.4	15
$CaCO_3$(Medium-41micron),gm	5.7	15

TABLE 4-5: PROPERTIES OF THE POLYMERIC Water Based Mud

PROPERTIES	WBM-1	WBM-2	WBM-3	WBM-4
DENSITY, lb/cu. Ft	66.9	67	67	67
RHEOLOGY @ 150^{O}F & 600RPM 300RPM 3RPM	43 28 4	43 27 3	43 27 3	43 27 3
10 Sec. gel, lb/100 sq. ft	4	3	3	3
10min gel. lb/100 sq. ft	6	4	5	4
PLASTIC VISCOSITY, cp	15	16	16	16
YIELD POINT,lb/100sq ft	13	11	11	11
PH	10.81	10.80	10.82	10.80
FILTRATE API,ml/30min	4.6	4.4	4.6	4.0
CAKE API, 32ND/inch	1	1	1	1
FINAL VOLUME, mls	563	565	565	565

4-1.3 Core Sample Preparation

Berea core samples of 5.14 cm diameter and length from 9.8 to 25.4 cm were cut from a long core. The porosity of the core sample was determined by saturation method. 3.5 wt.% KCl brine were used as saturation fluid. Pore size distribution was measured using centrifugal method.

4-1.4 Porosity by Saturation Method

A brine of known density (1.02222g/cc) is used to saturate the Berea core at room temperature. The following procedures were adopted for porosity measurement by saturation method:

1. The dry weight (W_1) of the core and the corresponding dimensions (i.e., Length (l) and diameter (d)) was measured.
2. Vacuum the air out of the core sample before saturating the core with brine for about 8 to 12 hours.
3. Using filtered KCl brine, saturate the Berea core at an overburden pressure of 2500psi for 12 to 24 hours.
4. Measure the weight of saturated sample (W_2). Then the porosity is calculated using the following equation:

$$porosity(\phi) = \left(\frac{(W_2 - W_1)}{\rho} / (\frac{\pi d^2}{4}) \right) X100\% \qquad 4\text{-}1$$

From this method, the average porosity of the Berea core studied is 21.4%.

4-1.5 Pore Size Distribution

A centrifugal method was employed to measure the pore size distribution of the Berea core samples tested.

If the porous rock is fully saturated with a wetting fluid, a non-wetting fluid may enter the pores only when a finite pressure is applied on that fluid which is greater than the capillary pressure. These capillary pressure measurements are based on the observation of the pressure required to force a non-wetting fluid into a rock at some given conditions of saturation. The equation of capillary rise is more accurately referred to as the radius of entry. Since flow channels in a rock system are by no means smooth or regular, the significant radius is then the radius at the point of entry for a given pore. Then, this may be expressed by the following equation:

$$P_c = \sigma_{wa} \cos\theta_{wa} \left[\frac{1}{r_1} + \frac{1}{r_2}\right] \qquad 4\text{-}2$$

Where P_c is the capillary pressure, δ_{wa} is the interfacial tension between the brine and sample and θ_{wa} is the contact angle. r_1 and r_2 are the principal radius of curvature of the interface. If we consider $r_1=r_2=r$, and solving for capillary pressure equation;

$$r = \frac{2\sigma_{wa} \cos\theta_{wa}}{P_c} \qquad 4\text{-}3$$

Knowing the values of δ_{wa} and θ_{wa}, the pore entry radius r can be determined for the corresponding applied pressure. Figure 4-3 shows the pore size distribution of the Berea core samples studied.

4-1.6 Particle Size Distribution of Calcium Carbonate

The particle size distribution of the calcium carbonate samples used as bridging additives in the XC-Polymeric water base mud system were measured using MICROSCAN II, by QUANTACHROME CORPORATION. It can measure the particle size distribution for the powder and slurries.

Accurate particle size determinations require that a powder of known density be well dispersed in a liquid of known density and viscosity. The $CaCO_3$ sample to be analyzed has the specific gravity of 2.71. The liquid must be the one in which the $CaCO_3$ is insoluble. Therefore, we selected distilled water as the sedimentation fluid. Besides, the fluid to be selected should have the viscosity such that the largest particle to be analyzed will remain suspended for at least a few seconds such that the liquid flow is laminar, as dictated by the Reynolds number. The liquid should also have a lower density than the powder.

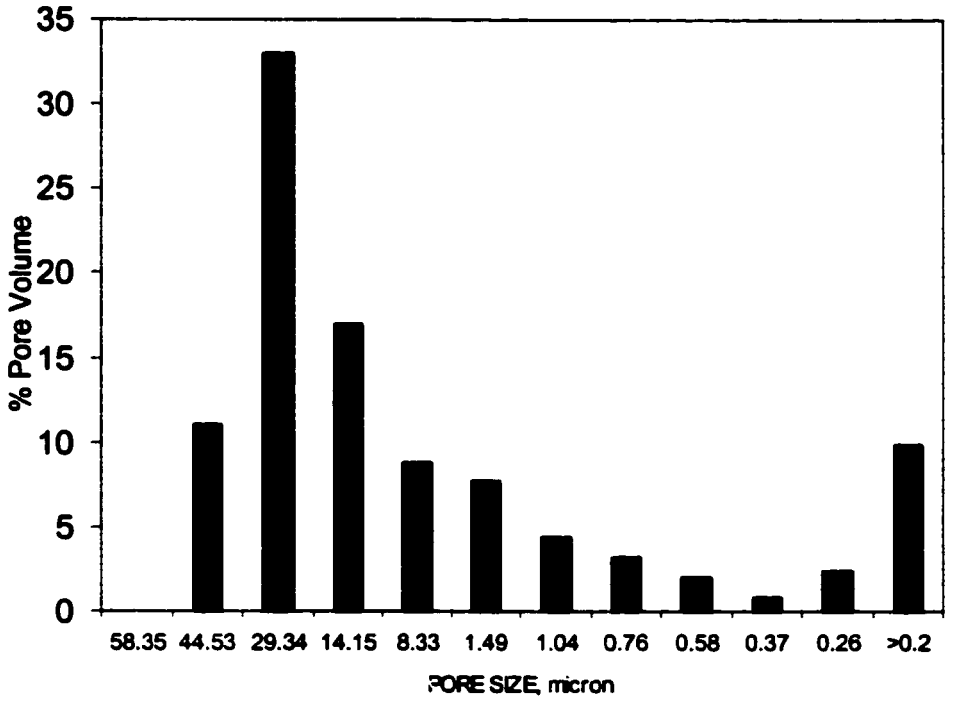

Figure 4-3: Pore Size Distribution for the Berea Core Sample studied

Prior to measuring the particle size distribution, it is essential that the particles be evenly dispersed in the sedimentation fluid. An appropriate amount of dispersant should be used for a better dispersion of the particles. For most powders, the usual concentration of wetting agent recommended by QUANTACROME is 0.1 weight % by volume of the dispersant. A good dispersing agent will cause a slow settling of the particles with linear interface between the liquid and powder and a small depth of sediment when settling is complete.

A 0.1 weight % by volume of tetra sodium pyrophosphate (TSPP) as dispersant was used in our case. An ultrasonic probing was also implemented for some 30minutes for each samples tested in the phase separator for the deagglomeration of the particle clusters, if any. Details and procedures of particle size distribution and bridging process is presented in appendix B. Figure 4-4 through 4-7 shows the particle size distribution of the four $CaCO_3$ samples analyzed. From the figure, it is determined that the median particle size of the four samples tested; sample A, B, C and D as 12, 8, 21 and 41μ respectively.

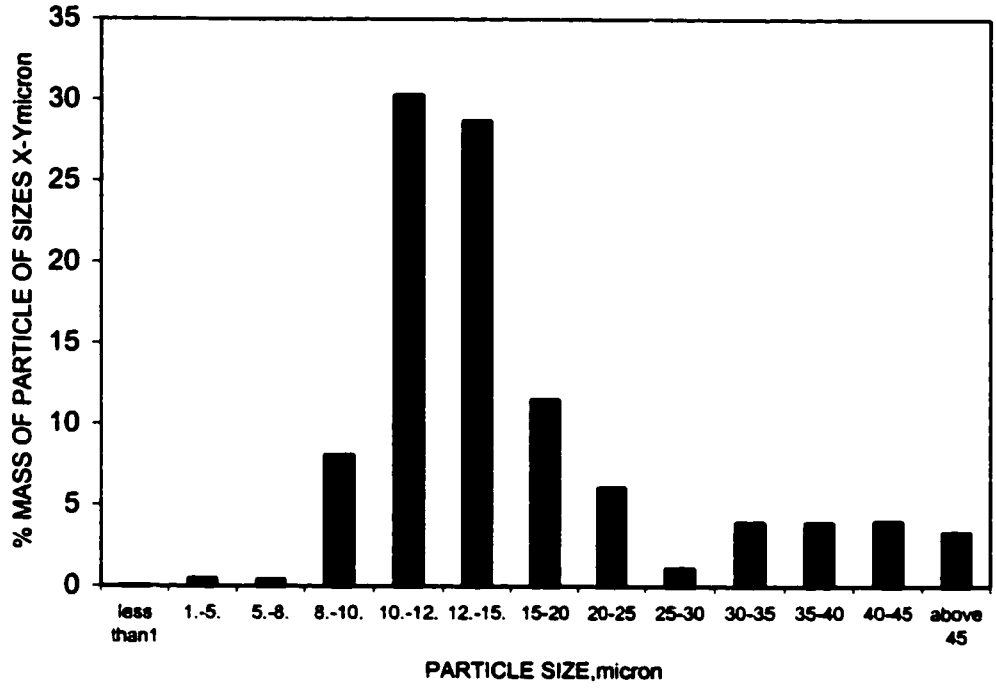

Figure 4-4: Particle Size Distribution of sample A by MICROSCAN II

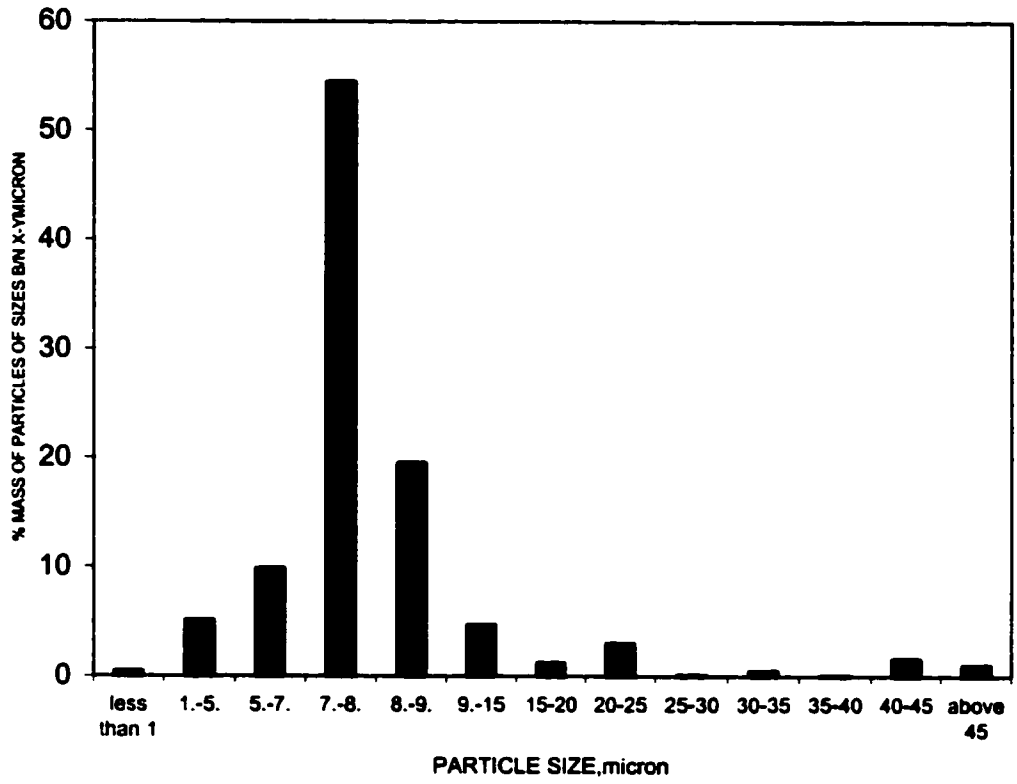

Figure 4-5: Particle Size Distribution of sample B by MICROSCAN II

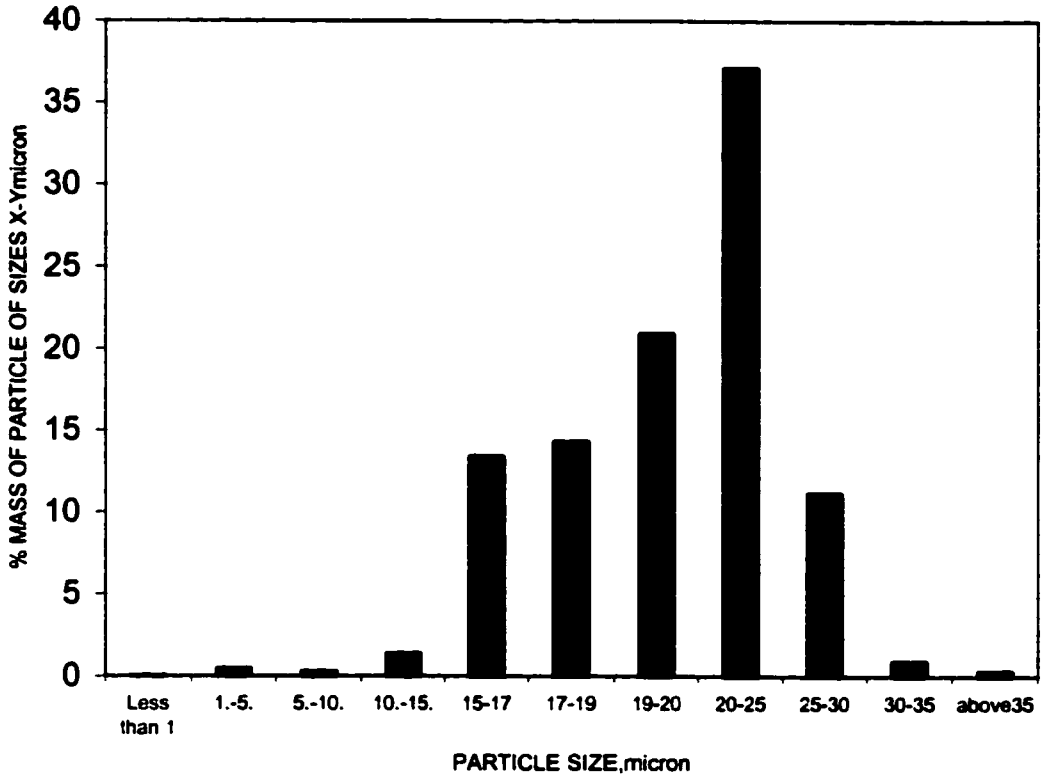

Figure 4-6: Particle Size Distribution of sample C by MICROSCAN II

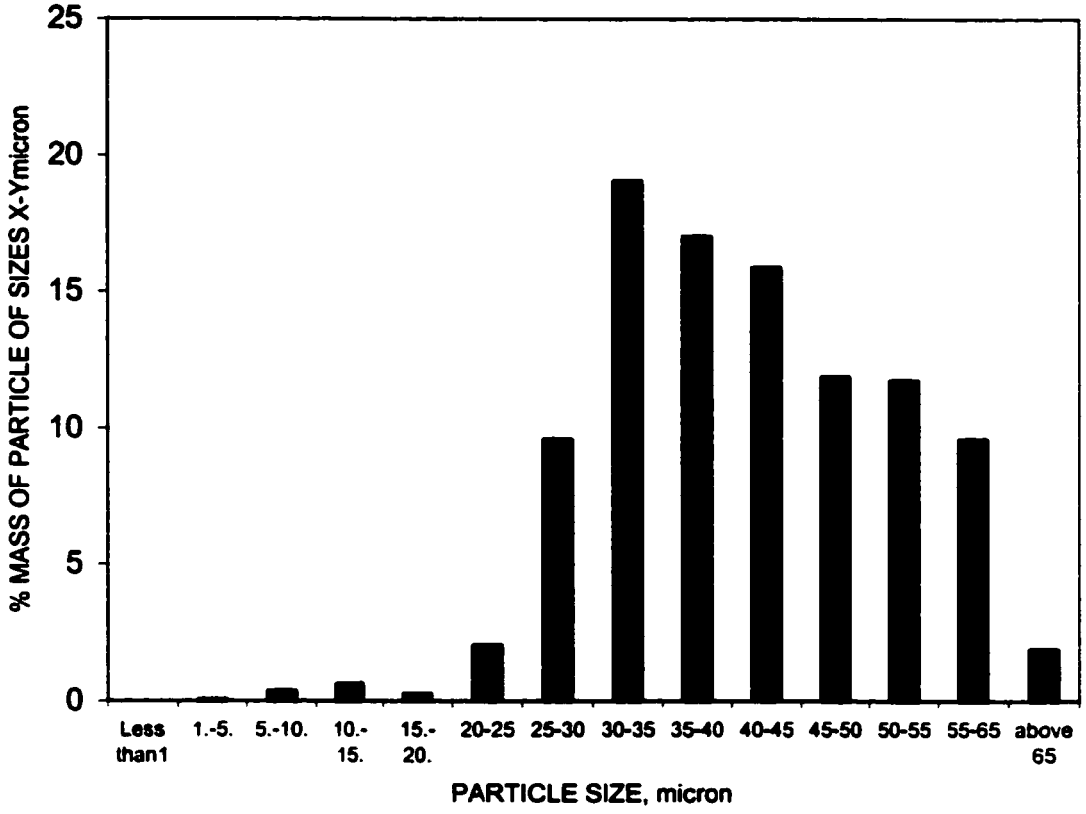

Figure 4-7: Particle Size Distribution of sample D by MICROSCAN II

4-2 ULTRASONIC EXPERIMENTAL SETUP AND METHOD

4-2.1 Theory

The Ultrasonic waves are pressure waves that are the same in nature as sound waves with the most important differences of their frequency. The audible sound is of frequency below 20,000Hz(cycle/sec), whereas ultrasonic has frequency greater than 20,000Hz.

Depending on the direction of particles movement during vibration, Ultrasonic waves are divided into four groups.

1. Longitudinal wave or Compressional waves
2. Shear waves or Transverse waves
3. Surface or Rayleigh waves
4. Guided (Plate/Lamb) waves

Longitudinal wave, which is the fastest of all, is used in the ultrasonic method. Shear waves can also be used. We will briefly discuss the two most important types of waves: longitudinal and shear waves.

1. Longitudinal/Compressional Wave

In this wave, the vibration or displacement of the particles of the medium takes place in the direction of the propagation of the wave. Or in other word, the particles move back and forth along the line in which the wave is traveling. In fact, the individual particle of the medium oscillate about their equilibrium position without there being any net movement of the medium.

2. Shear/Transverse Wave

Another form of propagation is that of transverse wave. In this case vibration occurs at right angles to the direction of the propagation. Shear waves can generally propagate through solids only because liquids and gases do not support shear stresses.

Ultrasonic wave doesn't travel through air. Therefore, the ultrasonic wave follows a zigzag path in the dry core sample and hence will have lower mean velocity profile compared to an oil saturated or sample after damage. Figure 4-8 shows the relative velocity of the damaged, saturated at residual water saturation and dry sample.

4-2.2 **Experimental Setup**

Figure 4-9 shows the Schematics of the experimental setup for the ultrasonic method. It contains a Panametric Pulser-Reciever (Model 5072PR), connected to a

500MHz Oscilloscope through panametric Pre-Amplifier. Two panametric Transducer (V403) are used to inject and receive ultrasonic waves generated by the pulser-Reciever.

Petroleum jelly is used as a couplant in order to remove the effect of any air entrapped between the surface of the transducer and the core.

An Ultrasonic pulse, generated in the Pulser-Reciever is passed through the core sample. The time taken for the ultrasonic wave to travel from the transmitter/pulser to the receiver is readout on the oscilloscope and will be transferred to the data acquisition system.

Berea core samples of 5.00 to 5.14 cm diameter and 9.8 to 25cm long were investigated. In this particular part of the test, we sent ultrasonic waves across the diameter of the core sample as shown in figure 4-10. The time taken for the ultrasonic wave to travel from the source transducer to the receiver was measured and displayed on the oscilloscope. These data were later transferred to the data acquisition system. The signal received was processed before being reported in order to avoid any random noises that are not part of the signals. Depending on situations, a noise filter was used in order to avoid any noise introduced from the environment. For each data points, the average of 64 samples was taken. Knowing the diameter of the core and the time, the Ultrasonic wave takes to traverse across the core, an Ultrasonic velocity is calculated as:

$$V=d/\Delta t \qquad 4\text{-}4$$

Where d is the diameter of the core sample and Δt transit time for the ultrasonic wave. Generally, for each core tested, the compressional velocity was determined under three different conditions:

1. Dry Samples:

For the dry sample, since the ultrasonic wave doesn't travel in air molecules, it follows a zigzag path and hence takes longer time compared to the oil saturated sample or sample after damage.

2. Oil Saturated Samples:

The velocities at this stage are considered as base line velocity. Because, it is this velocity profile that is used to determine if there is any extraneous material invading the formation and if so, by what extent.

3. Damaged samples:

At this stage, the sample is damaged at 100psi overbalance pressure, different flooding time and drilling fluids. As shown in figure 4-8, up to a certain particular point along the length of the core, the velocity profile of the sample after damage will be the same as that of saturated sample. This portion of the core is designated as lean or virgin

since this part of the core is not contaminated with drilling fluid particle and filtrate. Beyond a certain point, the velocity will start rising and ultimately attains a plateau. The incline in the slope of this profile is an indication of the increase in the particles and filtrates until the plateau is attained. The plateau at the dense end reflects that the porous medium is completely filled with drilling fluid particles and filtrate.

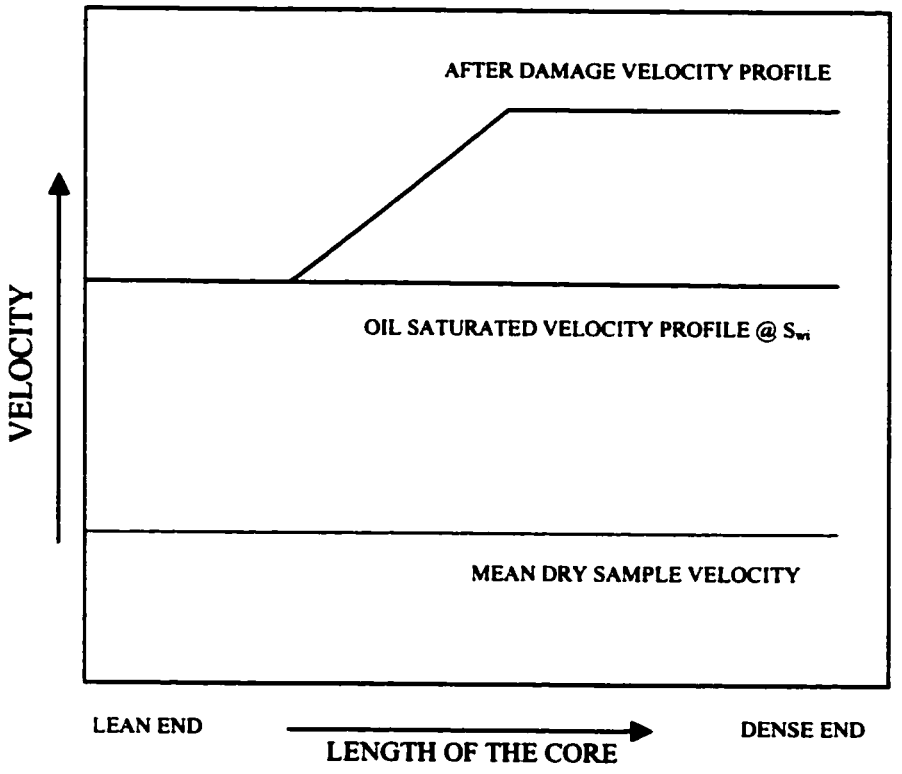

Figure 4-8: Schematics of the Relative Velocity profile for Dry, Saturated and damaged Sample

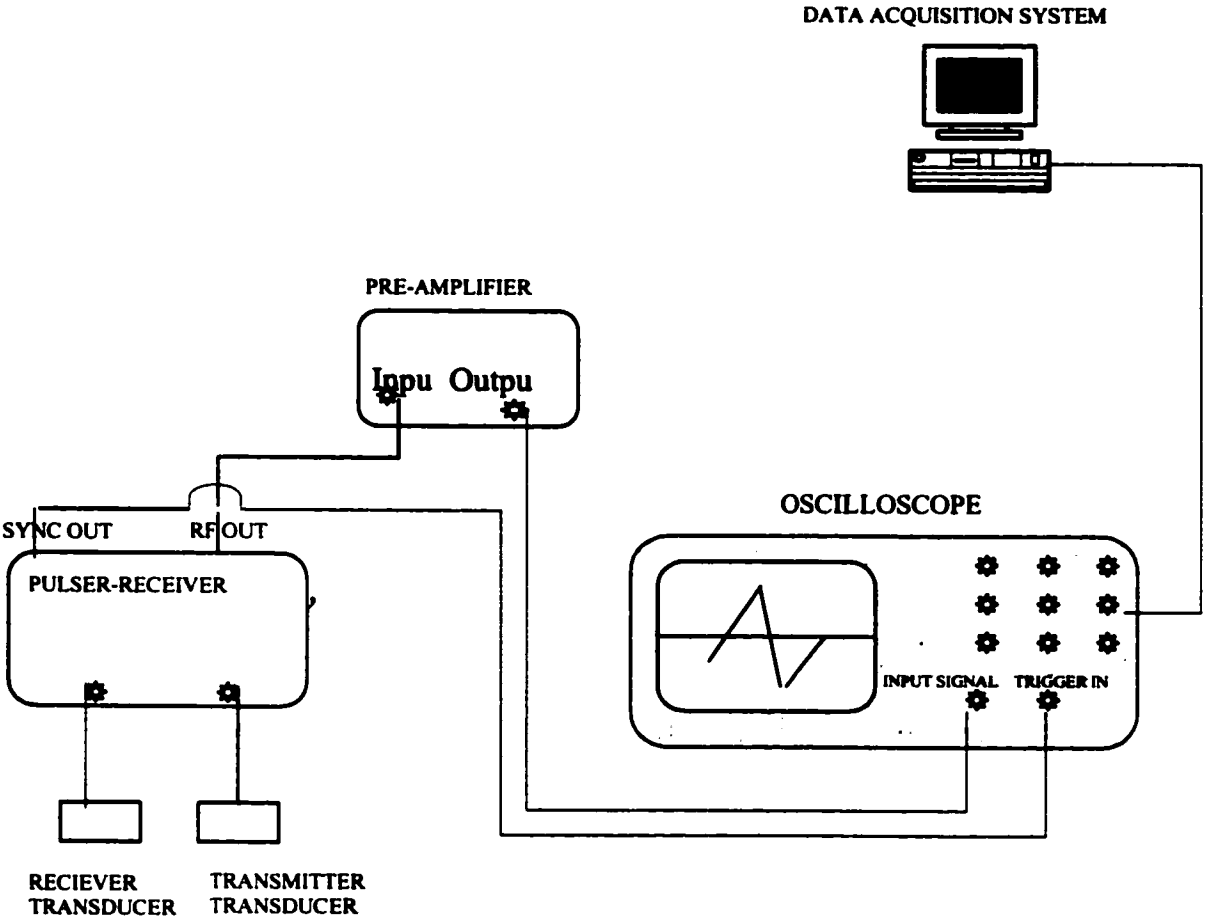

Figure 4-9: Schematic of the Ultrasonic Measurement Setup

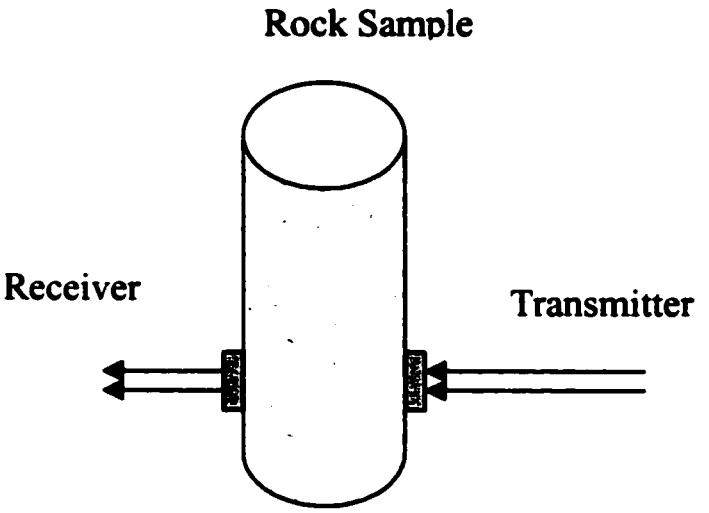

Figure 4-10: Position of the Core Sample for the Ultrasonic test

CHAPTER 5

RESULTS AND DISCUSSIONS

5-1 RESULTS

XC-Polymeric water-base mud with four different size Calcium Carbonate particles were formulated and used during this experimental work. The purpose of these experiments was to simulate drilling fluid circulation across the face of the core and studies the impact of particle size distribution on formation damage. These tests allow us to evaluate the potential for formation damage caused by the infiltration of drilling fluid solids and filtrates. The tests were conducted using Leak-Off experimental set-up. A non-destructive technique, based on ultrasonic wave propagation, method was also employed to identify the extent of formation damage in a Berea core samples. Details of each set-up and procedures are explained in the previous chapter.

The particle size analysis of calcium carbonate ($CaCO_3$) that was used as bridging additives in the XC-Polymeric water base mud system was performed with Scanning Electron Microscopy (SEM). SEM provides important qualitative information about the morphology and size of the particles. Samples for SEM imaging and analysis consist of

materials that are stable in a vacuum and under a high voltage electron beams. Details of the SEM analysis, procedures and particles size distribution analysis using QUANTACHROME II equipment for the four $CaCO_3$ samples is present in appendix B

In this chapter the experimental results are presented and discussed. An effort was also made to apply these experimental results to horizontal wells under certain specific condition. Experimental conditions that were kept constant throughout this experiment are listed in table 5-1. Composition and properties of the Water based muds are given in chapter 4

Table 5-2 and 5-3 presents the results of Ultrasonic and Leak-Off experiment respectively. Figure 5-1 through 5-10 shows the ultrasonic test results. Effect of particle size of the bridging additive in the water-based mud on the invasion depth is presented in Figure 5-11 through 5-14. Figure 5-15 to 5-18 shows the effect of flooding time on the invasion depth. Effect of bridging particle size on the return permeability is presented in Figure 5-19 through 5-22. Effect of flooding time on return permeability is presented in figure 5-23 through 5-26. Discussions of the results are presented in the following sub sections.

Table 5-1 Constant parameters for the Leak-off test

PARAMETERS	VALUES
Overbalance Pressure, psi	100
Temperature, ^{0}F	150
Confining pressure, psi	2500
Pore Pressure, psi	1000psi
Mud Flow Rate, cc/min	1.0

5-2 DISCUSSION OF RESULTS

5-2.1 Ultrasonic Test Results

We have used a new non-destructive method to measure an invasion depth by drilling fluid filtrates and particles on a Berea core samples at different conditions of flooding time and drilling fluids with different median particle sizes of the bridging additives. Figure 5-1 through 5-10 shows the results of this technique.

Variations in the velocity profiles between dry, oil saturated at residual water saturation (S_{wi}) and mud invaded samples are used as means to measure invasion depth. Therefore, the ultrasonic test was conducted for each samples at three stages: for dry, oil saturated at residual water saturation, and for the mud-laden states. During the ultrasonic measurement, the orientation of the core samples were kept in a particular position throughout the experiment with a reference line marked on the core samples. The purpose was to avoid any error in the velocity profile incurred due to disorientation of the sample's pore.

During the ultrasonic test, since the position of the core samples remains in the same vertical position throughout the test, one may expect that gravitational segregation of the fluids in the pore sample may affect the velocity profile. However, Khan et.al [31] proved that reverse orientation of the core samples does not significantly change the mud invaded velocity profile.

For the whole samples tested, the average dry samples velocity was 2131m/sec. Since we are dealing with Berea sandstone, which is believed to be a fairly homogeneous formation, we do not expect large heterogeneities. As Appendix C shows the largest velocity variation observed for the dry core sample is about 1.64% from the mean dry sample's velocity profile.

The velocity for the oil-saturated sample is used as the basis to determine an invaded portion of the core after damage. On the velocity profile for the mud invaded sample, starting from the lean end, there will be a point along the length of the core beyond which the damaged samples velocity is higher than the base line velocity. This point will actually determine the invasion depth. In order to show the contrast between the base line velocity and mud-damaged sample's, we multiplied the mean velocity profile of the dry sample by a factor of 1.25.

Figure 5-1 shows the ultrasonic velocity profile on Berea core sample tested (sample A-17) when flooded for 4hours with WBM-1 mud (i.e., when the median particle size of the bridging additives was 8μ). From the figure, one can fairly see the plateau toward the dense end. Later, this plateau diminishes and the velocity profiles declines until it attains the base line velocity, and maintains this velocity all the way through the lean end.

The plateau to the dense end is an implication that the porous media of the Berea core sample tested is completely filled with drilling fluid particles and/or filtrate. The decline of this profile is therefore an indication of partial invasion of the porous media by particles and/or filtrate until the base line velocity is attained. Once the base line velocity is attained, the velocity profile fairly maintained this velocity all the way to the lean end, which indicates that this portion of the core hasn't been affected by drilling fluid invasion. Therefore, this portion of the core sample is considered to be lean. From the point, the after damage velocity profile crosses the base line velocity profile; the invasion depth for this particular sample (sample A-17) is 5.05cm.

Figure 5-2 shows the ultrasonic velocity profile for sample A-20, when the core sample was flooded for 4hours with WBM-2 mud. From the figure we can fairly clearly see the portion of the core sample that is not affected by the drilling fluid invasion. But toward the dense end the plateau is not very much evident. Based on this velocity profile, the invasion depth for this particular test is 4.45cm.

Figure 5-3 through 5-7 shows somehow the same behavior as figures 5-1 and 5-2 explained above with the after damage velocity profile showing plateaus toward the dense end. Then these plateaus will be followed by the decline in velocity profile, until the base line velocity profile is attained. Once the after damage velocity profile attains the base line velocity, they will maintain this profile all the way through the lean end. The plateaus toward the dense end, however, is more clearer for the longer flooding time as shown in figures 5-8 to 5-10.

Table 5-2: Ultrasonic test result

SAMPLE #	PARTICLE SIZE(μ)	INVASION DEPTH (cm)
TIME =4Hrs		
A-17	8	5.05
A-20	12	4.45
A-23	21	4.3
A-22	41	3.7
TIME=10Hrs		
A-26	8	5.88
A-25	12	5.57
A-24	21	5.04
TIME=30Hrs		
A-28	8	13.15
A-19	12	10.95
A-29	21	9.9

Table 5-3: Leak-off test results

Sample #	Particle size(μ)	Absolute, Kabs (md)	Effective before damage, Keff1 (md)	Effective after damage, Keff2 (md)	Return Permeability, RP(%)
FLOODING TIME=4Hrs					
A-17	8	373.4	170	74.8	44
A-20	12	204.6	165	98.1	59.5
A-23	21	197	126	76.6	60.8
A-22	41	155	82	49.5	60.4
TIME=12Hrs.					
A-26	8	368.6	141.7	78.6	55.5
A-25	12	408	159.6	76.91	48.2
A-24	21	309	131.5	75.5	57.4
TIME =30Hrs.					
A-28	8	528	247	85.1	34.45
A-19	12	406	312.5	125	39.93
A-29	21	309.2	163.7	88.9	54.3

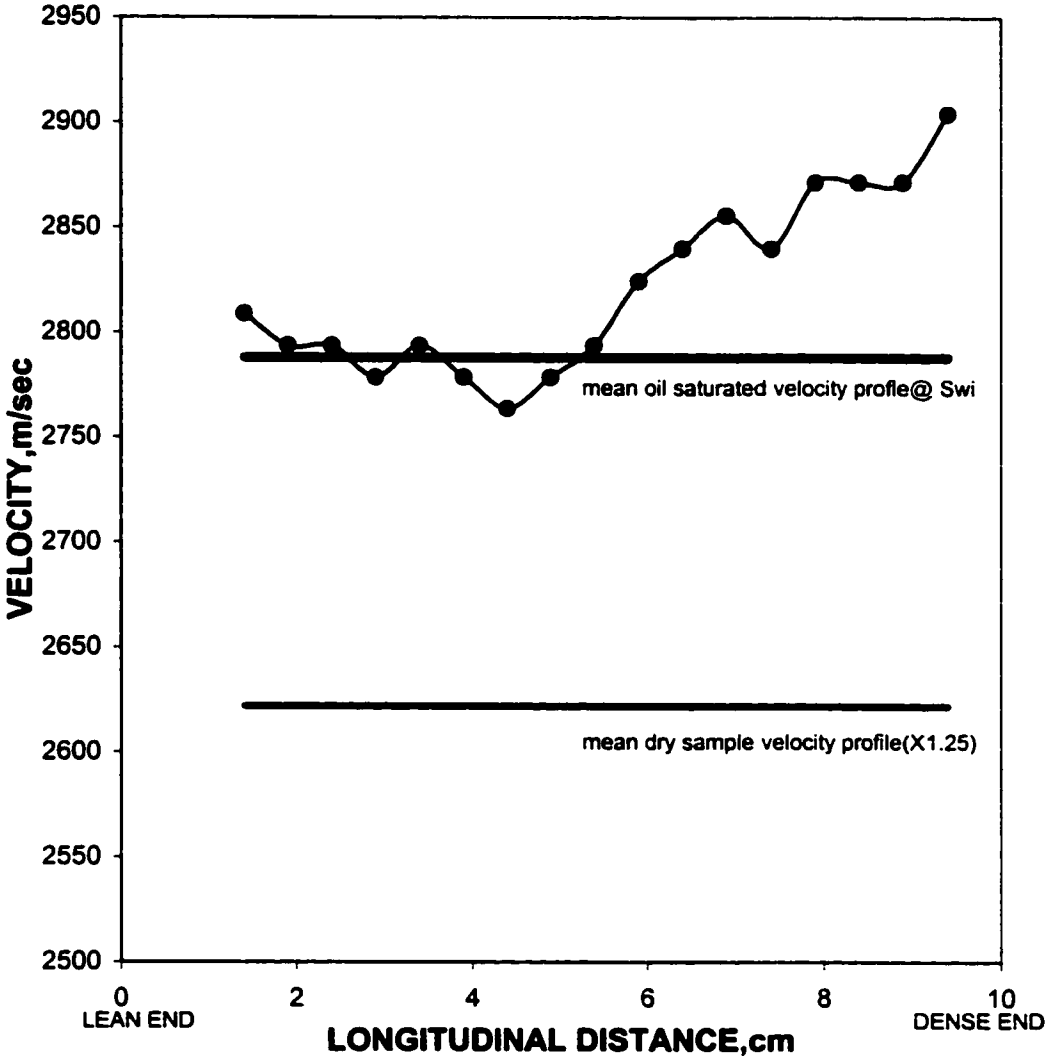

Figure 5-1: Ultrasonic Velocity Profile for sample A-17 (for 8μ $CaCO_3$ additives, 4 Hrs Flooding time)

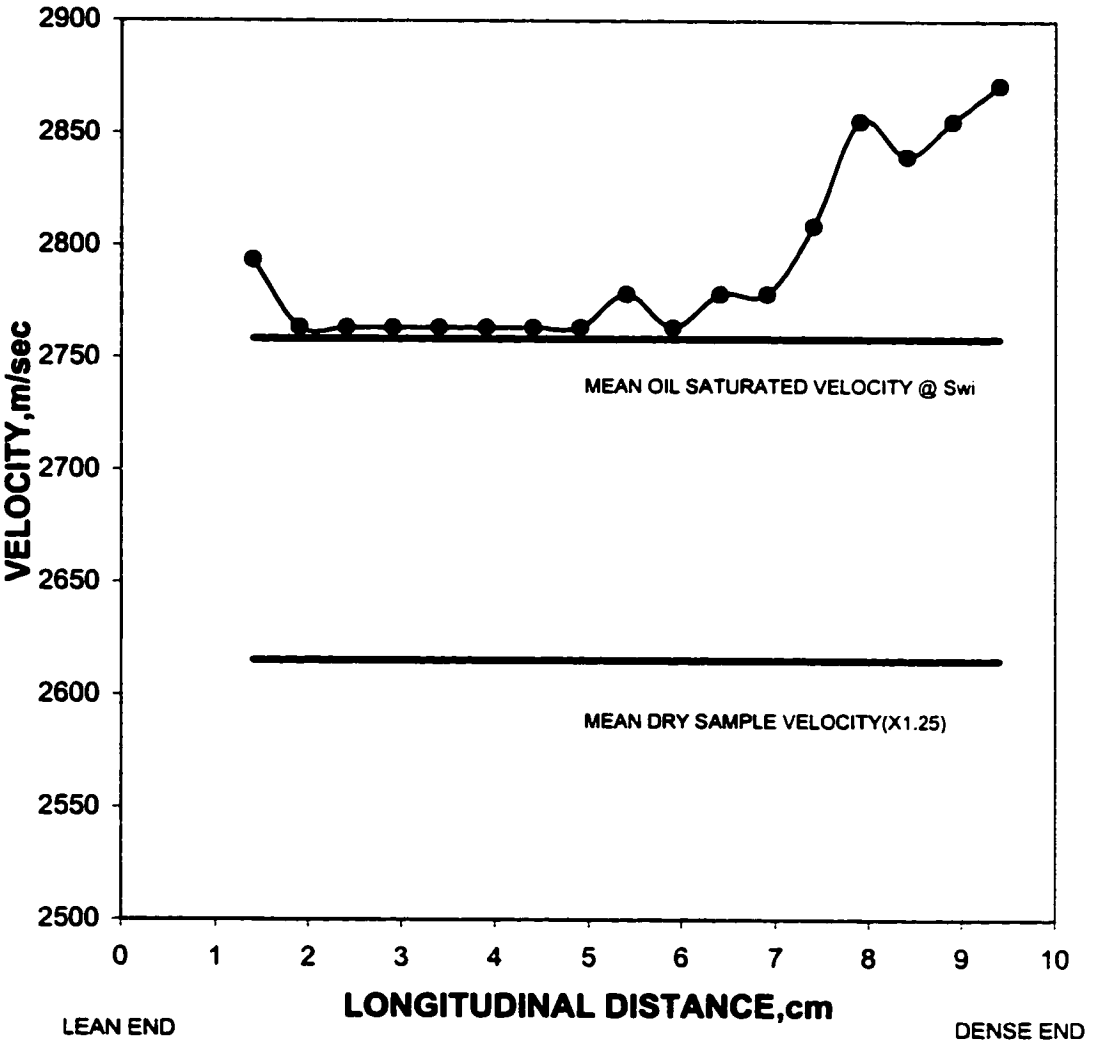

Figure 5-2: Ultrasonic Velocity Profile for sample A-20(for 12μ $CaCO_3$ additive, 4 Hrs flooding time)

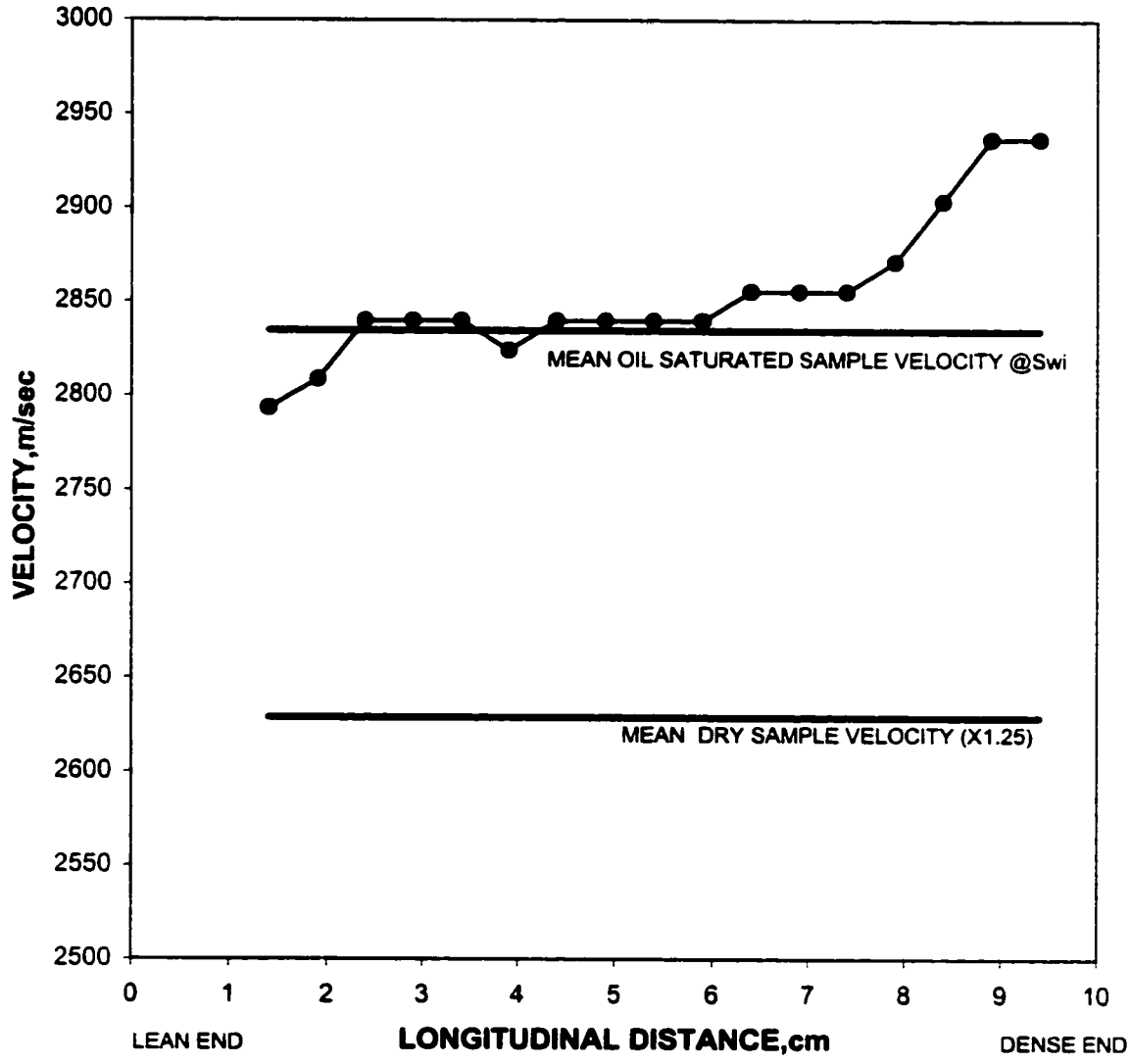

Figure 5-3: Ultrasonic Velocity Profile for sample A-23 (for21μ $CaCO_3$ additive, 4 Hrs Flooding time and)

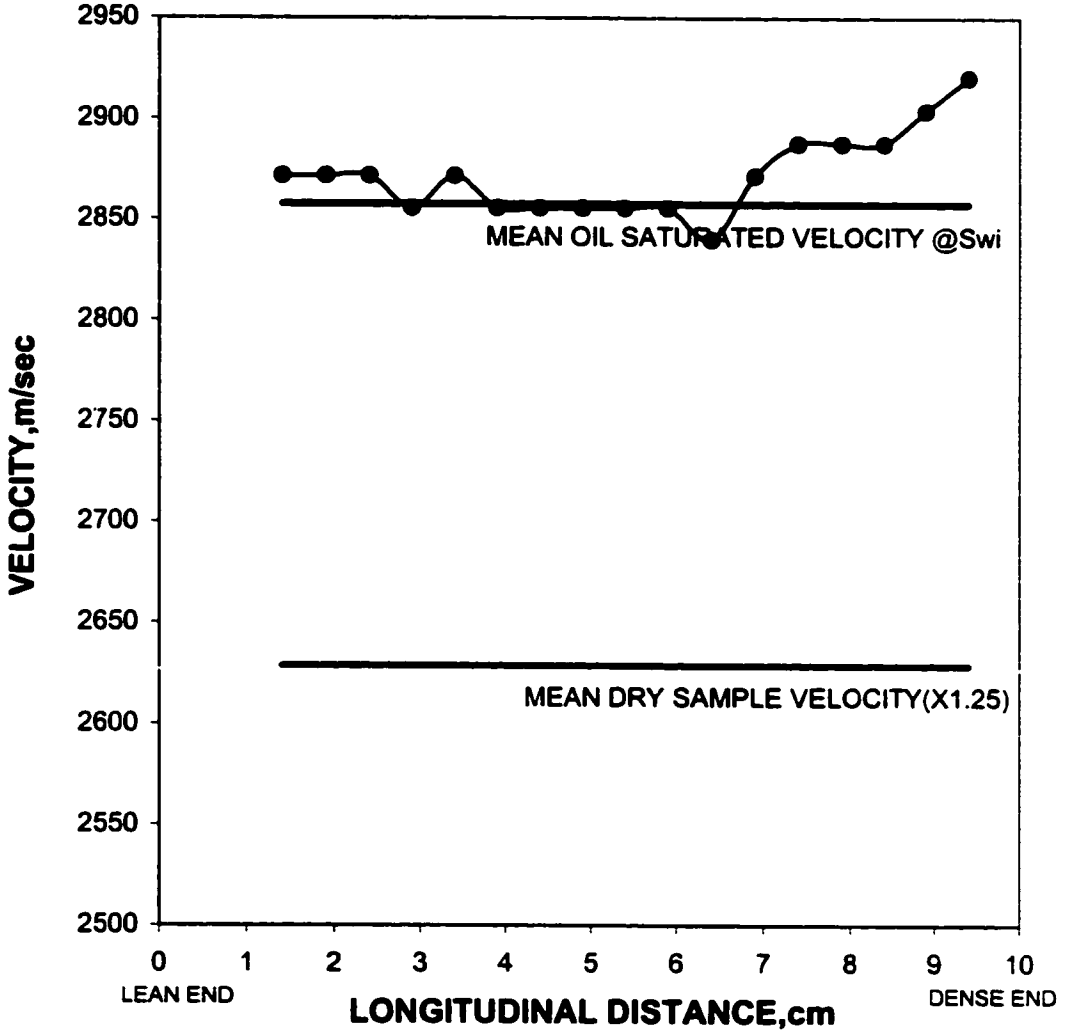

Figure 5-4: Ultrasonic Velocity Profile for sample A-22(for 41μ $CaCO_3$ additive, 4 Hrs flooding time)

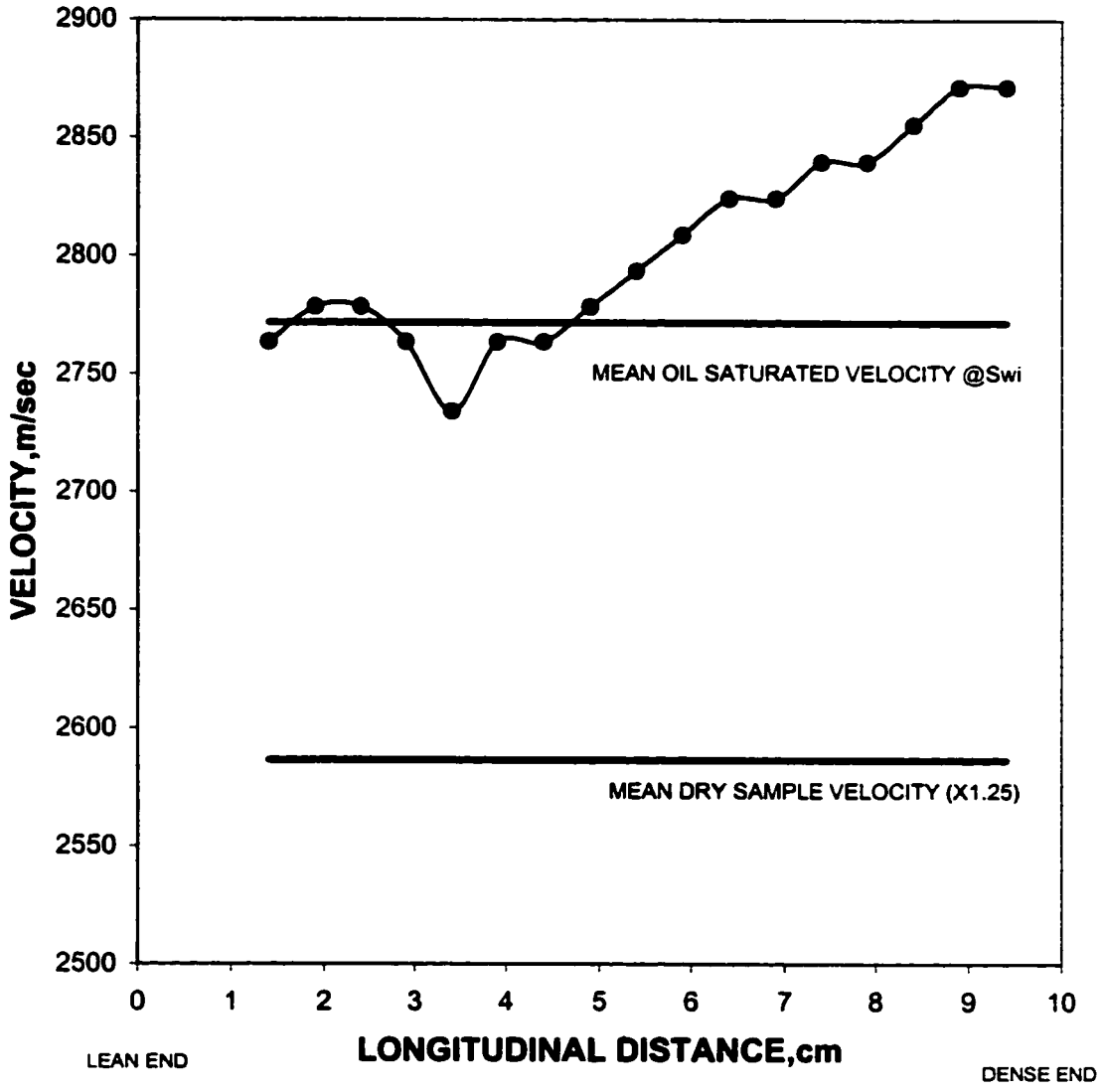

Figure 5-5: Ultrasonic Velocity Profile for sample A-26(for 8μ $CaCO_3$ additive,12 Hrs flooding time)

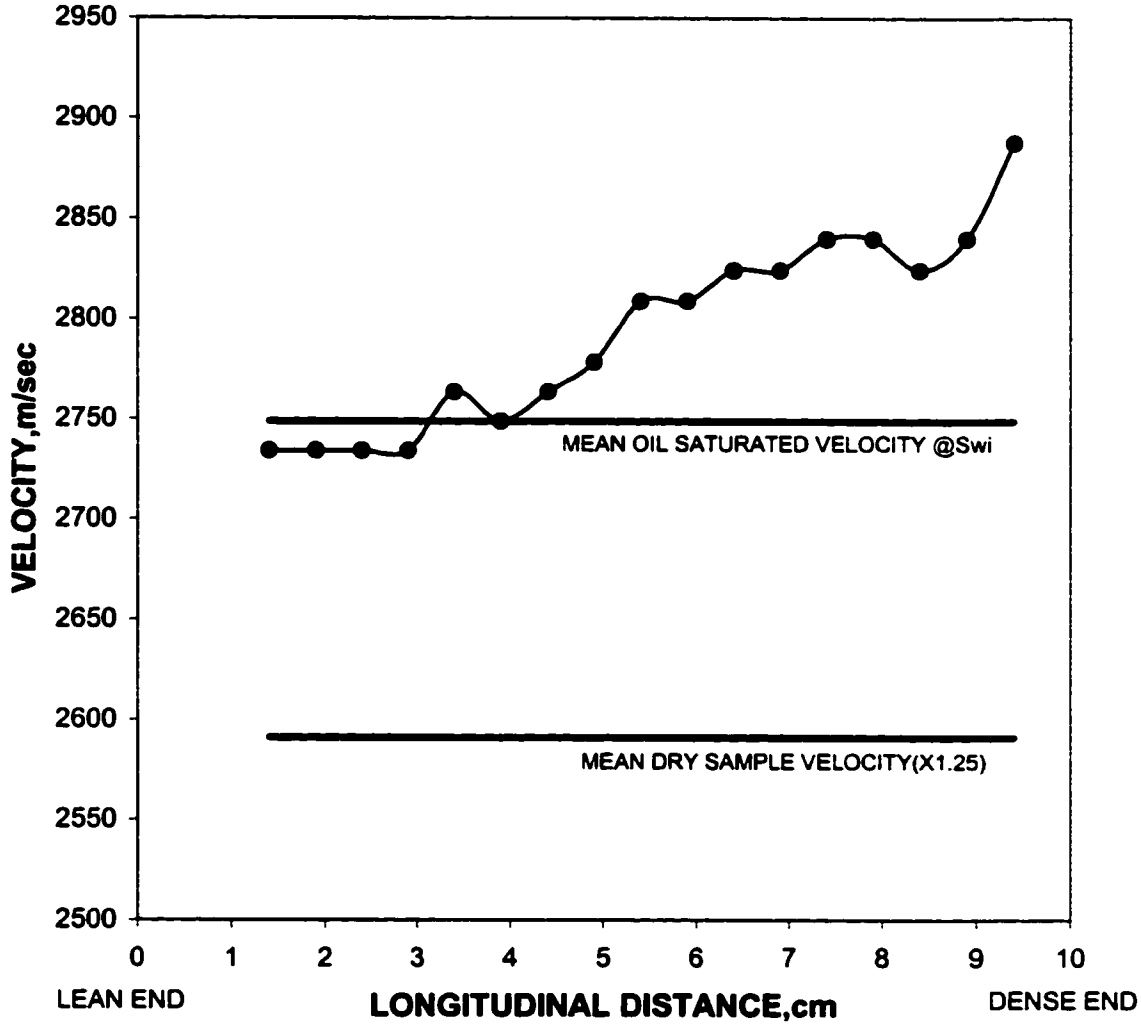

Figure 5-6: Ultrasonic Velocity Profile for sample A-25(for12μ $CaCO_3$ additive,12 Hrs flooding time)

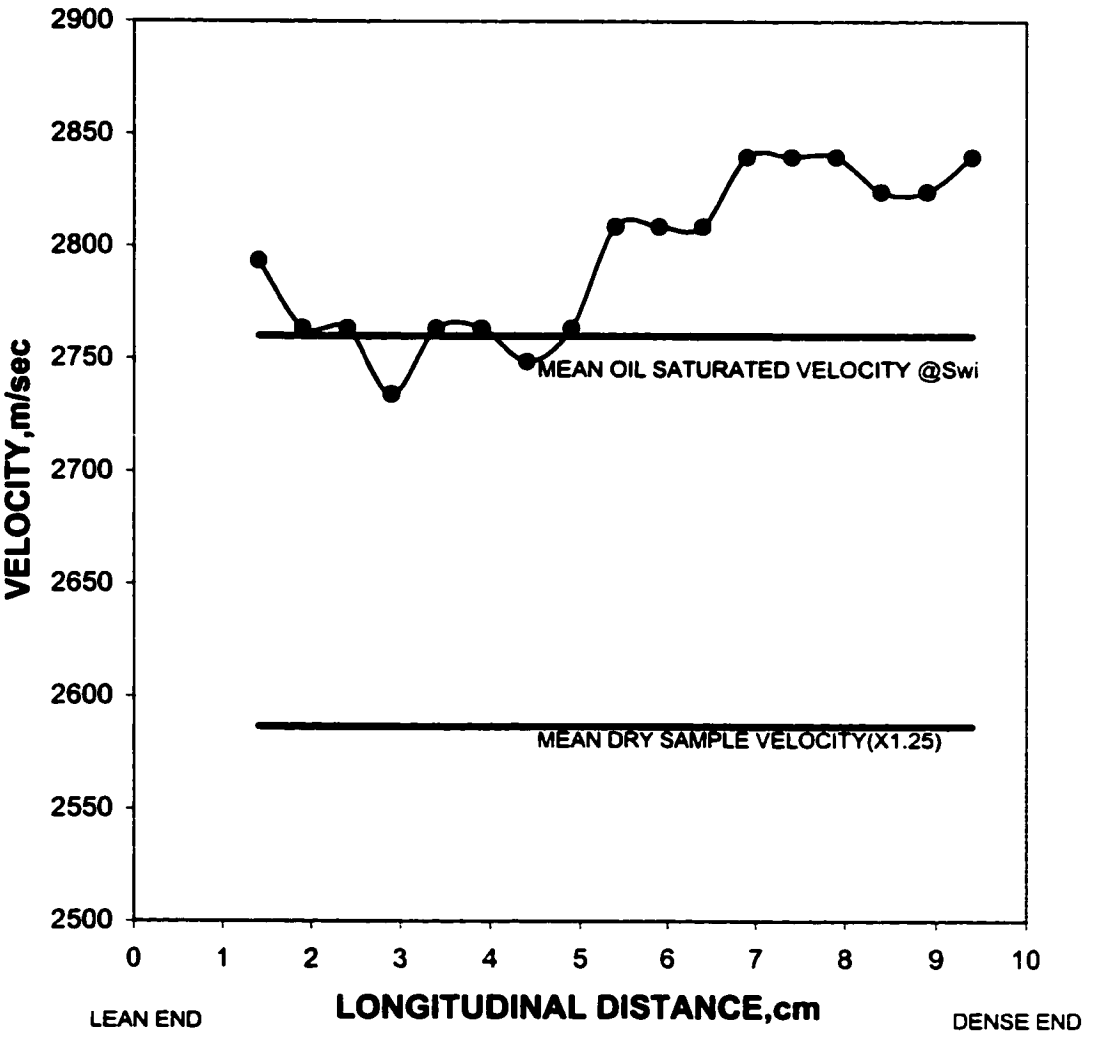

Figure 5-7: Ultrasonic Velocity Profile for sample A-24 (for21μ $CaCO_3$ additive,12 Hrs flooding time)

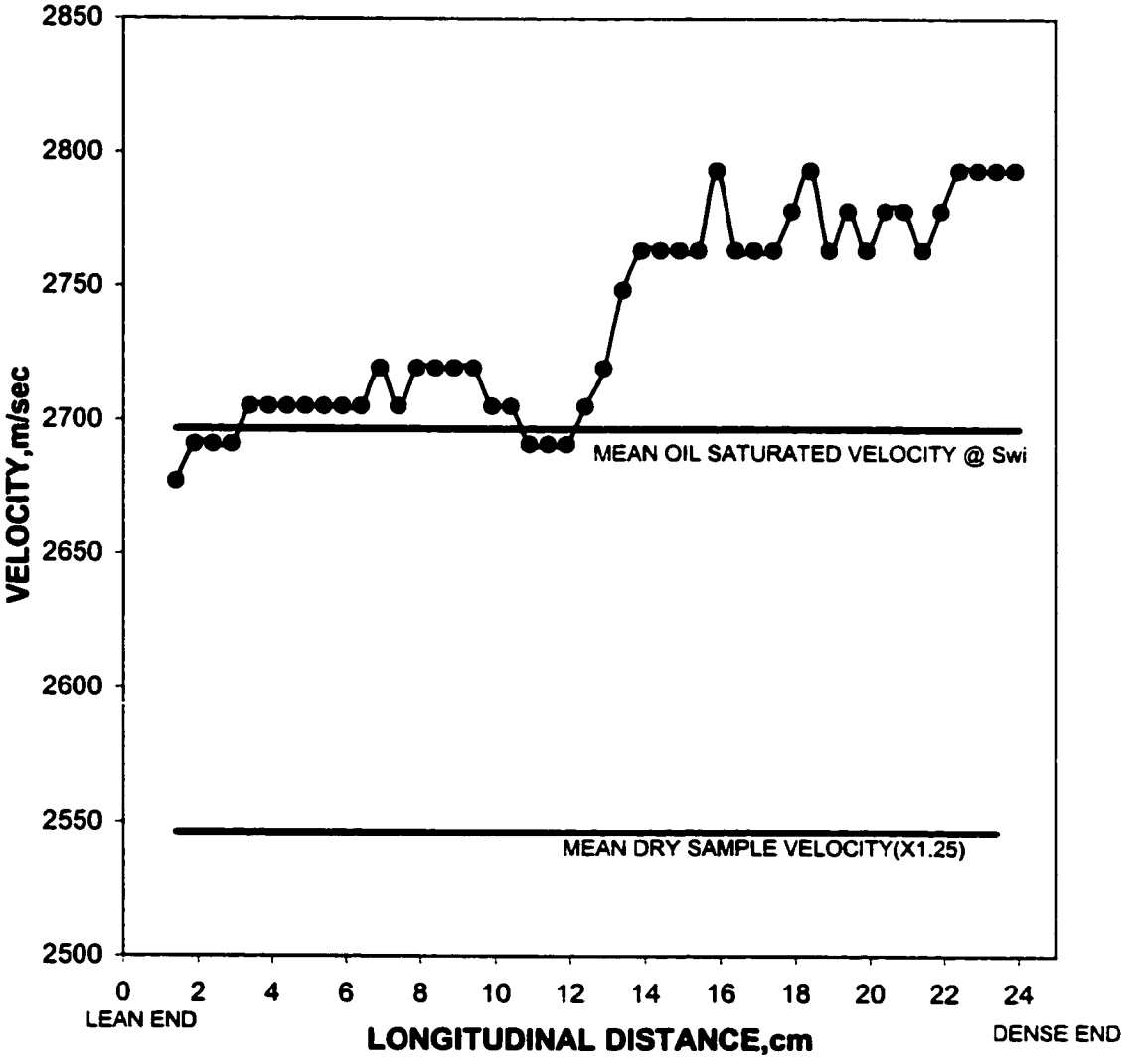

Figure 5-8: Ultrasonic Velocity Profile for sample A-28 (for 8μ $CaCO_3$ additives, 30 Hrs flooding time)

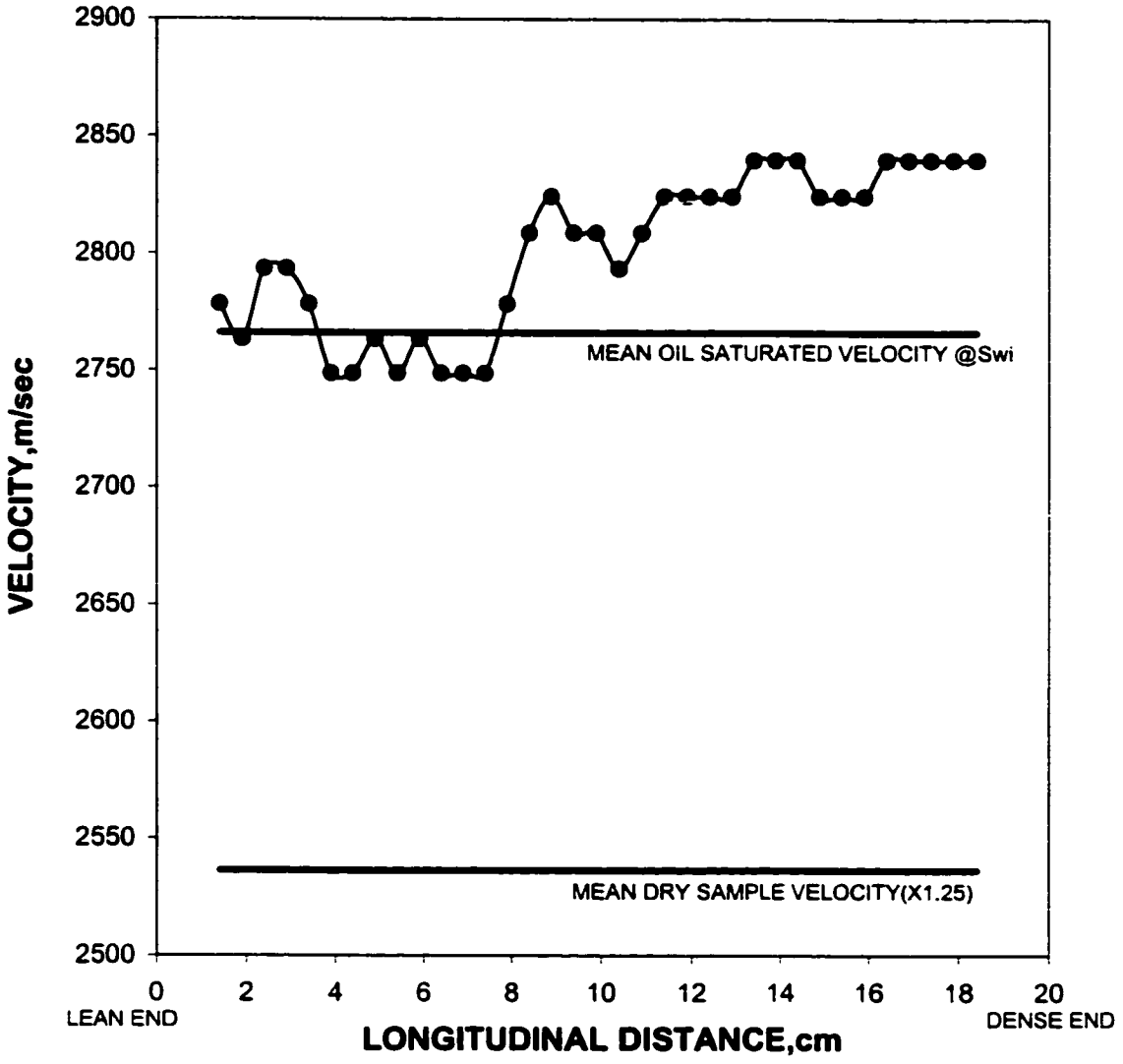

Figure 5-9: Ultrasonic Velocity Profile for sample A-19(for 12μ $CaCO_3$ additive, 30 Hrs flooding time)

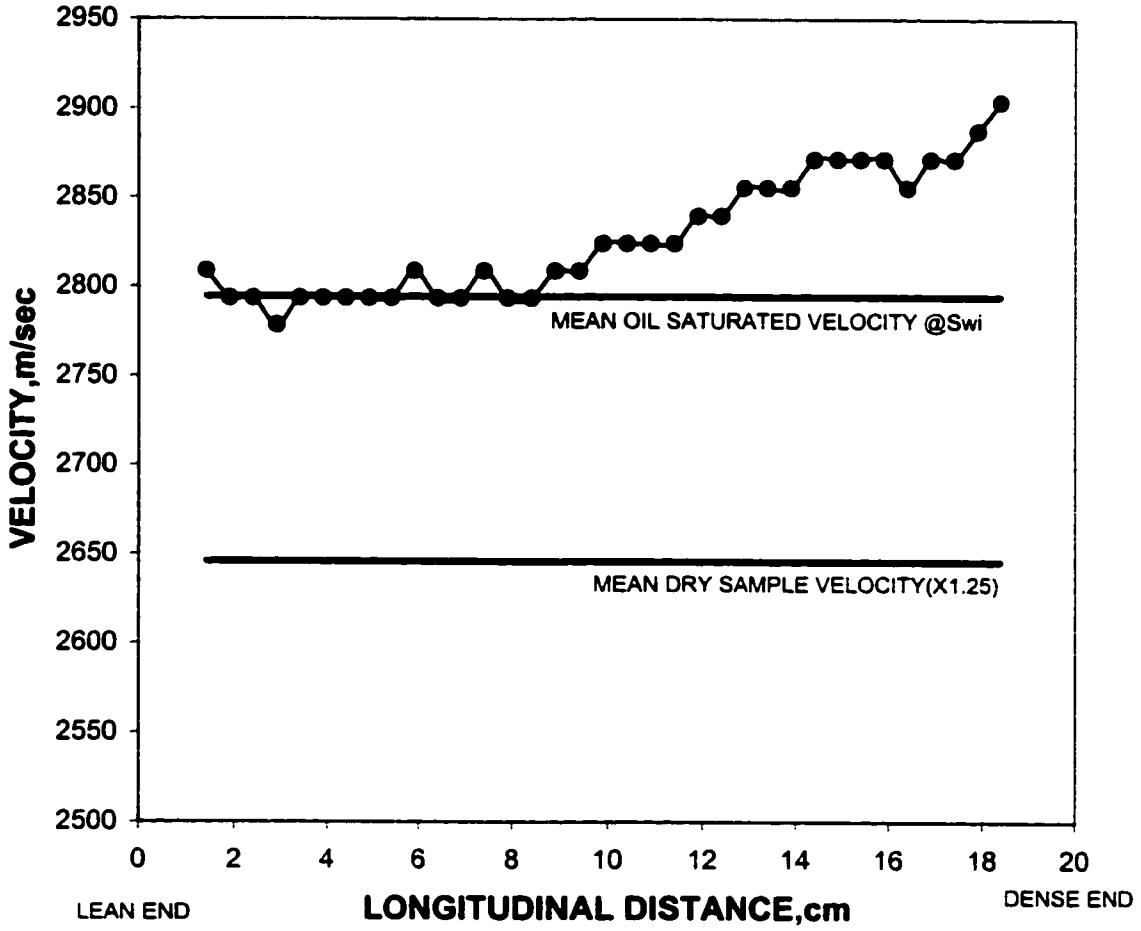

Figure 5-10: Ultrasonic Velocity Profile for sample A-29(for 21μ $CaCO_3$ additive, 30 Hrs flooding time)

5-2.2 Invasion Depth

Four different sizes of Calcium Carbonate particles ($CaCO_3$) were used as bridging additives in the water based mud formulations. Although formation damage occurs with all mud during drilling, it is possible to minimize solids invasion and formation impairment by adding bridging material to the mud. These bridging materials are chosen by matching its size to the formation pore sizes. In this study, the pore size distribution was calculated from the capillary pressure data measured from centrifugal technique as presented in chapter 4.

Effect of Particle size

Figure 5-11 through 5-14 presents the effect of particle size on an invasion depth. From these figures, it is evident that invasion depth decreases with increase in the particle size of the bridging additive used in the polymeric water based mud system. Figure 5-11 shows the effect of bridging particle sizes on invasion depth for the four hours flooding experiment. From the figure, it can be seen that as the median particle size of the bridging additive increases from 8 to 41 micron, the invasion depth decreases by 1.35cm. It is also interesting to note that increasing the $CaCO_3$ bridging additive from 8micron to 12micron decreases the invasion depth by more than 40 %.

Figure 5-13 for instance clearly shows this effect. As one can see, when the size of the median $CaCO_3$ particles in the drilling fluid system was increased from 8 micron to 21 micron, the invasion depth decreases from 13.15 to 9.9cm. Increasing the particle size

from 8 to 12 microns results in decreasing the invasion depth by about 68%. Further increase in particle size beyond 12 microns results in a decrease of the depth of invasion by only 32%. Figure 5-14 shows a steep rate of invasion depth decline up to the 12micron. Above this value, the rate of invasion depth decline is much smaller.

Generally, the result of this study shows a decrease in invasion depth with increase in particle size. It may not be the case for the particle sizes beyond the range of the particle size studied. For example, back in 1957, Glenn and Slusser[2] studied the effect of injected mud particle size distribution on formation damage. They conducted filtration experiment on porous samples with muds containing different particle sizes. Their experimental result showed that a certain particle size distribution in the mud system is required for a given pore size distribution for minimum permeability impairment.

Recently, Ajay and Sharma [30] reported that to minimize formation damage due to drill-in fluids, solids must be sized to satisfy two important criteria: i) they must be large enough to not invade the rock, and ii) they must be small enough to form filter cake that effectively filters drill solids and polymers from filtrate entering the formation.

Effect of flooding time

Figures 5-15 through 5-18 show the effect of flooding time on the invasion depth. It is evident from these figures that invasion depth by filtrates and drilling fluid particles increases with flooding time. Figure 5-15 presents the invasion depth versus flooding time when Berea core samples were exposed to the WBM-1 (i.e., when the core samples were exposed to the polymeric water-based mud, with the median particle size of the bridging additive used was 8microns). When the flooding time was 4 hours, the observed invasion depth was 5.05cm, or up to the 4hours flooding time the invasion depth was increasing at the rate of 1.263cm per hour. Whereas increasing the flooding time to 30hours has increased the invasion depth by 8.1 cm or from the 4 hours flooding time onward, the rate of invasion depth was 0.31cm per hours.

Figure 5-16 presents the invasion depth versus flooding time plot for the WBM-2 mud system where the median particle size in the mud system was 12 micron. The trend of this plot is the same as in the case of figure 5-15 with higher invasion depth rate increment being up to the 4hours flooding time at the rate of 1.113cm per hours. Beyond the 4hours flooding time, the rate of invasion increment was 0.25cm per hours. Figure 5-17 also shows the same trend with higher invasion depth rate increment being observed to the first four hours flooding time when the core sample was flooded with the WBM-3 mud. Up to the 4hours flooding time, the observed rate of invasion increment was 1.08cm per hours and beyond the 4 hours flooding time the rate was 0.215cm per hours.

It is also evident that the rate of invasion depth increment with flooding time decreases as the size of the particles in the drilling fluid system was increased. This is actually due to the fact that larger particles added were able to bridge pore entries (internal or surface) and subsequently results in smaller openings which could be easily bridged by smaller particle and hence minimizes the filtrate and/or particles invasion.

The larger invasion depth observed in the first 4hours flooding time is due to the absence of well-established, low permeable filter cake to protect the formation from the invasion by filtrates and drilling fluid particulates down to colloidal sizes. But once the filter cake was established, the invasion of formation by filtrates and particles has declined as evidenced by the decline of rate of invasion beyond the 4hours flooding. Mud particles invasion mainly occurs during the initial mud spurt loss before an external mud cake has been formed. [32] It is also our observation that more than 50% of the filtrates were collected at the effluent in the first half or at most one hour of flooding for the experiments conducted.

One of the critical factors in the design of non-damaging fluids to prevent or reduce an invasion depth is the sizing of particles in the drilling fluid system to obtain a surface bridge on the formation face with minimum in-depth solids penetration. This can only be achieved by proper selection of bridging particle in relation to the formation pore opening.

Field experience indicated that the largest particle size, which should be used as a bridging additive in the water based mud system, is about one-half the diameter of the pore to be sealed; bridging occurring when the plurality of the carbonate particles attempted to simultaneously enter the pore. [33,34]

Bridging solids provide the basic structures for the building of a filter cake to prevent loss of fluid and solid particles into a permeable formation. Particle size distribution should be carefully controlled with an objective of obtaining a filter cake of maximum density; i.e., the closest possible packing. Close packing reduces cake porosity and total solids required for an effective bridging. It is generally accepted that a wide range of solids particle size is needed to allow the process of large-to-small close order packing.

5-2.3 Return Permeability

Effect of particle size

Figure 5-19 to 5-22 shows the effect of particle size on the return permeability. It is evident from the figures that return permeability will increase with particle size. Figure 5-19 presents the plot of a return permeability versus particle size for the four hours flooding experiment. When the core sample was exposed to the WBM-1 mud, the

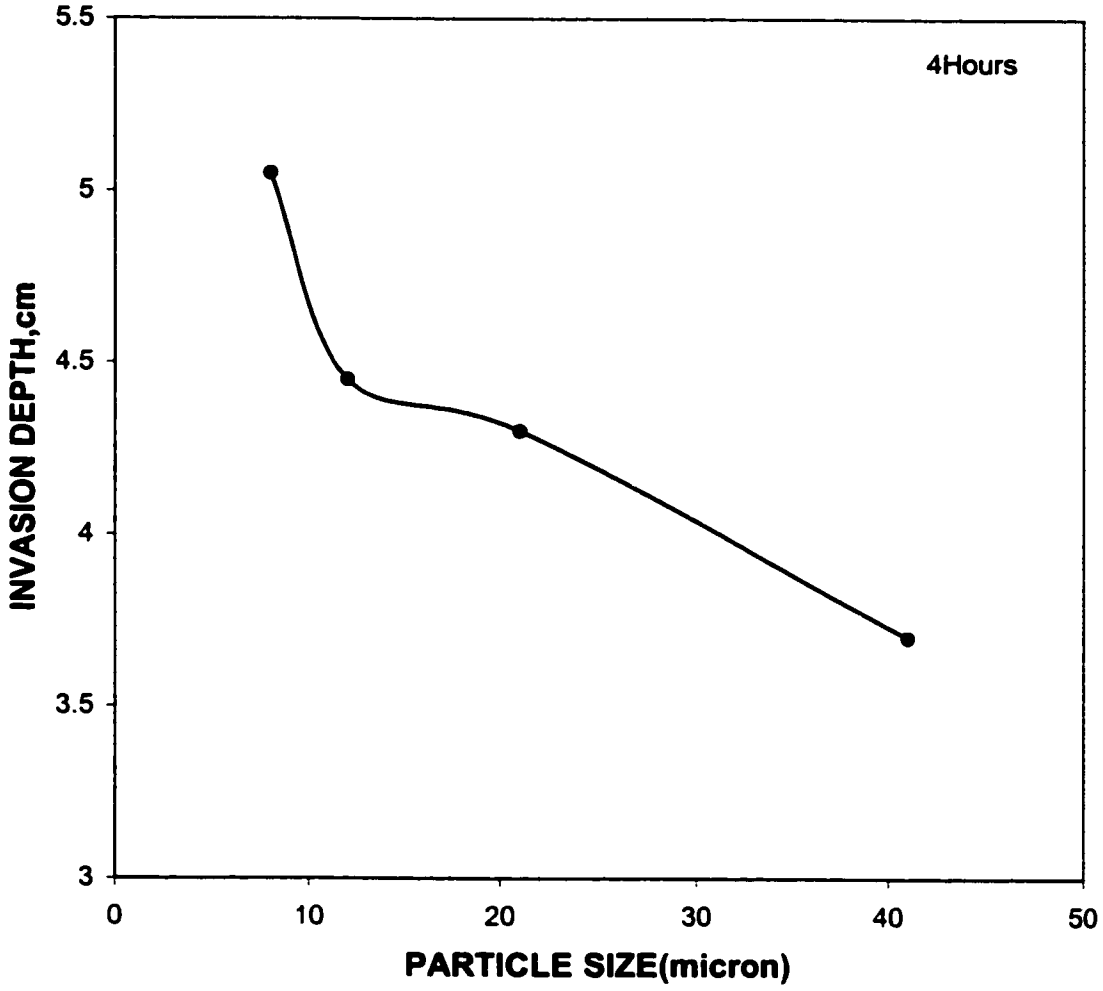

Figure 5-11: Effect of Particle size of Calcium Carbonate used in the WBM on the invasion depth(for the 4hours Flooding Time).

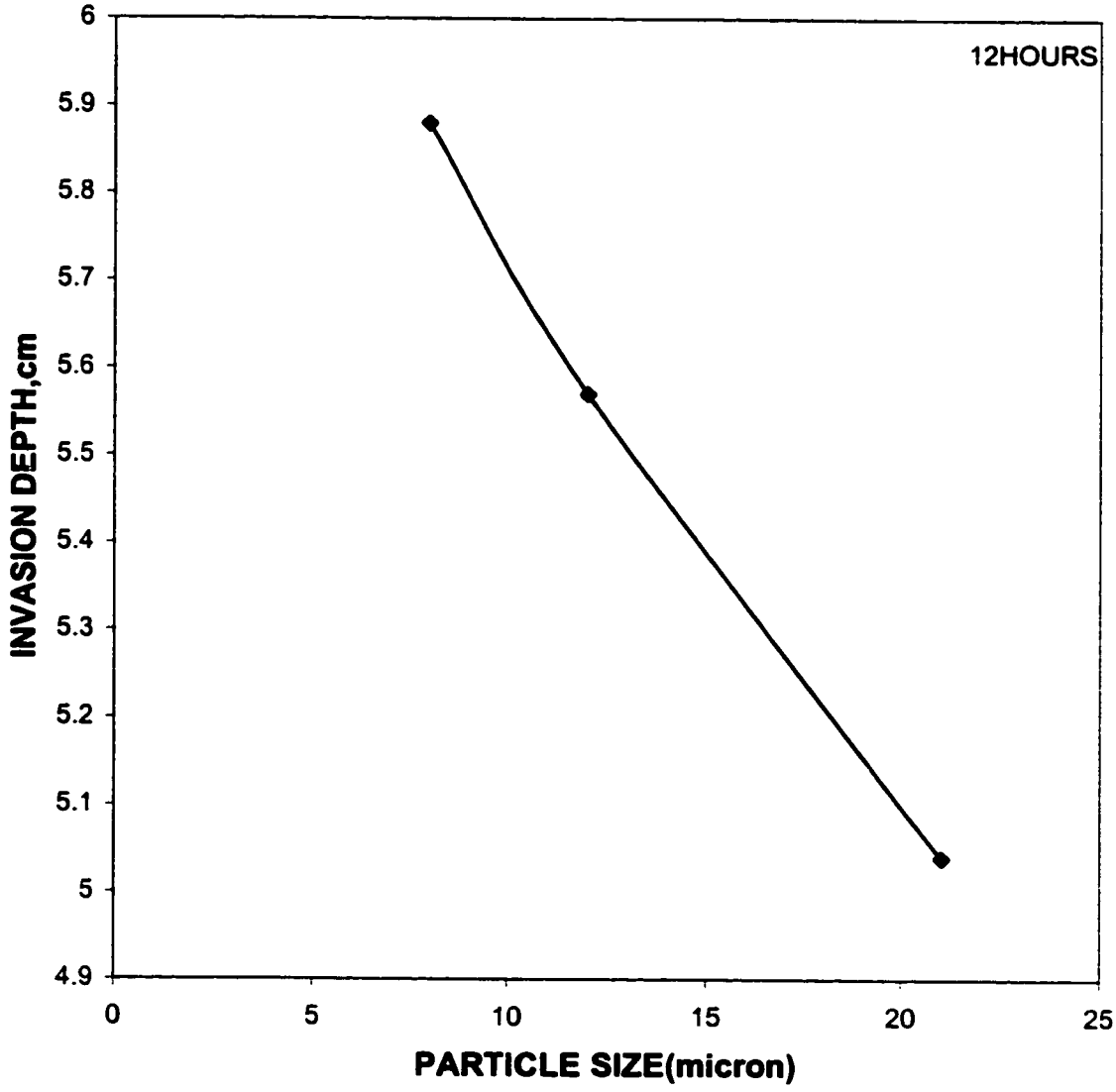

Figure 5-12: Effect of Particle size of Calcium Carbonate used in the WBM on the invasion depth (for the 12hours Flooding Time).

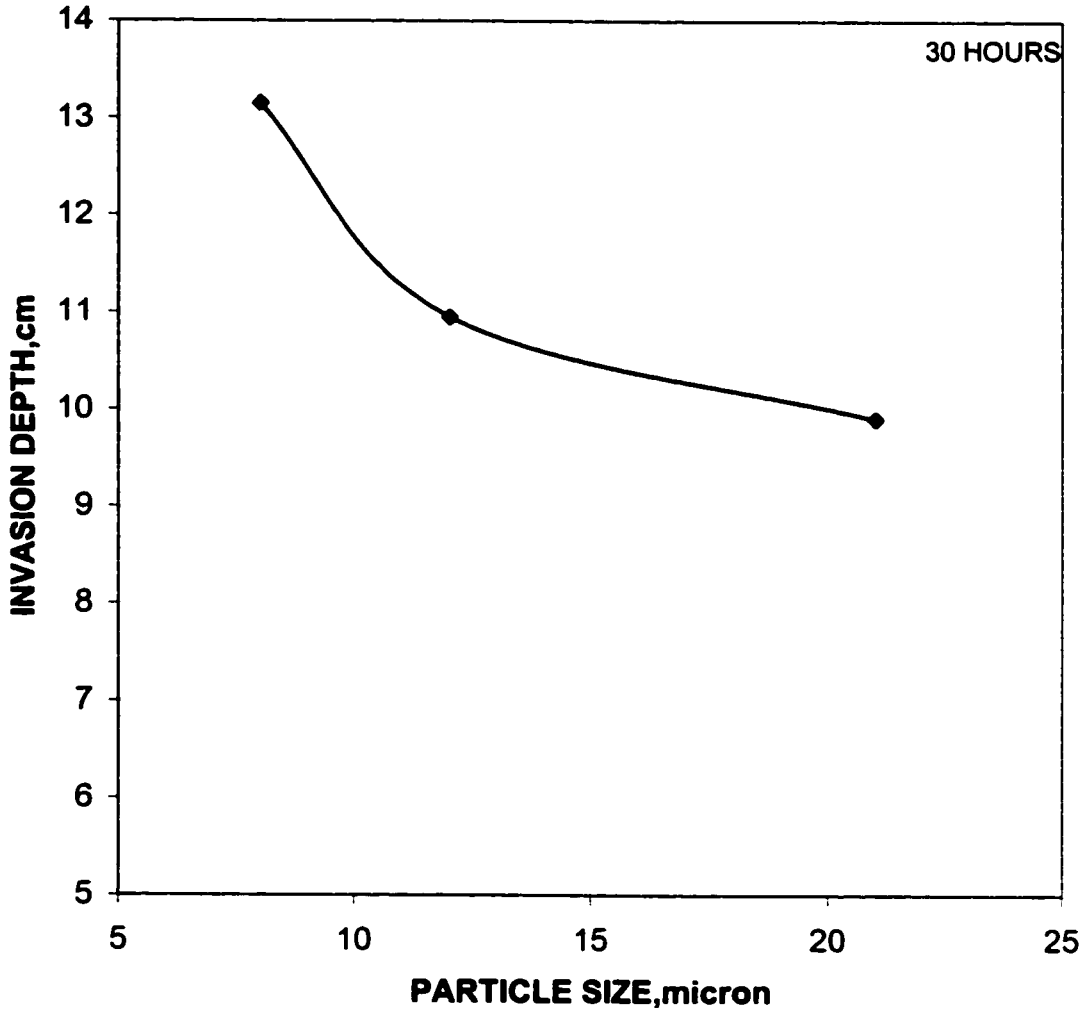

Figure 5-13: Effect of Particle size of Calcium Carbonate used in the WBM on the invasion depth(for the 30hours Flooding Time).

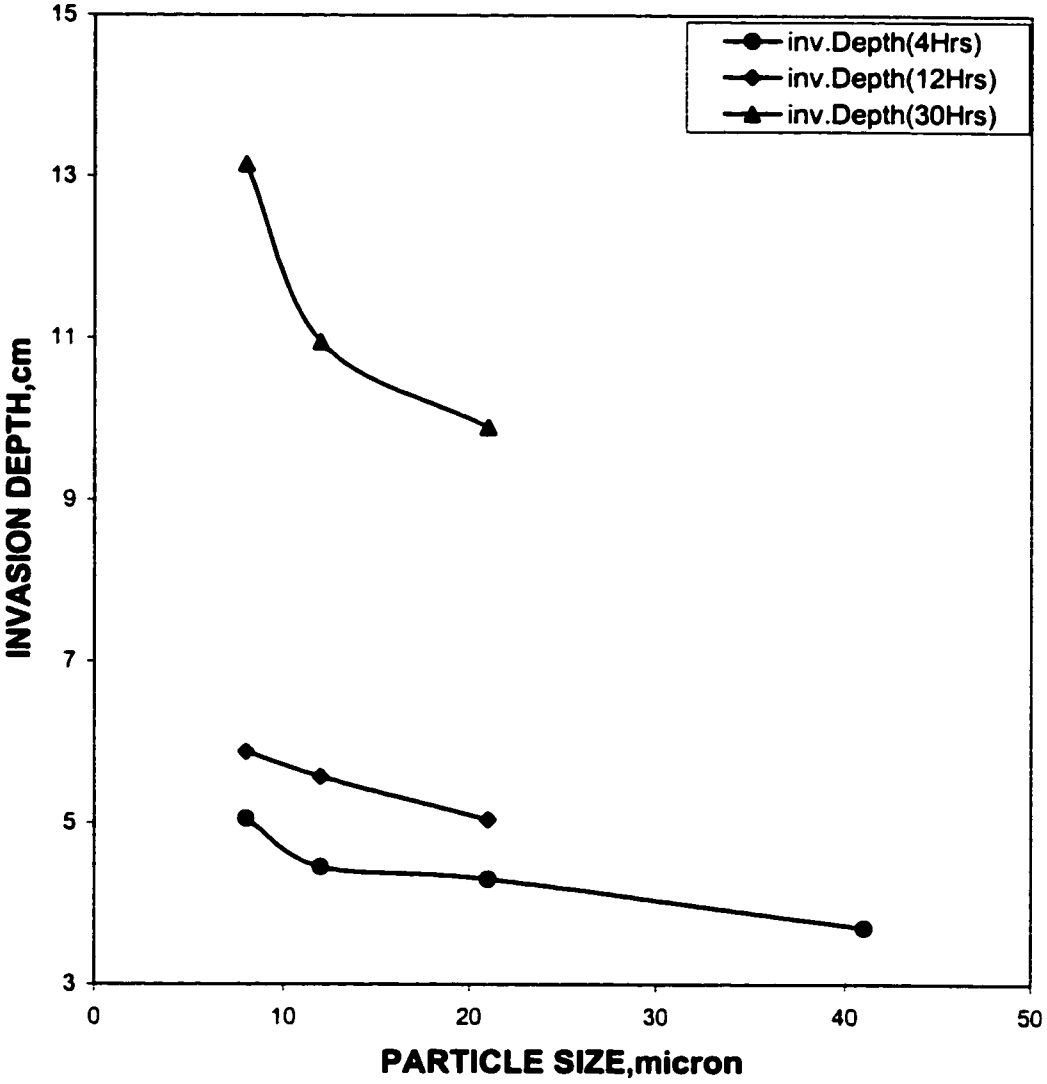

Figure 5-14: Effect of Particle size of Calcium Carbonate used in the WBM on the Invasion depth.

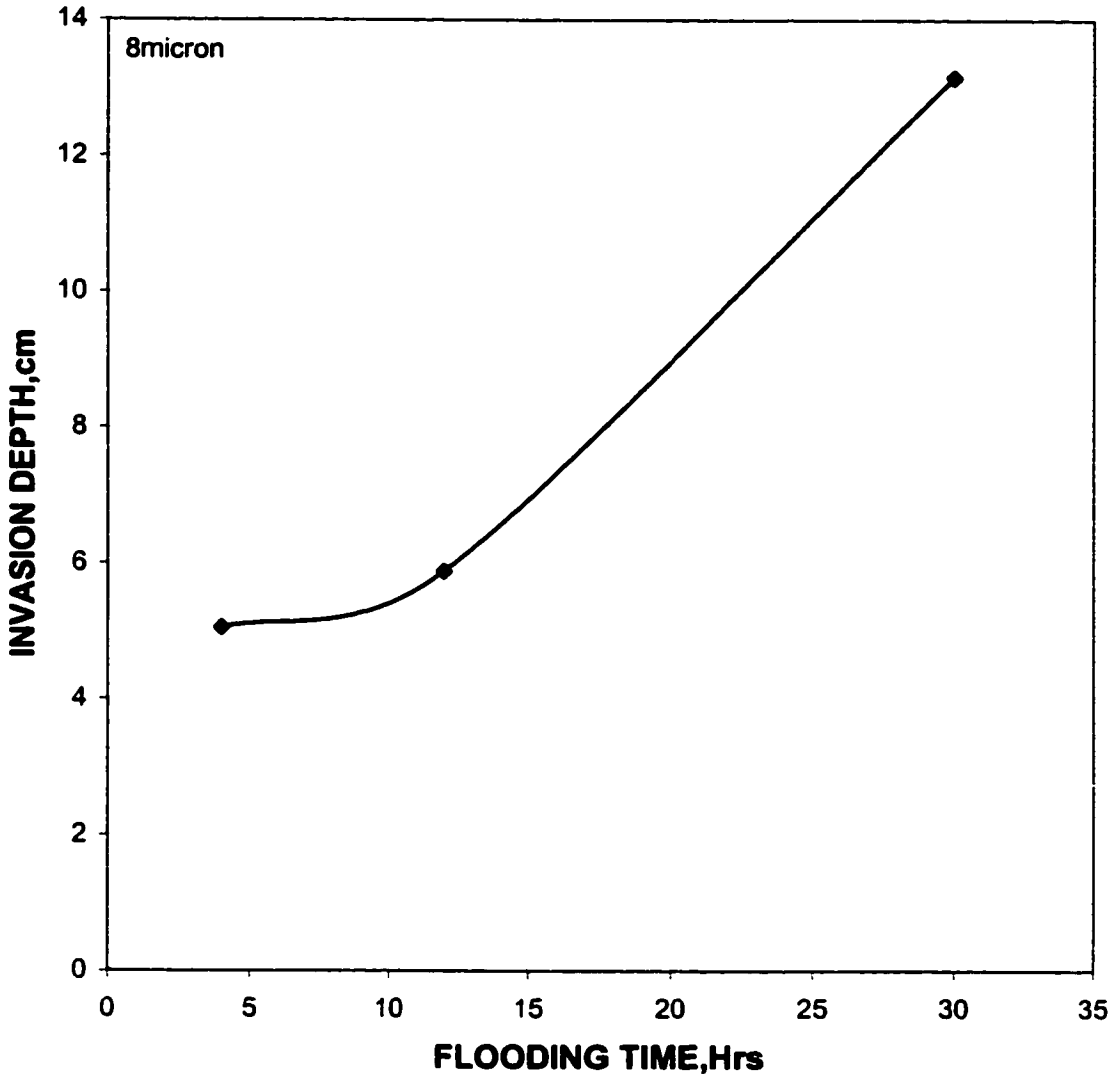

Figure 5-15: Effect of Flooding Time on the Invasion Depth(for 8micron $CaCO_3$ Bridging Additive)

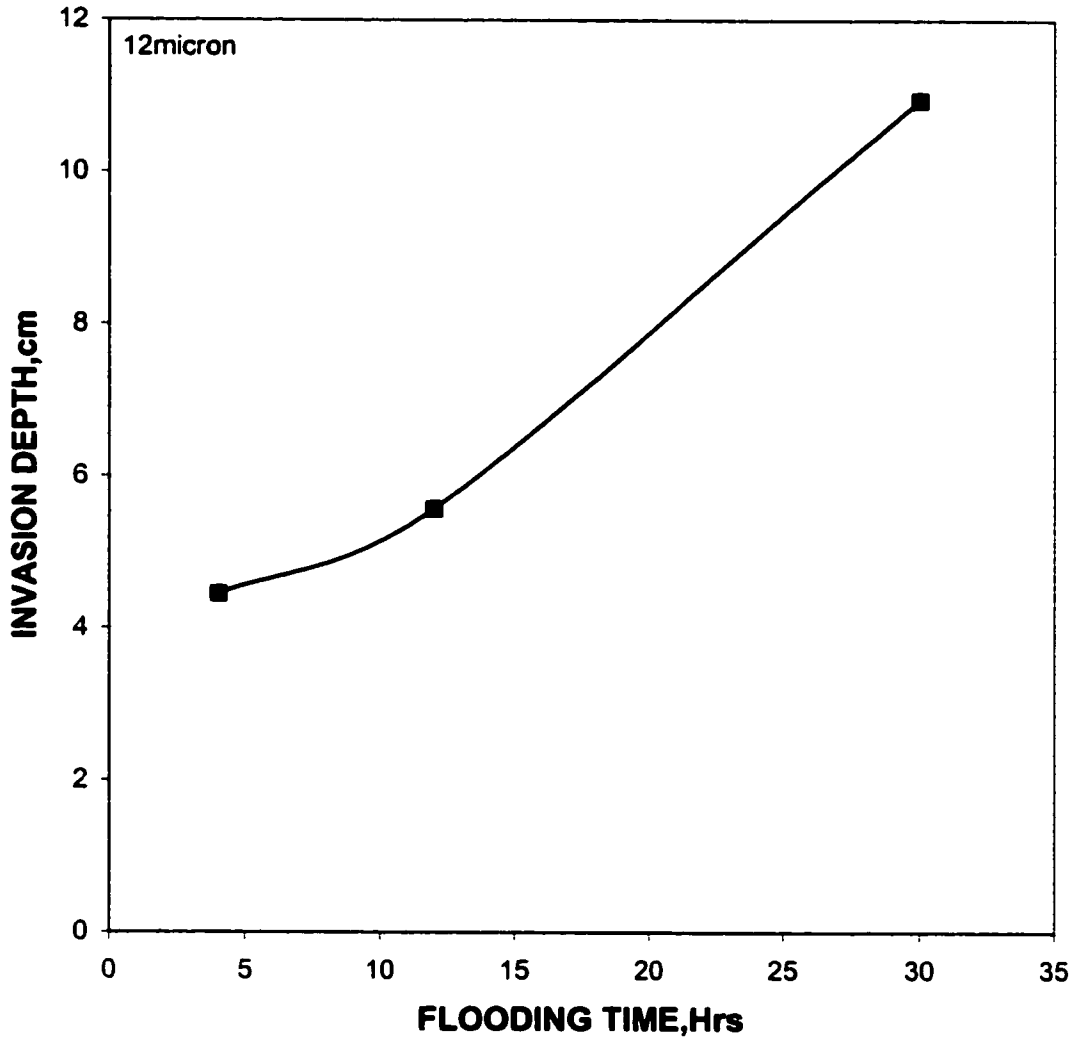

Figure 5-16: Effect of Flooding Time on the Invasion Depth(for 12micron $CaCO_3$ bridging additive)

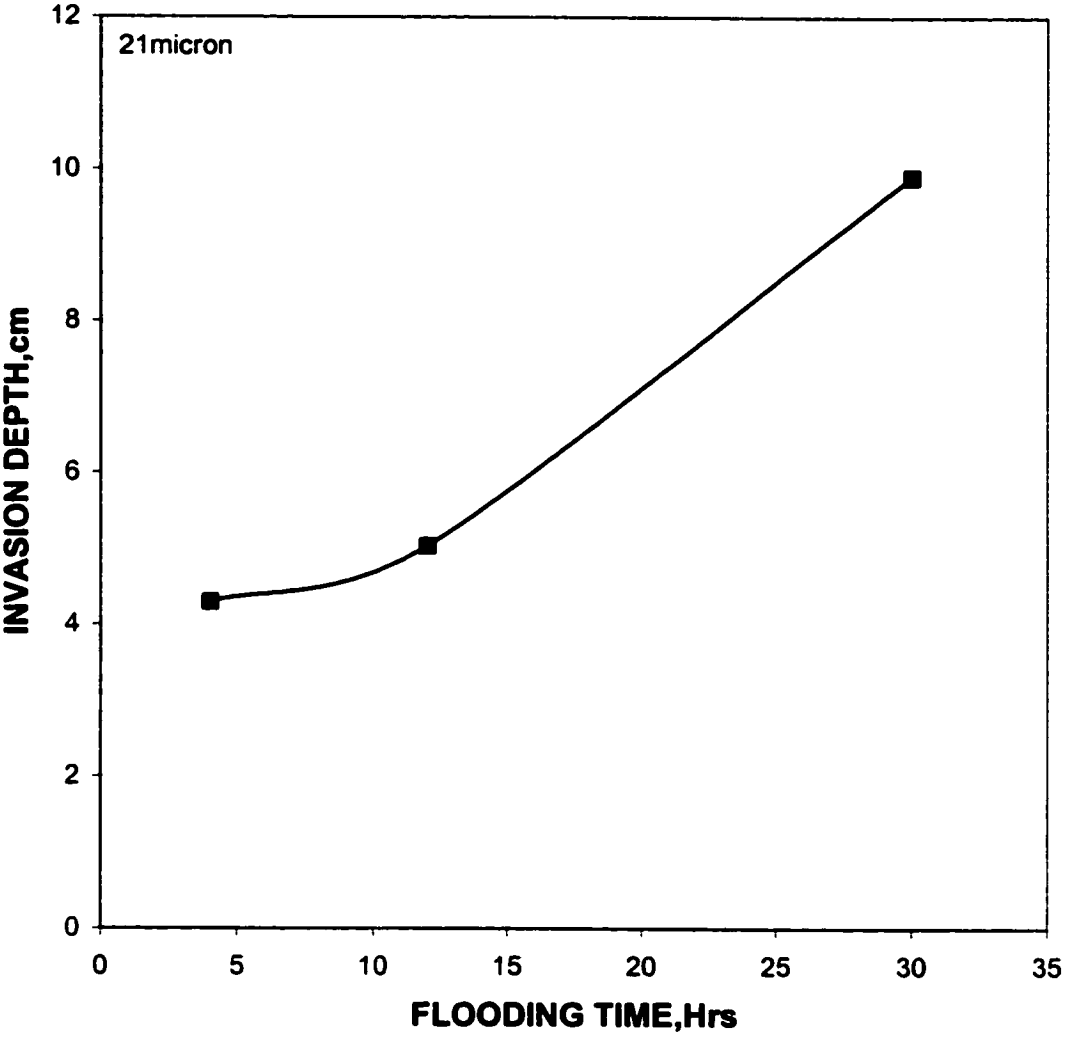

Figure 5-17: Effect of Flooding Time on the Invasion Depth(for 21micron $CaCO_3$ bridging additive)

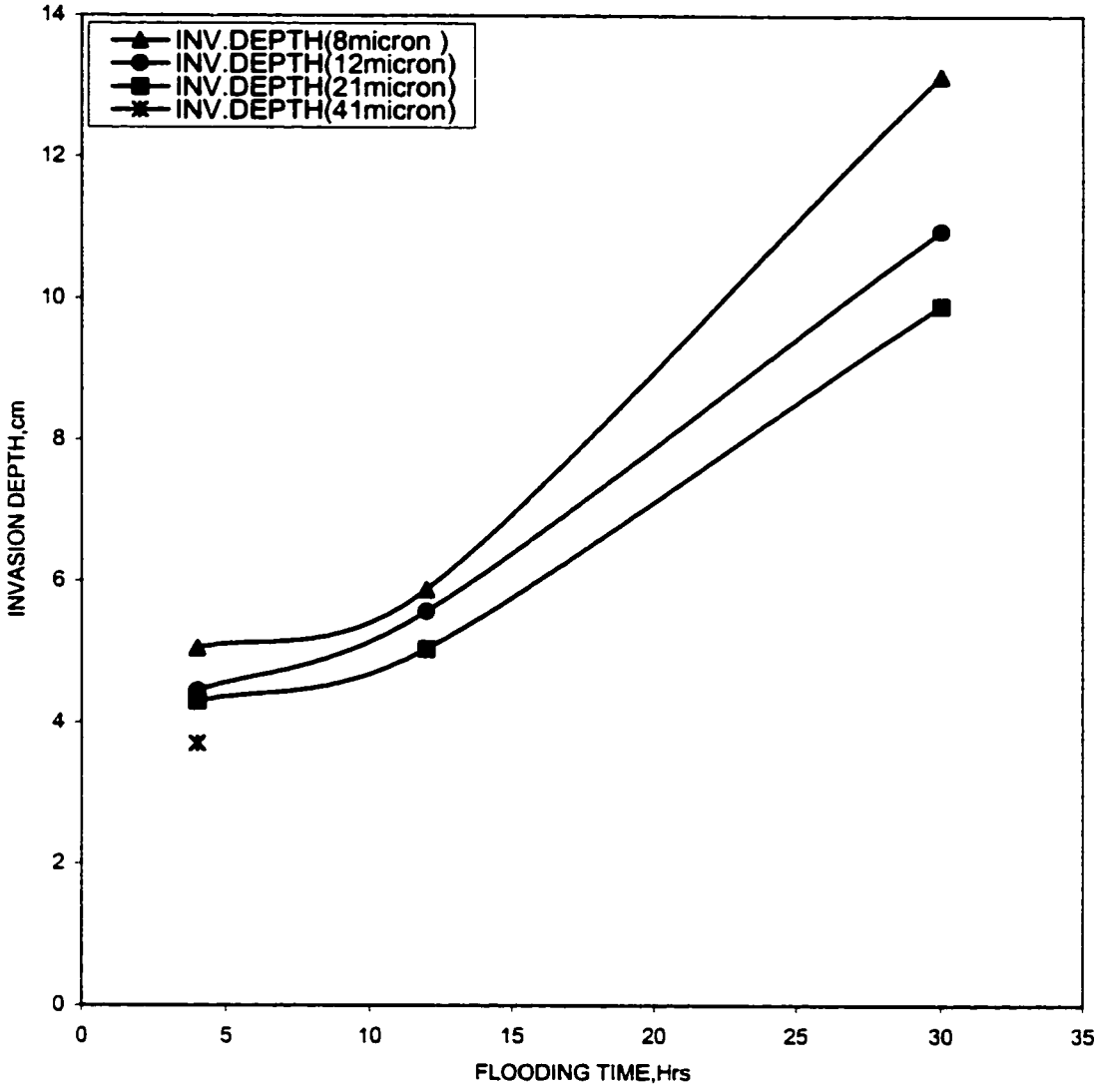

Figure 5-18: Effect of Flooding Time on the Invasion Depth

observed return permeability was 44%. Increasing the median particle size to 12 microns has increased the return permeability by 15.5%, or an increase in the return permeability of 3.88% per micron of the bridging particle size was observed. Further increase in the bridging particle size to 21micron has introduced an increment of only 1.3% or 0.144% per each micron increment of the bridging particle size. It is evident that beyond the 12micron particle size, the graph is almost flat. About 92% of the return permeability is recovered only by increasing the particle size from 8 to 12microns. Beyond the 12microns the graph is almost flat. But for higher flooding time, as shown in figure 5-21, the effect of particle size on return permeability doesn't show the same behavior as when the formation was flooded for four hours.

Effect of flooding time

Figure 5-23 through 5-26 presents the effect of flooding time on the return permeability. It is clear from the figures that the return permeability will decrease with increase in flooding time. Figure 5-23 shows the return permeability versus flooding time plot when the core samples were flooded with the WBM-1 mud. The return permeability of the core samples after it was flooded with the mud for 4 hours was 44% whereas; at the end of 30hours flooding, the return permeability was 34.45%. That is, a decrease of the return permeability by 9.55% or a decline in the return permeability of 0.3673% per hours.

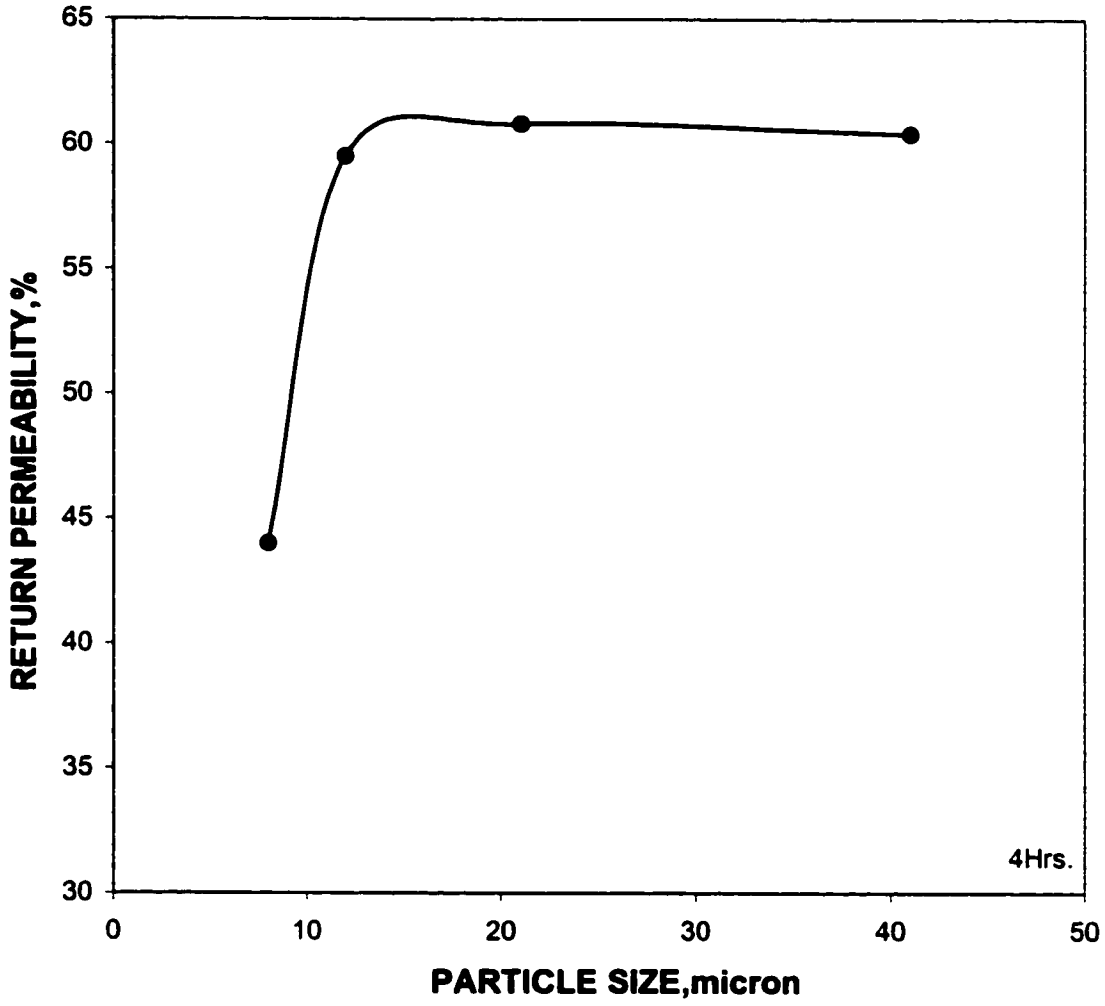

Figure 5-19: Effect of Particle Size on the return permeability for 4 Hrs. flooding time.

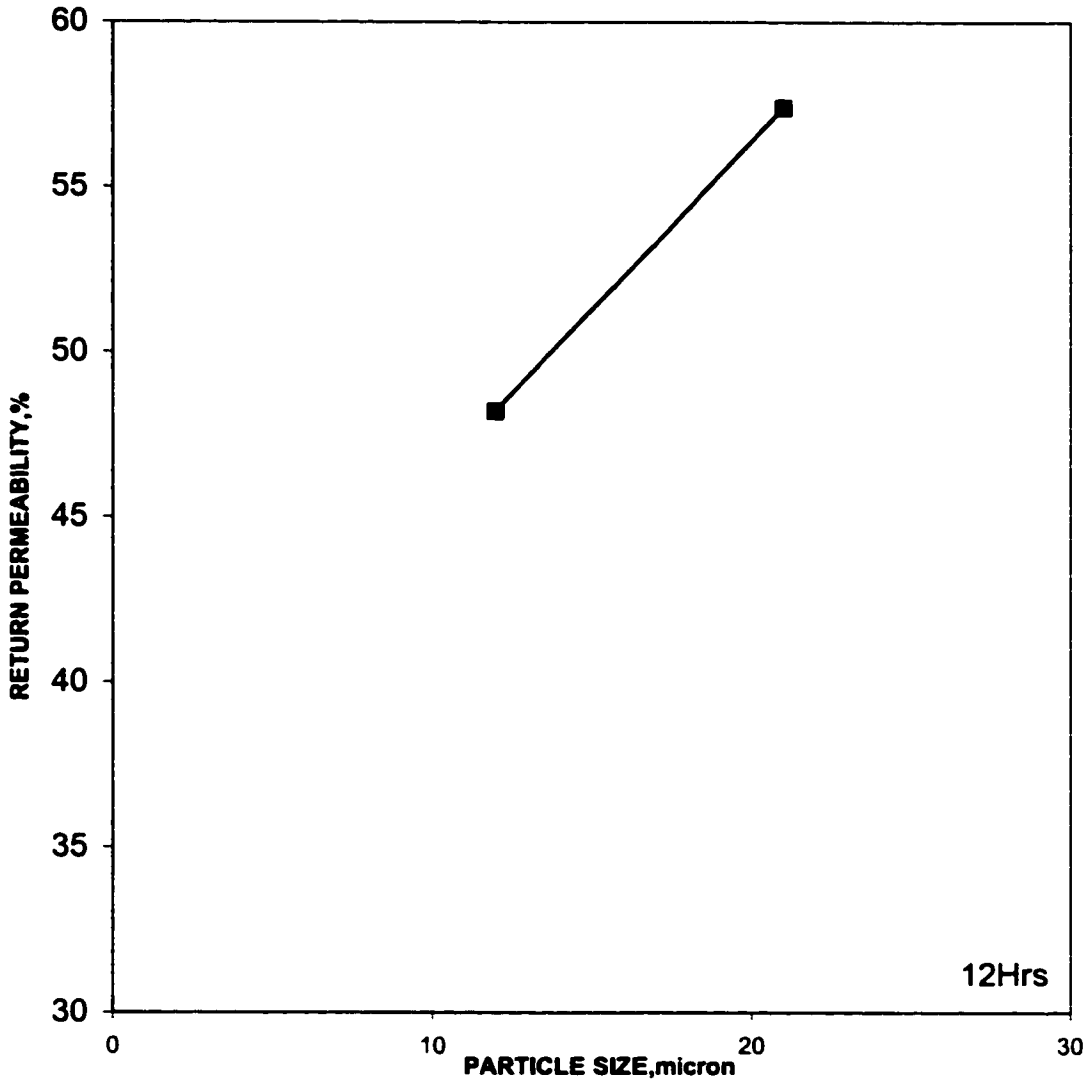

Figure 5-20: Effect of Particle Size on the return permeability for 12 Hrs. flooding time.

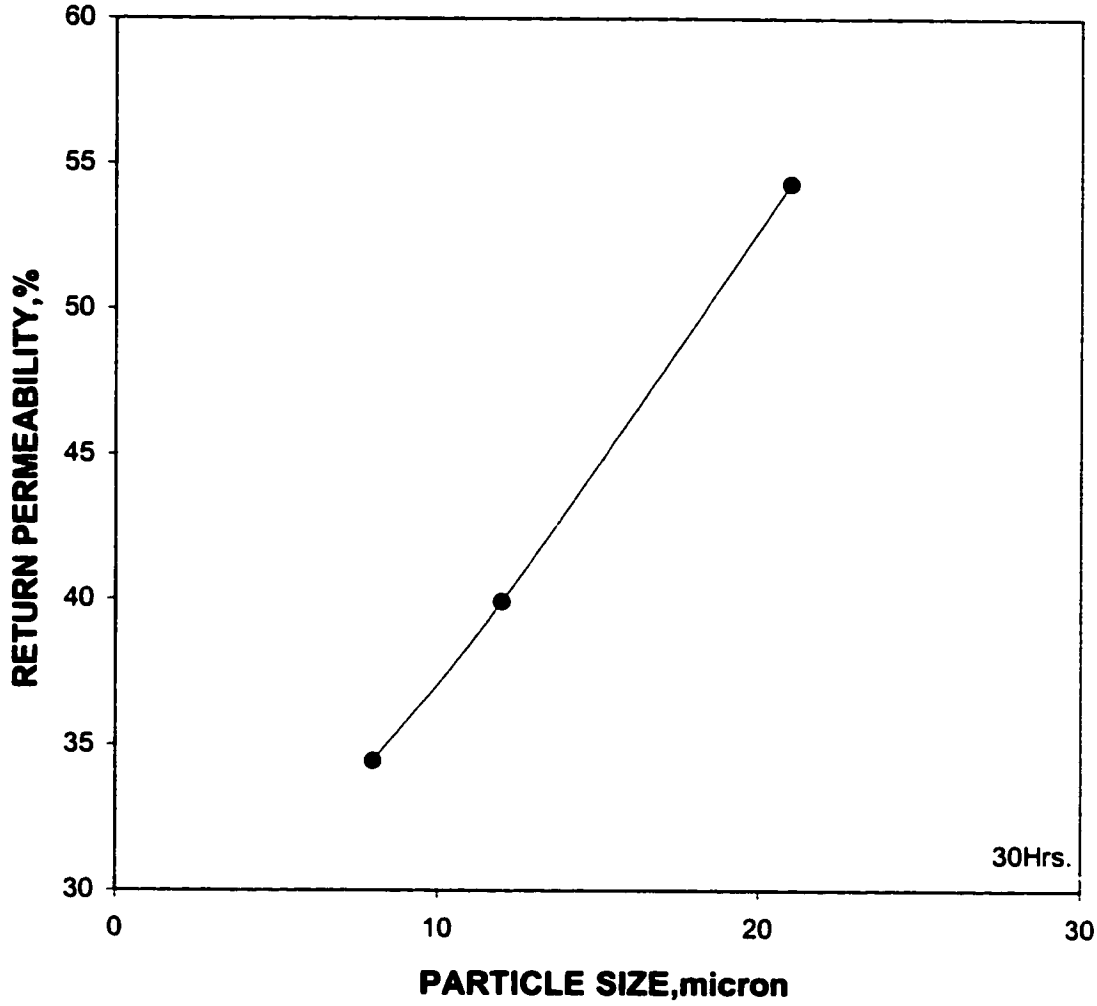

Figure 5-21: Effect of Particle Size on the return permeability for 30 Hrs. flooding time.

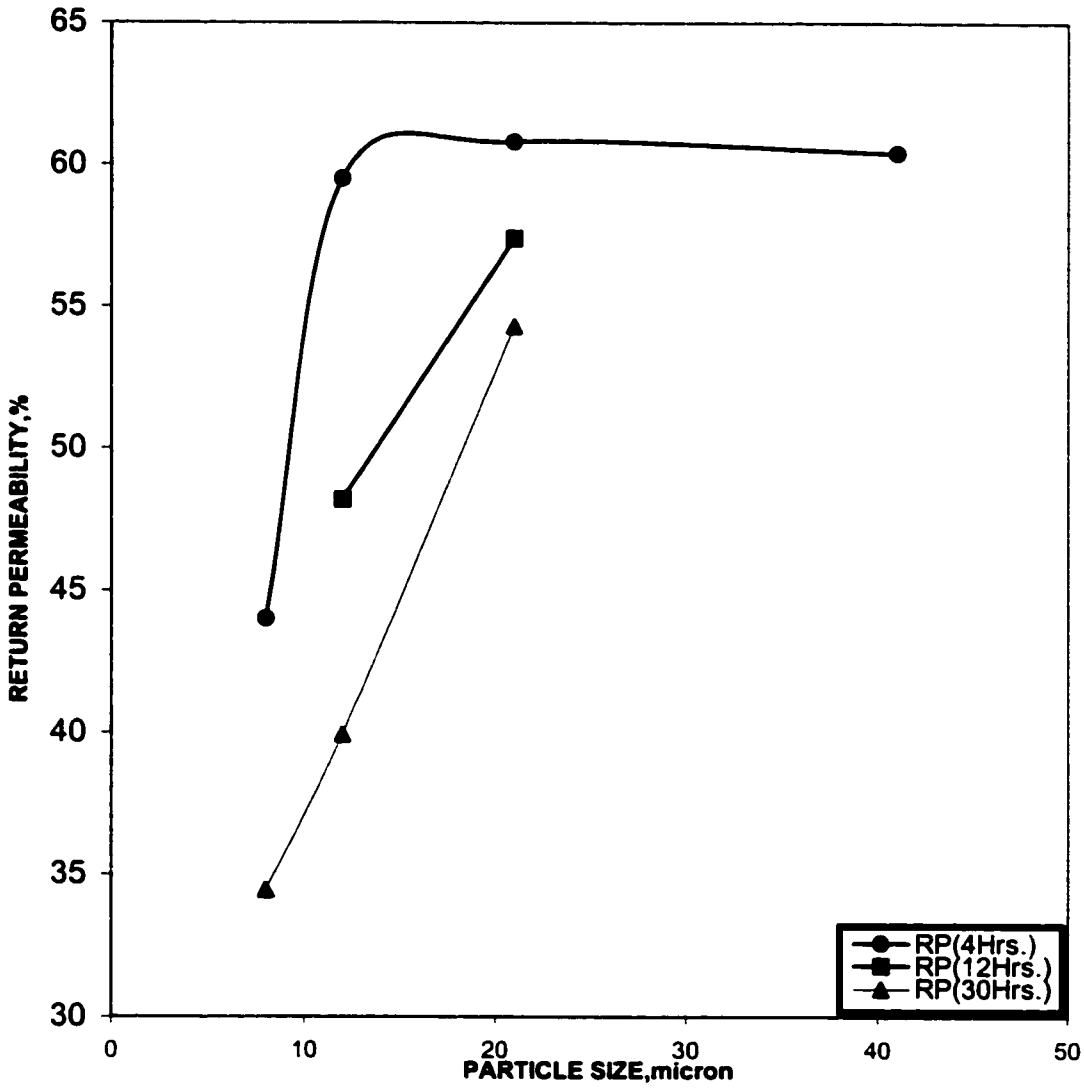

Figure 5-22: Return Permeability as function of Size of Bridging Particle($CaCO_3$)

Figure 5-24 presents the return permeability versus flooding time plot when the median particle size of the bridging additives used in the mud system was 12 microns. For the 4hours flooding time, the observed return permeability was 60%, which is much higher than the case when the median particle size in the drilling fluid system was 8microns. When the flooding time was increased to 30hours, the return permeability has reduced by 20%, or a decline in the return permeability of 0.77% per hour was observed after the 4hours flooding time.

Figure 5-25 also presents the return permeability versus flooding time when the Berea core sample was flooded with the WBM-3 mud (i.e., when the median particle size of the drilling fluid system was 21micron). After the 4 hours flooding time, the return permeability observed was 60.4%. When the flooding time was increased to 30 hours, a reduction in the return permeability was 6.1%, or in other word, a decline in the return permeability at the rate of 0.235% per hour was observed, which is lower than the case when the core sample was exposed to the WBM-2 mud.

In sizing of solids for use in the drill-in fluids and completion fluids, usually attention is given on minimizing the invasion of solids into the formation. The rule of thumb that has been mentioned earlier in this chapter ensures that sized solids do not invade the formation and cause permeability reduction. However, as shown experimentally by Ajay and Sharma [30] when only calcium carbonate particles were used, no damage was observed in the cores. Whereas the addition of a biopolymer (Xanthan

Gam); or use of Biopolymer alone induced very significant formation damage as shown in figure 5-27.

Therefore, from the above facts, it is clear that in sizing particles for drilling fluids, it is important to consider not only the invasion depth of the bridging particles but also the invasion of particulates down to colloidal sizes like the polymers. By properly sizing the particles not only to minimize the invasion depth into the formation, but also to effectively filter out the smaller polymers and other colloidal particulates, it is possible to achieve minimum formation damage.

7.2.4 Skin Factor

The pressure drop in a well per rate of flow is controlled by; the resistance of the formation, the viscosity of the fluid and the additional resistance concentrated around the well bore resulting from the drilling, completion and production operation. According to Van Everdingen [35], this additional pressure drop caused by this additional resistance is defined as skin effect, denoted by the symbol S. It was Van Everdingen [35] and William Hurst [51] who introduced the concept of skin factor to the petroleum industry. This skin effect considerably detracts from a well's capacity to produce. Hawkin's equation [46] is used to calculate skin factors based on the experimental result and an assumed wellbore radius of 0.3ft.

$$S = \left(\frac{k_e}{k_a} - 1\right) \ln\left(\frac{r_a}{r_w}\right) \qquad 5\text{-}1$$

Where K_e and K_a are permeabilities of the core before damage and the altered zone permeability after damage respectively. Wellbore and altered zone radii are denoted by r_w and r_a respectively.

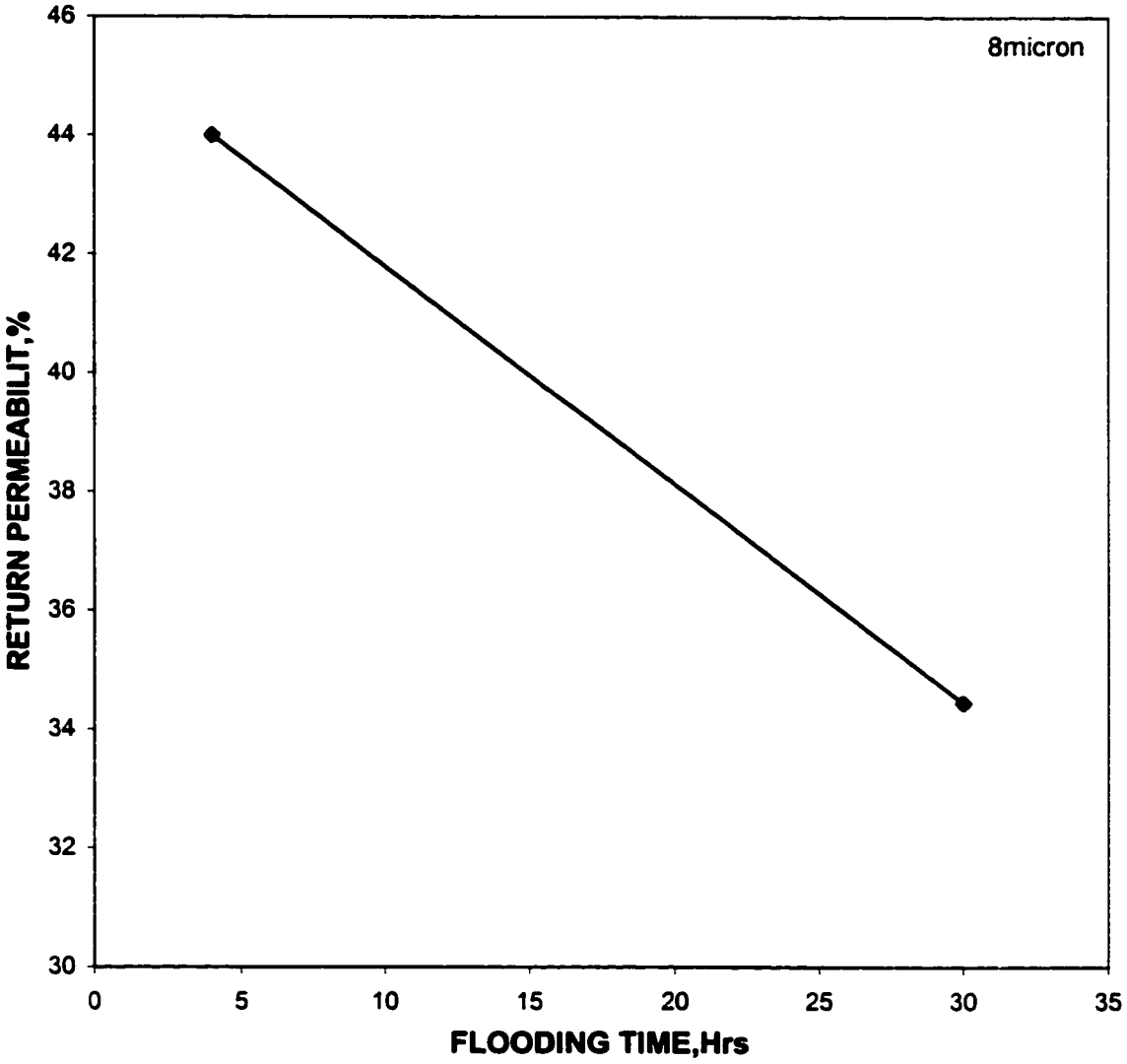

Figure 5-23: Return Permeability as function of Flooding Time (for 8micron $CaCO_3$ Bridging Additive)

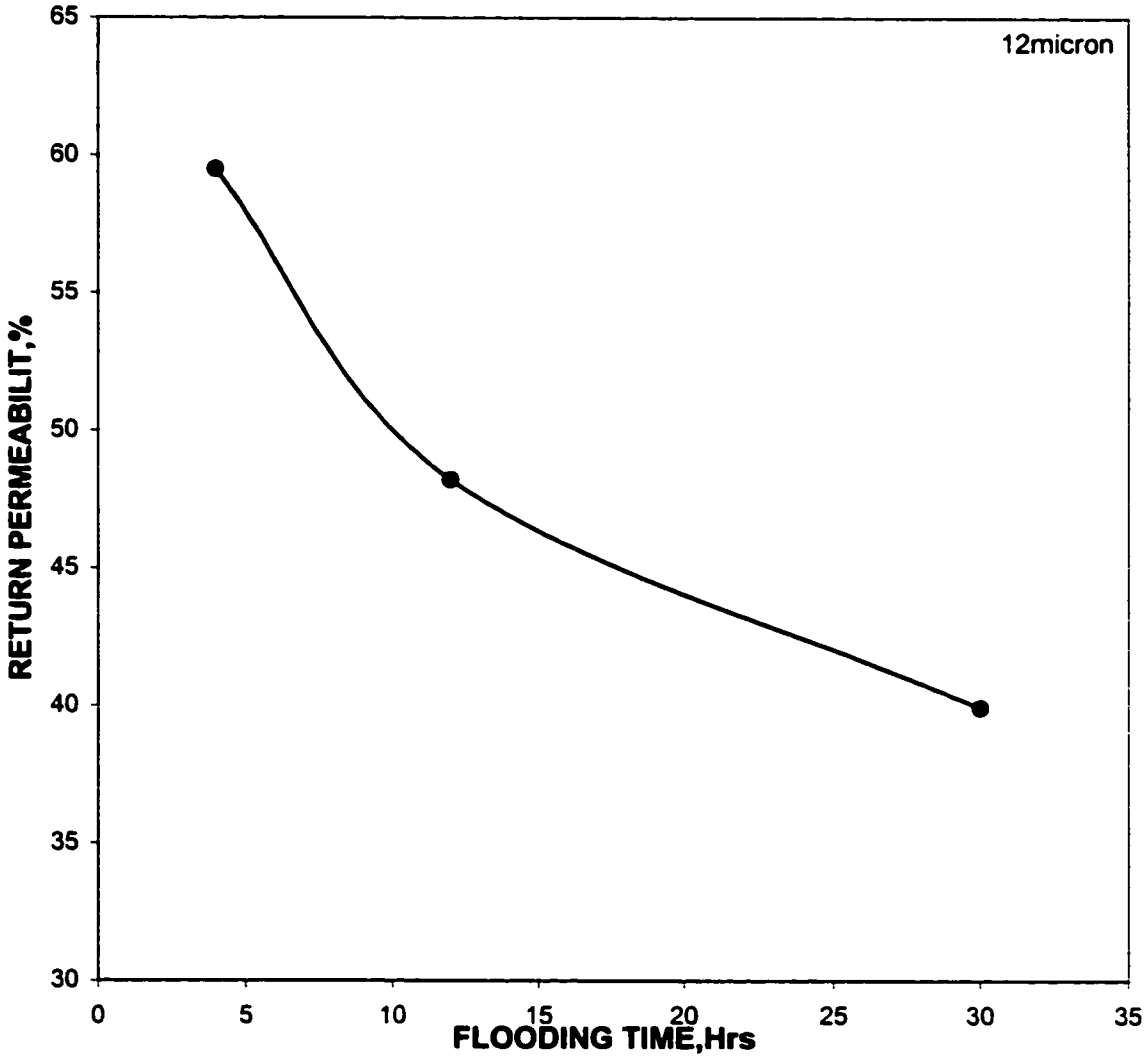

Figure 5-24: Return Permeability as function of Flooding Time (for 12micron $CaCO_3$ Bridging Additive)

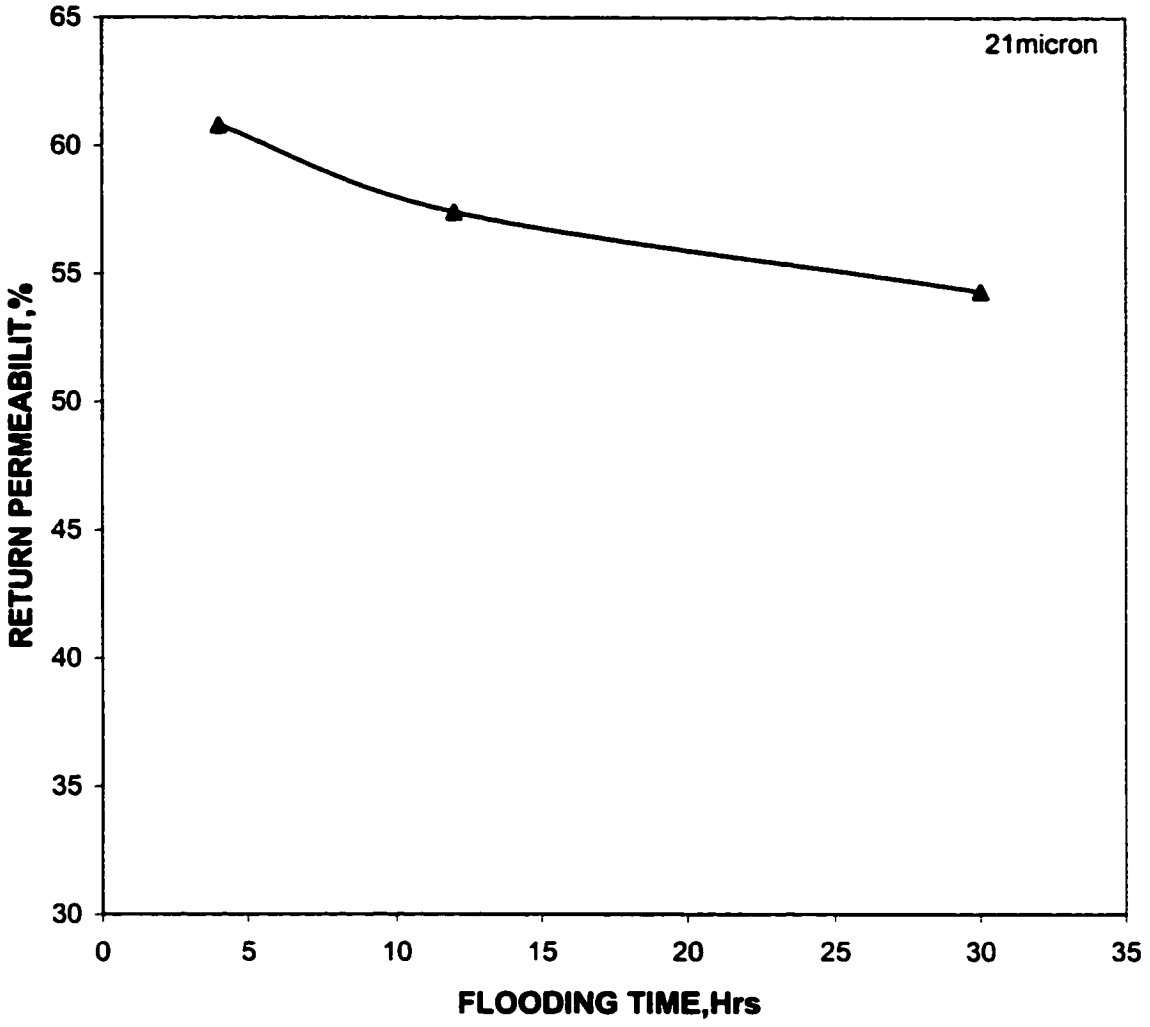

Figure 5-25: Return Permeability as function of Flooding Time (for 21micron $CaCO_3$ Bridging Additive)

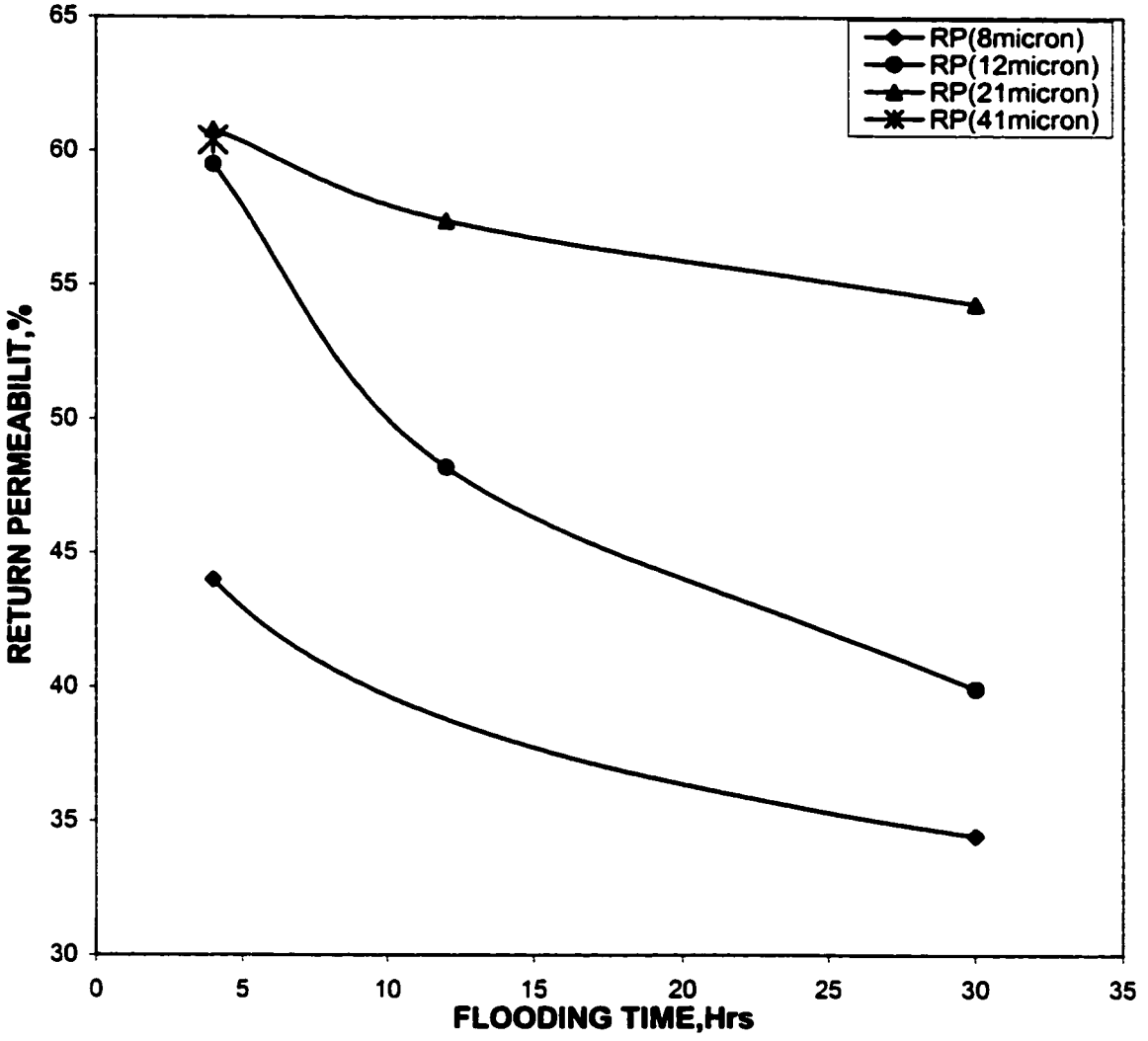

Figure 5-26: Return Permeability as function of Flooding Time

Effect of Particle size

Figure 5-28 through 5-31 presents the effect of particle size used in the polymeric water based mud system on the skin factor. It can be clearly seen from the figures that the skin factor is declining as particle size is increased. Figure 5-28 shows that when particle size is increased from 8 to 12 micron, the skin factor has dropped by about 50%. After 12 microns of the bridging additive, the influence of increasing particle size further has little effect on the skin profile.

Effect of flooding time

The effect of flooding time on the skin factor is shown in figure 5-32 through 5-35. As the exposure time of formation to the drilling fluid increases, more and more filtrates and particle will encroach deep into the formation. After back flow or during production there is portion of the porous media that is permanently occupied by these drilling fluid particles or filtrate that can cling around wall of the pore throat. These particulates or filtrate reduce the productivity of the well by further increasing the pressure drop at the well bore. Since skin factor is a function of invasion depth and return permeability, a decrease in the return permeability and an increase in the invasion depth will increase the skin factor. As flooding time increases, permeability impairment and invasion depth increases which will result in an increase of the skin factor.

Figure 5-32 shows the effect of flooding time on skin factor for the WBM-1 mud system. From the figure it can be seen that the skin factor increases with flooding time. It is also interesting to note that as particle size increases the rate of skin increment per hour of the flooding decreases. For the 8micron particle size, the rate of skin increment per hour of flooding time is 2.12. When the median size of the bridging additive in the drilling fluid system was increased to 12 and 21microns, the corresponding rate was 1.45 and 0.63 per hours of flooding time respectively.

5-2.5 Skin Distribution Along Horizontal Well

Formation damage around a horizontal well is neither radial nor uniform throughout the length of the well bore. The damage zone is expected to be a truncated cone-like shape, extending from the heel end to the toe end. The shape and distribution of damage around a horizontal well would reflect the horizontal-to-vertical permeability anisotropy and the time of exposure to the drilling fluid during the drilling operation. It is obvious why mud filtrate penetration would generate a truncated cone with larger base near the vertical section of the well. For the three XC-Polymeric water based mud system, a linear type interpolation of the skin profile is given in figure 5-36.

If we assume a 2000ft horizontal well is to be drilled and the rate of drilling is 100ft/day, then the first 100ft of the horizontal well section will be exposed to the drilling fluid filtrate invasion for 20days, the next 100 ft to 19days, and so on, until the last 100ft section to only one day of filtrate invasion. Therefore, the skin distribution along the

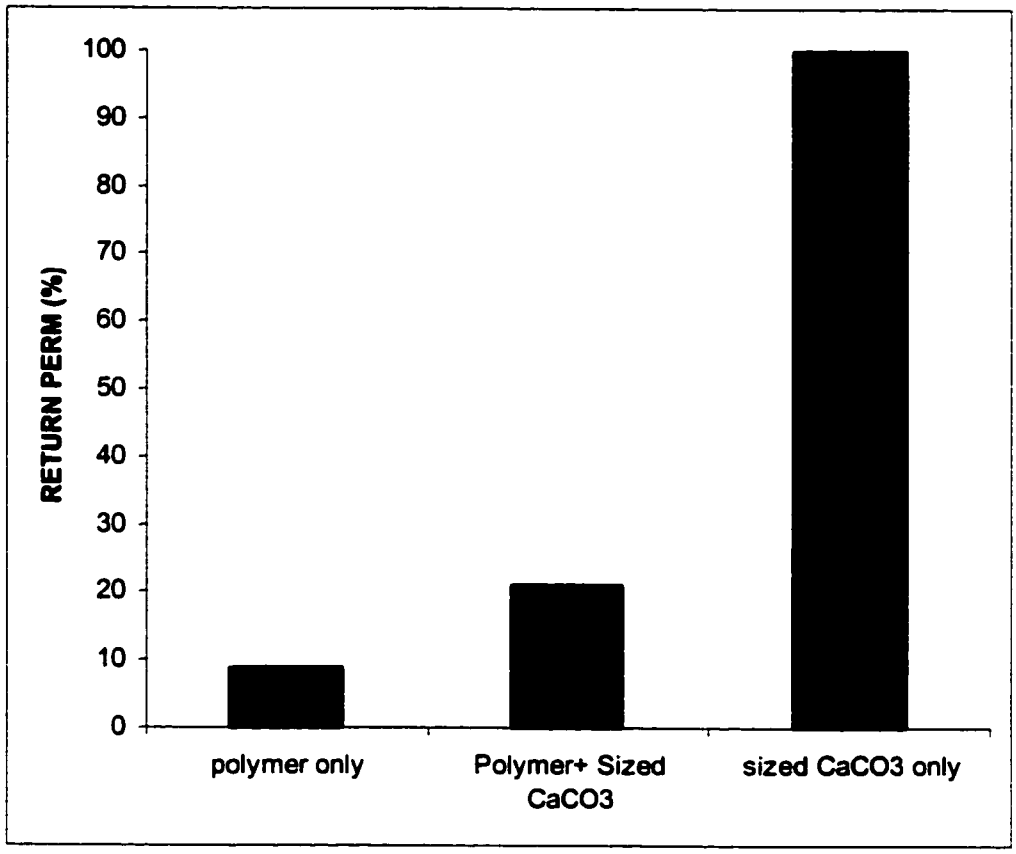

Figure 5-27: Effect of Biopolymer on permeability damage (After Sharma & Suri, 2001)

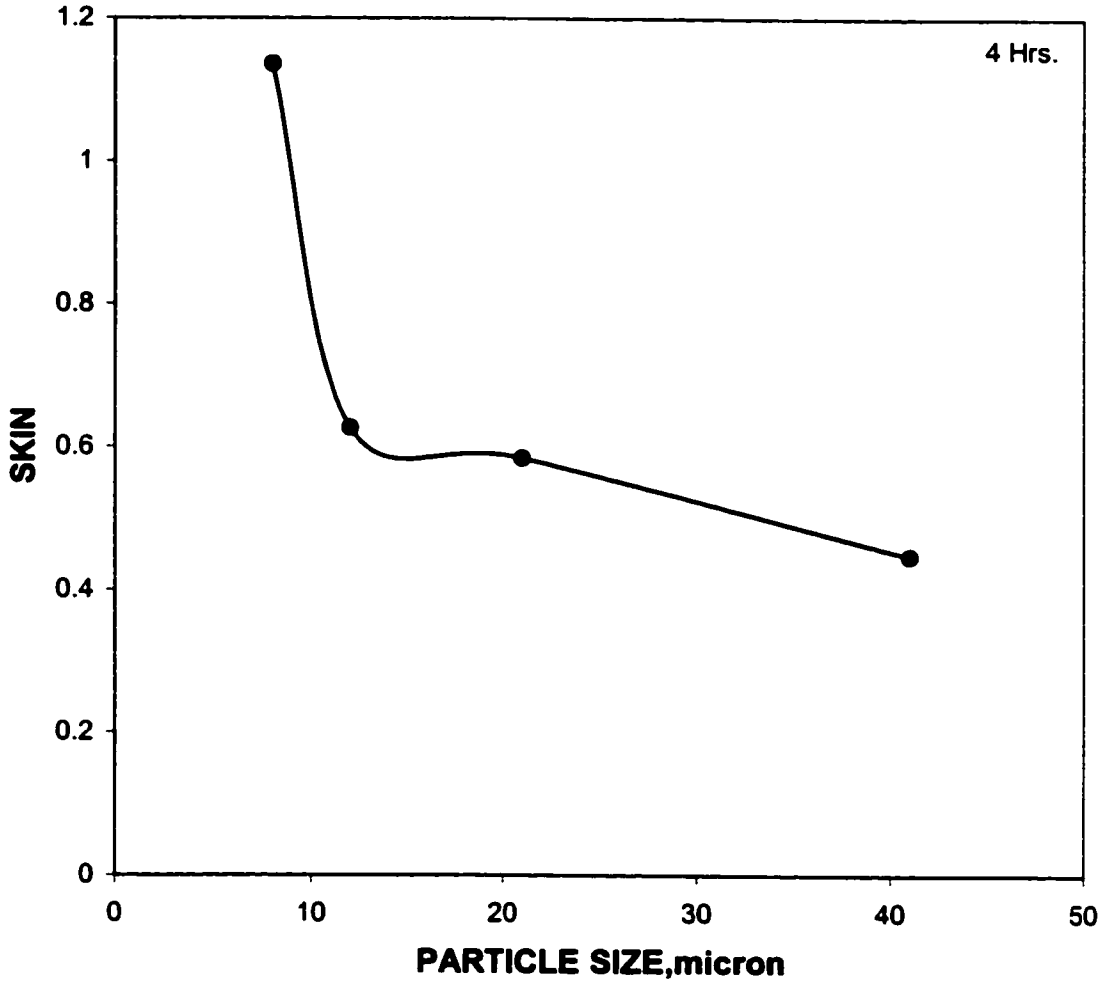

Figure 5-28: Effect of particle size used in the WBM on the skin for 4 Hrs flooding time.

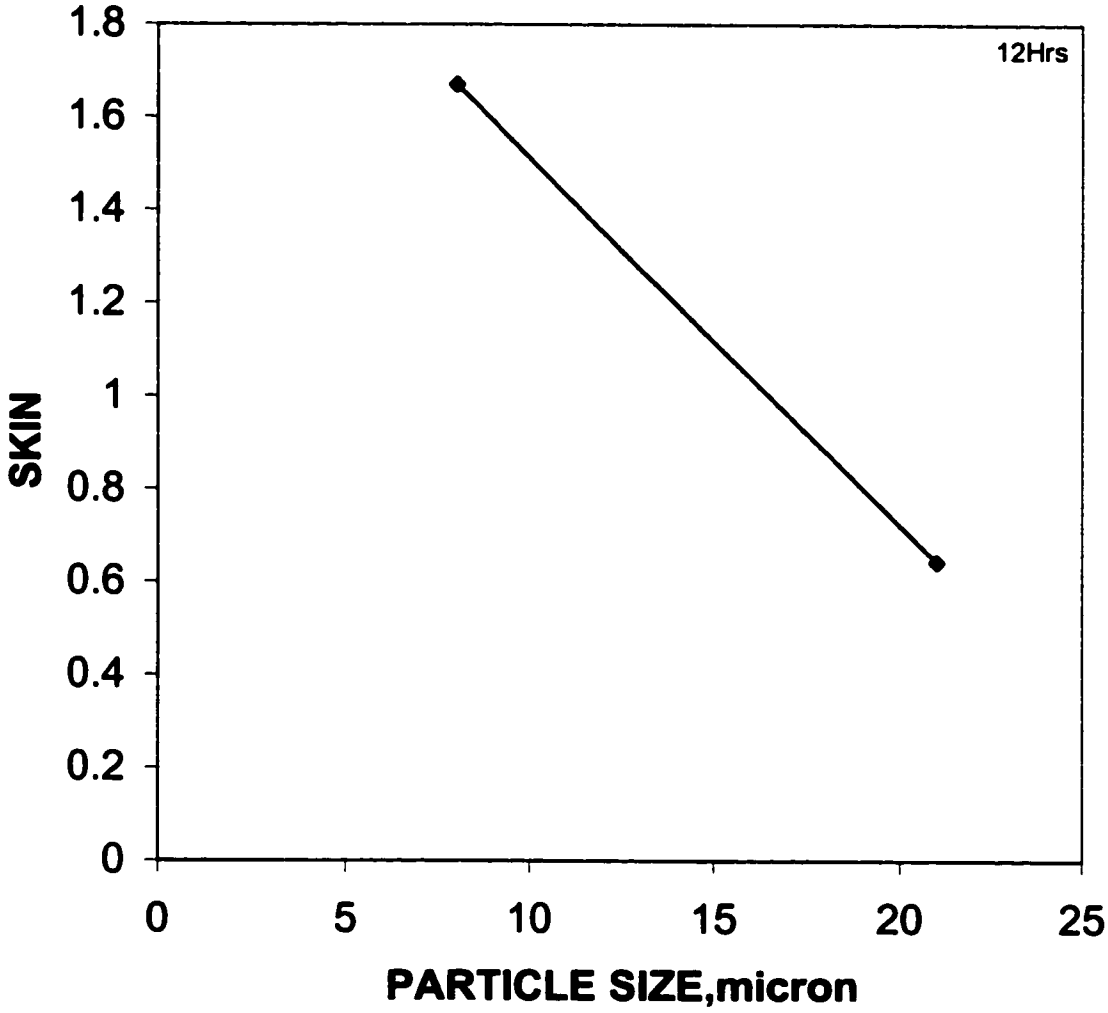

Figure 5-29: Effect of particle size used in the WBM on the skin for 12 Hrs Flooding Time.

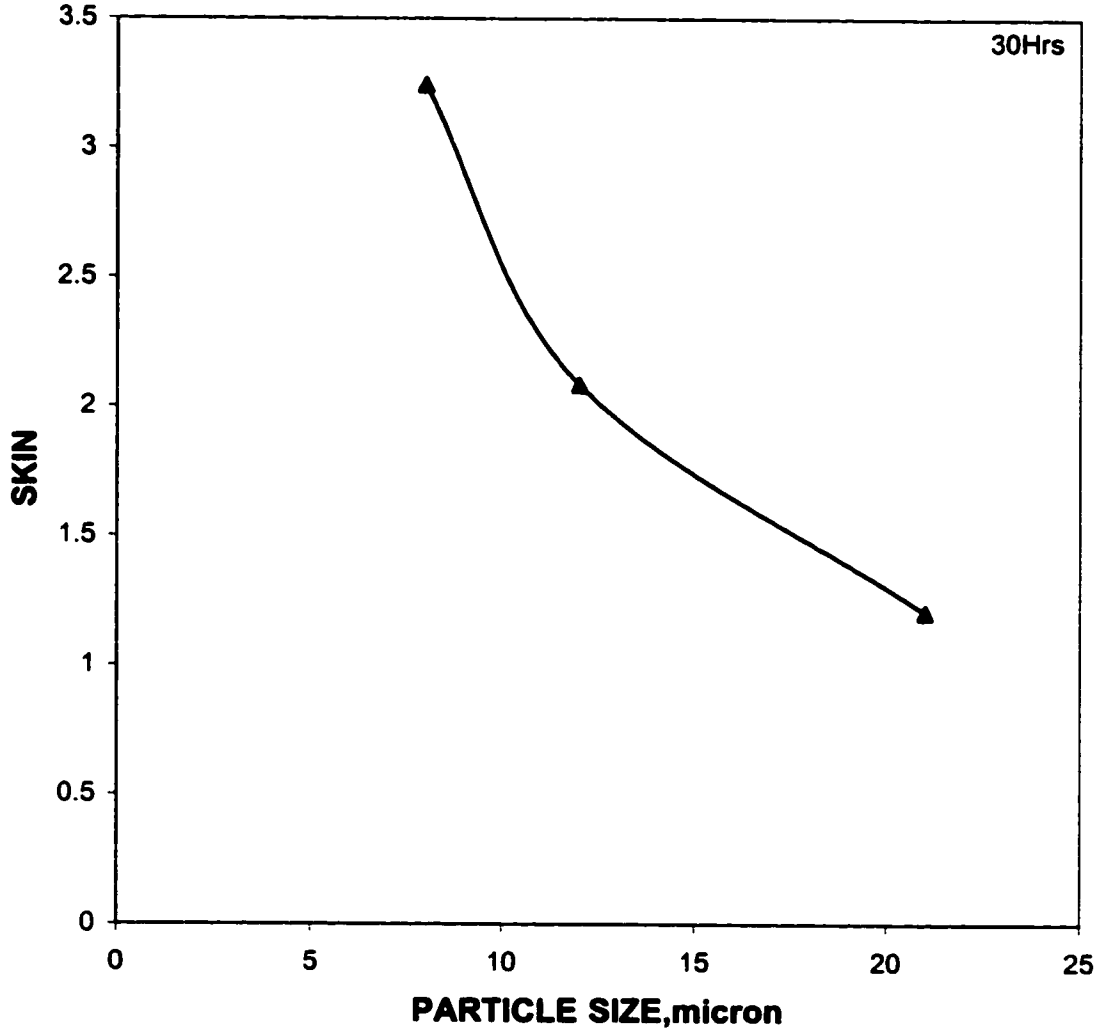

Figure 5-30:Effect of particle size used in the WBM on the skin for 30 Hrs Flooding Time.

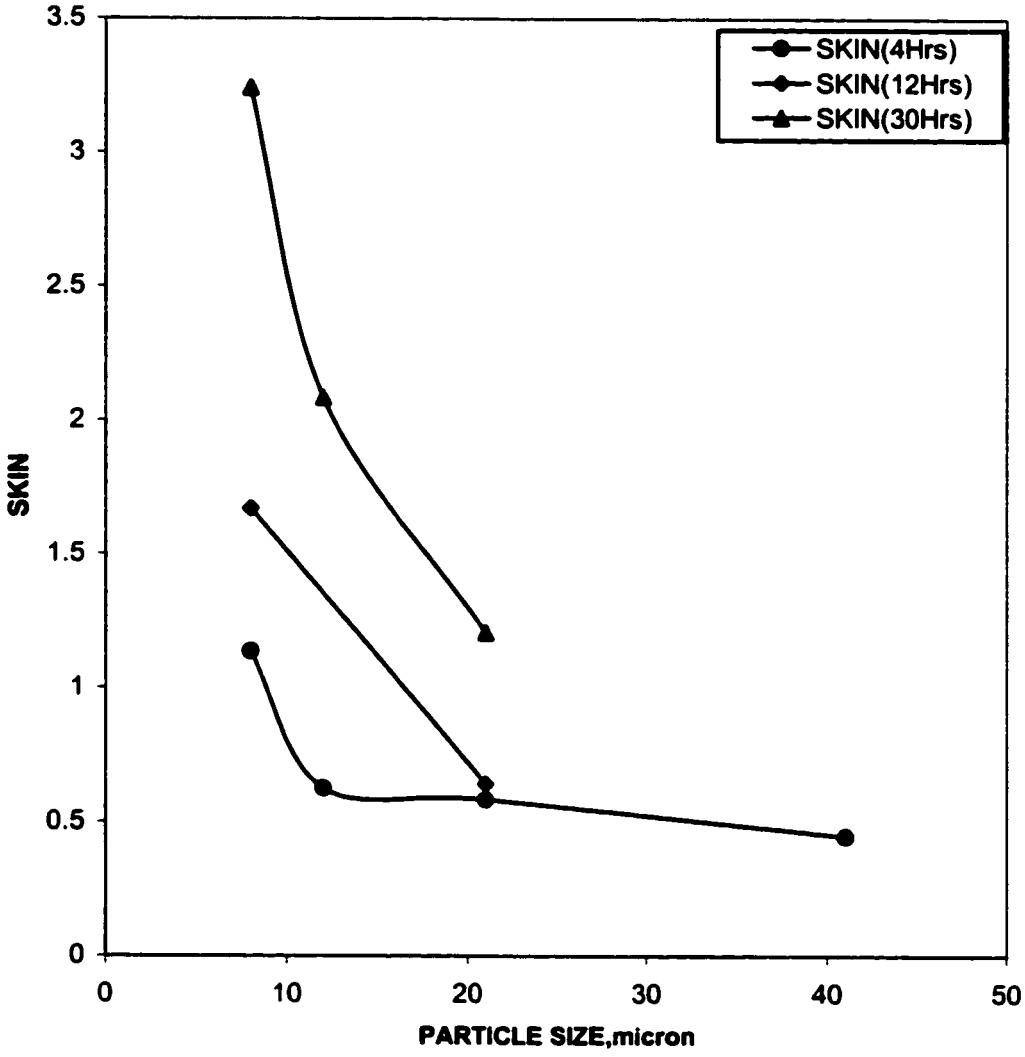

Figure 5-31: Effect of particle size used in the WBM on the skin.

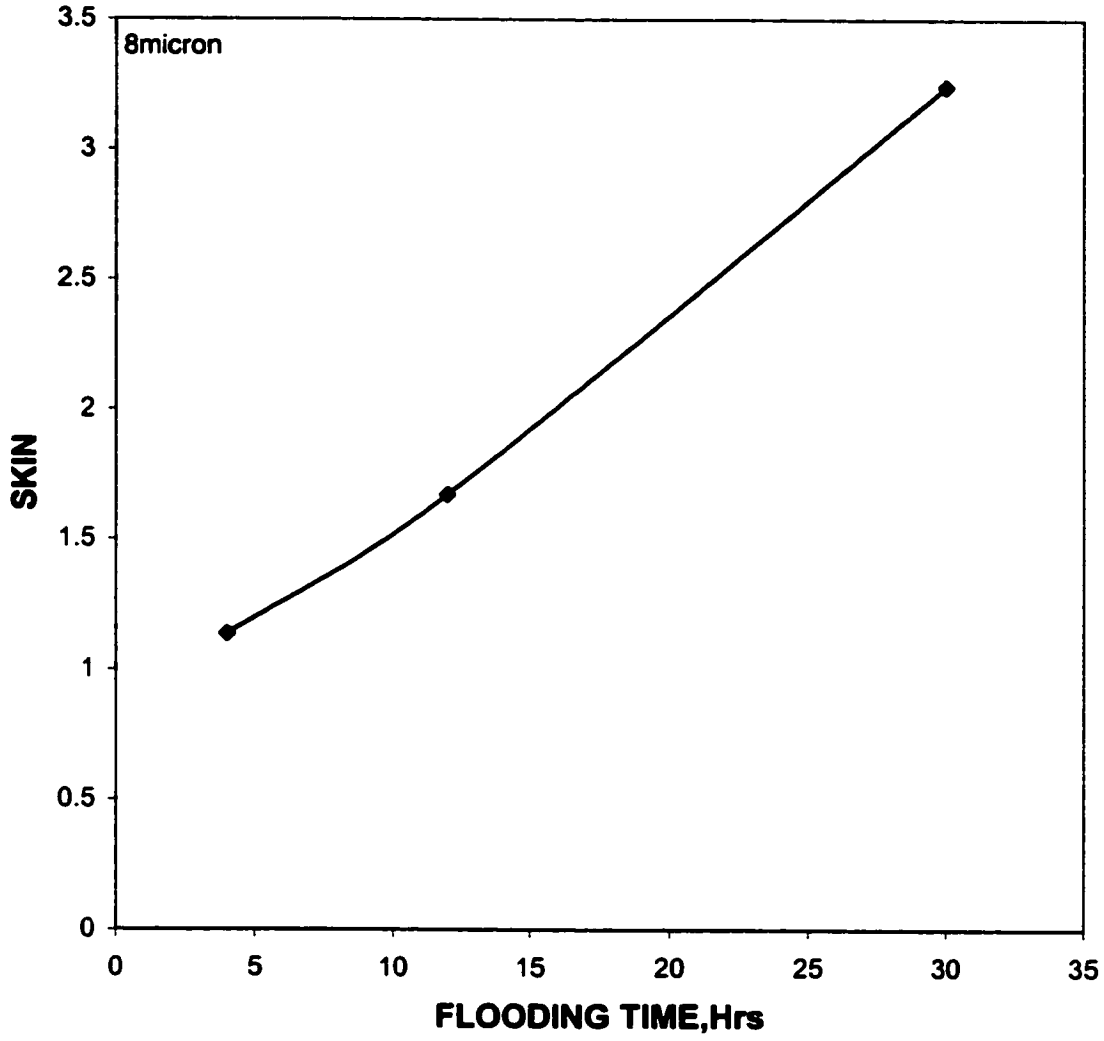

Figure 5-32: Effect of Flooding Time on the Skin for 8μ $CaCO_3$ Bridging Additive in the WBM system.

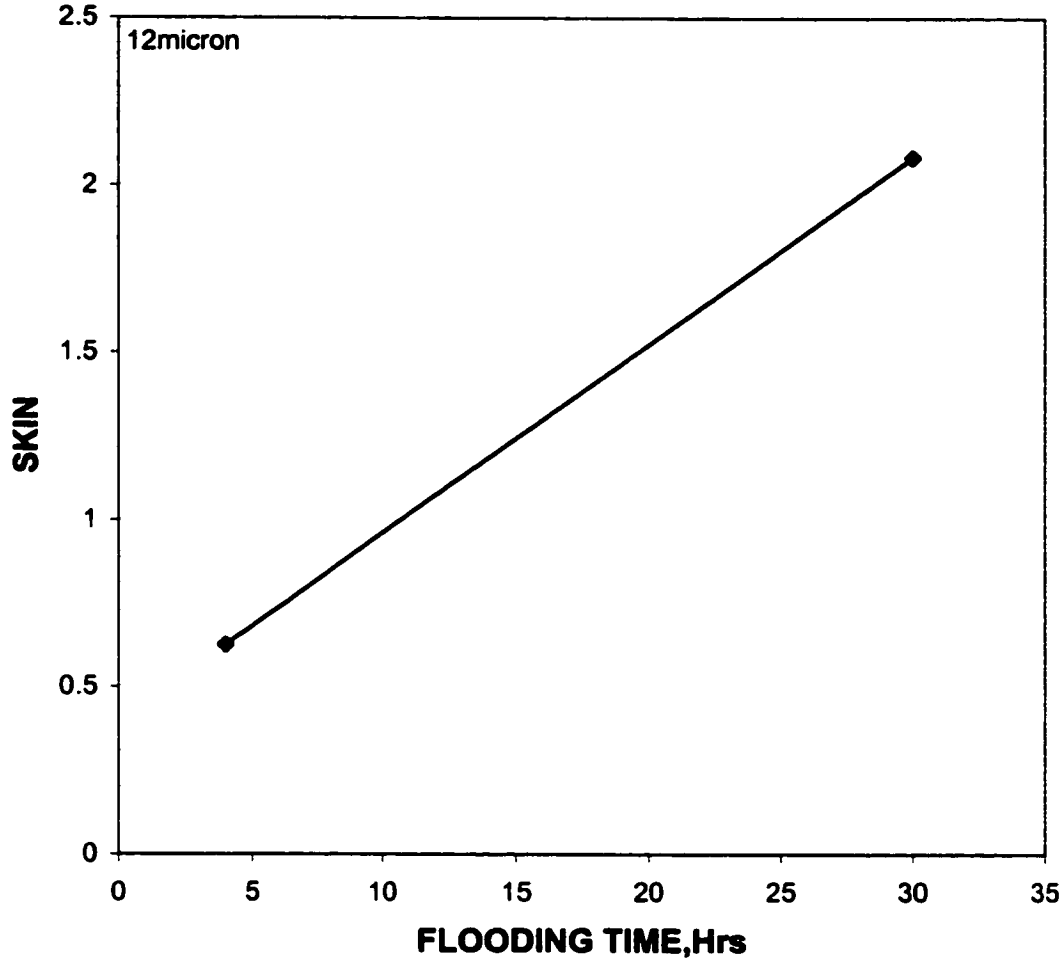

Figure 5-33: Effect of Flooding Time on the Skin for 12μ $CaCO_3$ Bridging Additive in the WBM system.

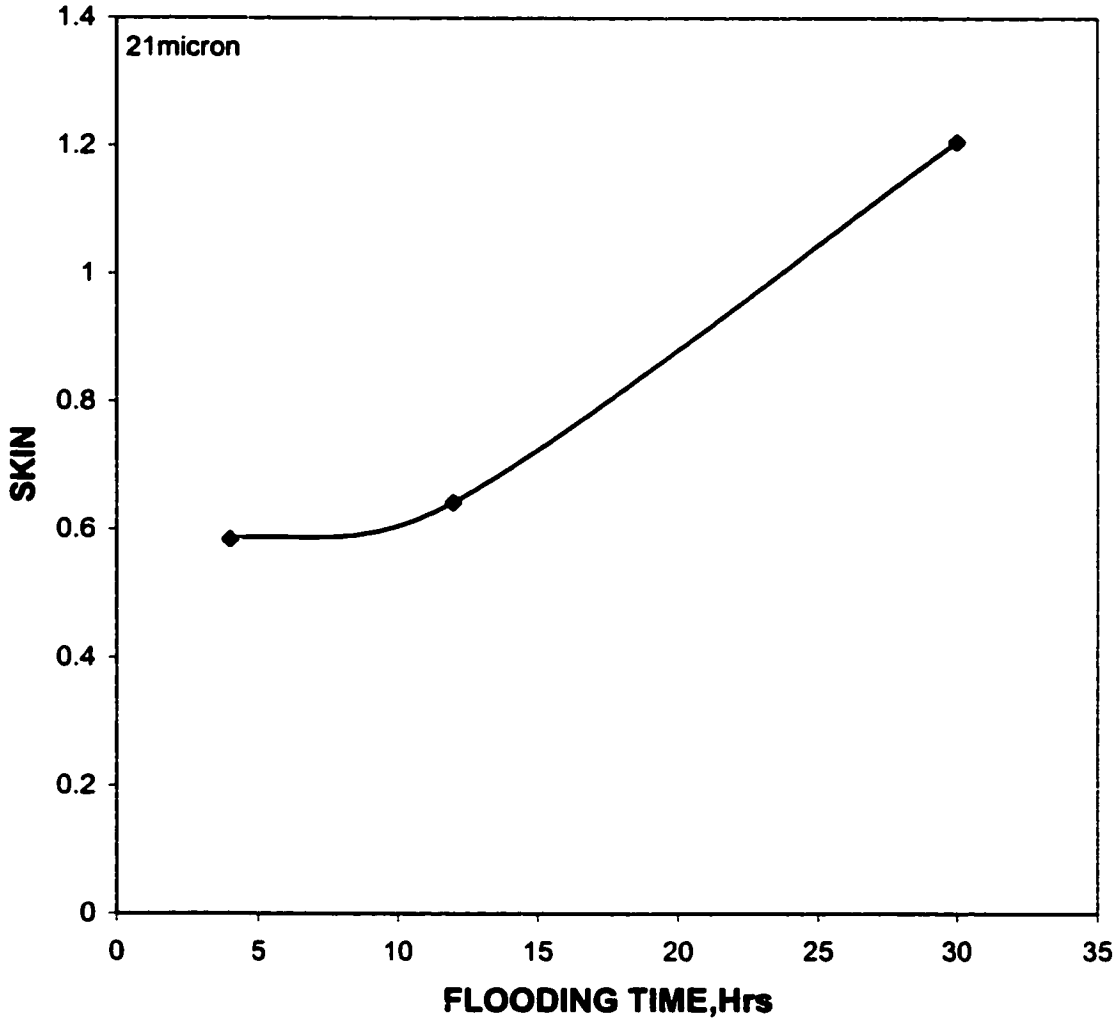

Figure 5-34: Effect of Flooding Time on the Skin for 21μ $CaCO_3$ Bridging Additive in the WBM system.

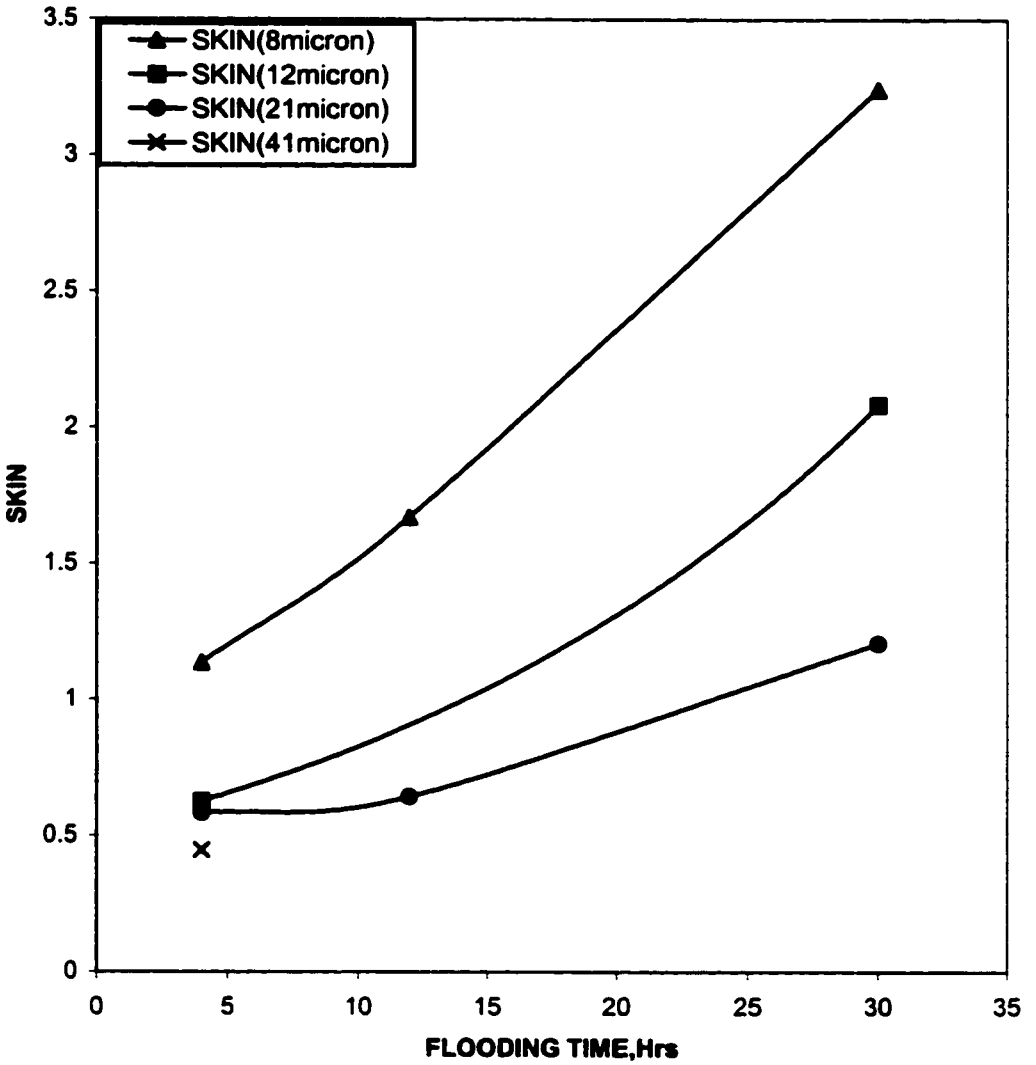

Figure 5-35: Effect of Flooding Time on the Skin Factor.

horizontal wellbore when the formation around the wellbore was exposed to the water-based mud system can be calculated based on the following equation:

$$Skin(x) = 24 * Slope * \frac{(L-x)}{ROP} + \text{int}\,ercept \qquad 5\text{-}2$$

Where Skin (x) is the skin factor at a certain distance x from the heel side of the wellbore, L is the horizontal wellbore length, slope and intercept are the slope and intercept of the linear type interpolation of the skin profile for the three mud systems at 100psi overbalance as shown in figure 3-37; and ROP is rate of penetration. In our case ROP is assumed to be 100ft/day.

Figure 5-37 presents the expected skin distribution along the horizontal wellbore for the 2000ft horizontal well length when it was drilled with the three types of drilling fluid at an overbalance pressure of 100psi.

Based on equation 5-2 or from figure 5-37, when the horizontal well was drilled using the XC-Polymeric water based mud: WBM-1, WBM-2 and WBM-3, the expected skin factor at the heel end is about 41, 28 and 13 respectively. Toward the toe end, since the time the drilling fluid remains in contact with the formation decreases, the corresponding skin factor will also declines. At the toe end skin factor is negligibly small, which is equal to the intercept of the equation 5-2 or values of the intercept given in figure 5-36.

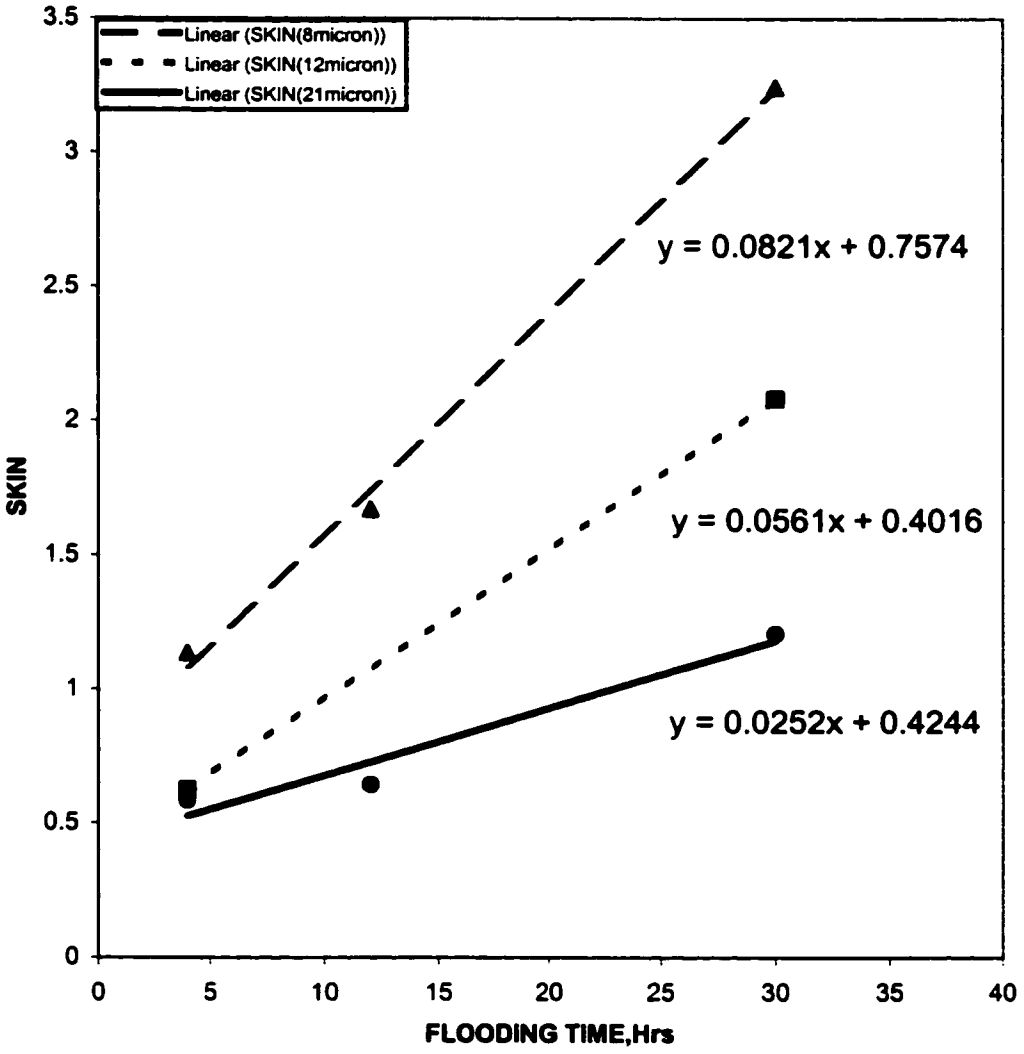

Figure 5-36: Linear-type interpolation for the skin profile at 100psi overbalance when the core sample was flooded with XC-Polymeric Water Based mud WBM-1, WBM-2 and WBM-3.

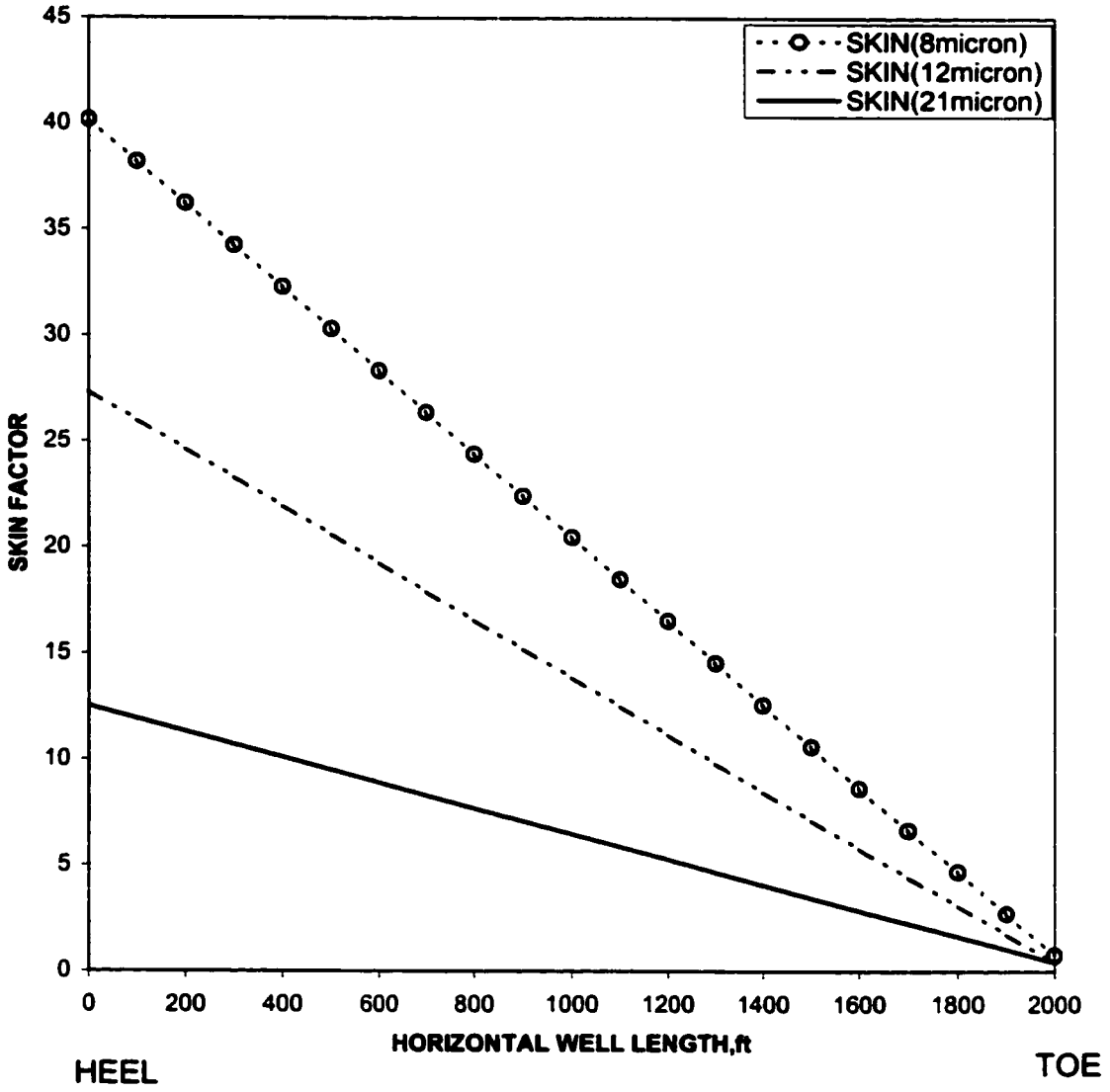

Figure: 5-37: Skin profile along the horizontal wellbore for the three types of drilling fluid system under 100psi overbalance

CHAPTER 6

CONCLUSION AND RECOMMENDATION

6-1 CONCLUSION

In this study, a Leak-Off experiment was conducted to investigate the impact of calcium carbonate additive particles size and flooding time on the formation damage. A new ultrasonic technique, which is a non-destructive method, was implemented to measure the corresponding invasion depth in Berea core samples. Four different sizes of $CaCO_3$ samples were used as bridging additives to prepare polymeric water based mud system. We also made an effort to apply our experimental result in a horizontal well under specific condition. Based on the result presented, the following conclusions can be drawn.

- The invasion depth was found to vary as a function of the $CaCO_3$ particulate size used in the drilling fluid and the contact time with the formation.

- As particle size in the XC-Polymeric water based mud system was increased, the invasion depth decreases. More than 40% decrease of an invasion depth was

observed by increasing the median particle size of the bridging additive from 8 to 12 micron. This could be related to Abrams rule of thumb which states that for a better formation protection the median particle size of the bridging additives used in the polymeric water based mud system should be slightly greater than $1/3^{rd}$ of the median pore throat diameter.

- As flooding time was increased, permeability impairment and invasion depth was observed to increase, which resulted in an increase of the skin factor.

- The rate of invasion by drilling fluid filtrates and particles is observed to decrease as flooding time increases. The reason for the largest rate of invasion for the first 4 hours flooding is due to the absence of a well-established, low permeable filter cake to protect the formation from invasion by filtrates and drilling fluid particles.

- In sizing particles in the drilling fluids, it is important to consider not only the invasion of particles, but also the invasion of particulates down to the colloidal sizes like the polymers.

- It is possible to achieve minimum formation impairment by properly sizing the particles, not only to minimize the invasion depth into the formation, but also to effectively filter out the smaller colloidal particulates like the polymers in the drilling fluid system.

6-2 RECOMMENDATION

For the range of median particle size used in the drilling fluid system, our result generally shows an increase in the return permeability and a decrease in an invasion depth with increase in the particle size. The range of the particle size studied may not be sufficient enough to generalize the claim of lower invasion depth or higher return permeability with larger particle size. Therefore, more investigation in recommended in order to determin as to what will happen if we further increase the particle size without affecting the rheology of the drilling fluid.

NOMENCLATURE

C(h,t)	Concentration of particles in suspension in the liquid at height, h and time t
D	Diameter of particles, micron
d	diameter of the Berea core, cm
F_b	Buoyant force, dyne
F_d	Drag force, dyne
F_g	Gravitational force, dyne
k_e	Permeability of the core sample before damage, md
k_a	Altered zone permeability, md
L	Length of the horizontal well,ft
m	Particles mass,gm
m_0	mass of suspended particlesat time t=0, gm
m_s	Mass of solids in volume element, V_f of the fluids
P_c	Capillary pressure, dynes/cm^2
S	Skin factor
ROP	rate of penetration, ft/day
r_a	Altered zone radius, ft
r_w	Wellbore radius, ft
V	Settling velocity, cm/sec
V_s	Sloids volume, cc
V_f	Liquid volume
W_l	weight of berea core before saturation, gm

W_2 weight of Berea core after saturation,gm

x distance along the horizontal well from heel end, ft

μ_f Fluid viscosity

θ_{wa} contact angle between brine and oil

σ_{wa} Interfacial tension between particle and water

β Vertical to horizontal permeability anisotropy

ϕ Porosity of Berea core, fraction

ρ_f Fluids density

ρ_s Particles density

ρ Density of brine, gm/cc

Δt the time for the ultrasonic velocity takes to traverse across the core sample, micro-second

REFERENCES

[1] **Joao Queiroz and Renato L. dos Santos:** " Evaluation of a Damaged Zone Caused by Water-Based Polymeric drill-in-fluid",SPE#58742, presented at International Symposium on Formation damage Control held in Lafayette, Louisiana 23-24 February 2000.

[2] **Glenn,E.E. and Slusser, M.L.**: "Factors Affecting Well Productivity-I. Drilling Fluid Filtration", Drilling & Production Practice, API 103-10, 1957

[3] **A. Abrams, William:** "Mud Design To Minimize Rock Impairment Due To Particle Invasion", SPE 5713, JPT, May 1977.

[4] **C. Gruebeck and R.E. Collins**: " Entrainment and Deposition of Fine Particles in PorousMedia", October 1982.

[5] **Claus Marx, S.S. Rahman:** " Evaluation of Formation Damage Caused by Drilling Fluid, Especially in Pressure Reduced Formation" , JPT, Nov 1987.

[6] **S.D. Joshi**: " A Review of Horizontal Well and Drainhole Technology", 62nd Annual Technical Conference and Exhibition of SPE Engineers, Dallas, TX, 27-30 September 1987.

[7] **S.D. Joshi**: " Augmentation of Well Productivity With Slant and Horizontal Wells", JPE,June 1988

[8] **Gernard Renard, J.M. Dupuy:** " Formation Damage Effect on Horizontal Well Flow Efficiency", JPT, July 1991.

[9] **S.S. Rahman, C. Marx:** "Laboratory Evaluation of Formation Damage caused by Drilling Fluids and Cement Slurry", JCPT Nov-Dec 1991.

[10] **Reza Ghofrani and M.A. Mazeel Alboudi**: " Damage Caused by Clay Based and Clay-Free Inhibitive Fluids in Sandstone Formations", SPE 23815, SPE International Symposium on Formation Damage Control, Lafayette, Louisiana, 26-27 Feb. 1992.

[11] **Abdul R. Ismail, James M. Peden and Azmi M. Arshad:** " The Effect of Solids Concentration and Formation Characteristics on Formation Damage and Permeability Recovery", SPE 28762, Asia Pacific Oil & Gas Conference , Melbourne, Australia, 7-10 November,1994.

[12] **Jose Tova,Intevep S.A. ,J.J. Lummus, D.S. Sarma and Ali Pilehvari:** "Formation Damage Studies on Reservoir Rocks Using Water-Base and Oil-Base Muds", SPE#27349, presented at SPE International Symposium on Formation Damage Control held in Lafayette, Louisiana, 7-10 February,1994.

[13] **N.G. Gruber, K.L. Adair:** " New Laboratory Procedures for Evaluation of Drilling Induced Formation Damage and Horizontal Well Performance", JCPT May 1995.

[14] **D. Langeron, J. F. Argillier:** " An Integration Experimental Approach for Evaluating Formation Damage Due to Drilling and Completion Fluids", SPE-30089, European Formation Damage Conference, Hague, Netherland, 15-16 May' 1995.

[15] **Yidan Li, Elisabeth Rosenberg and J.F. Arguillier**: " Correlation Between Filter Cake Structure and Filtration Properties of Model Drilling Fluids", presented for the SPE Int'l symposium on oilfield chemistry held in San Antonio,TX, U.S.A., 14-17 February 1995.

[16] **Jack D. Lynn:** "Evaluation of Drilling Fluids Using a Closed Loop Dynamic Slurry Circulation System",SPE#29833, presented at the SPE Middle East Oil Show ,Bahrain 11-14 March 1995.

[17] **R. Ghofrani, Y. Zhang and V. Boach:** " New Method in Evaluating the Formation Damage in Laboratory Investigations", SPE 35151, International Symposium on Formation Damage Control, Lafayette, Louisiana, 14-15 Feb. 1996.

[18] **D.B. Burnett and R.M. Hodge:** " Laboratory and Field Evaluation of the Role of Drill Solids in Formation Damage and Reduced Horizontal Well Productivity", SPE 37125, SPE International Conference on Horizontal Well Technology held in Calgary, Canada, 18-20 November1996.

[19] **J. Yan, G. Jiang & X. Wu:** " Evaluation of Formation Damage Caused by Drilling & Completion Fluids in Horizontal Wells", the JCPT ,May 1997, vol.36, Issue # 5

[20] **S.B. Toulekima, D.D. Mamora and R.A. Wattenbarger:** " The Effect of Skin Location, Production Interval and Permeability on Performance of Horizontal Wells", ", Journal of Petroleum Science & Engineering, Vol.2, Issue No. 1 pp. 63-69, February 1997.

[21] **S.T. Saleh, R. Rustum, W.El-Rabaa and M.R. Islam:** " Formation Damage With a Horizontal Wellbore Model", Journal of Petroleum Science & Engineering, Vol.2, Issue No. 1 pp. 87-99, February 1997.

[22] **Jack D. Lynn:** " Drilling Damage Associated with Water-Based Fluids", Lab Research and Development Center, Dhahran, Saudi Arabia, 1998.

[23] **T. Azizi, H. Chen and S.S. Rahman:** " Management of Wellbore Instability and Formation Damage by Improved Drilling Mud Design", IADC/SPE#47786, presented at the 1998 IADC/SPE Asia Pacific Drilling Confernce held in Jakarta, Indonesia, 7-9 September 1998.

[24] **D.G. Longeron, J. Alfenore and G.P. Guillaume**: " Drilling Fluids and Permeability: Performance Evaluation of Various Mud Formulations", SPE#48988, presented at the 1998 SPE Annual Technical Conference and Exhibition, held in New Orleans, Louisiana, 27-30 September,1998.

[25] **J.D. Lynn and H.A. Nasr-El-Din:** " Formation Damage Associated with Water-Based Drilling Fluids and Emulsified Acid Study" SPE# 54718, presented at the 1999 SPE European Formation Damage Conference held in The Hague, The Netherlands, 31 May-1June 1999.

[26] **D.G. Longeron, J. Alfenore, N. Salehi and S. Saintpere:** " Experimental

Approach to Characterize Drilling Mud Invasion, Formation Damage and Cleanup Efficiency in Horizontal Wells with Openhole Completions", SPE #58737, presented at International Symposium on Formation damage Control held in Lafayette, Louisiana 23-24 February 2000.

[27] **Mike R. Chambers, Darrell B. Hebert and Chris E. Shuchart**: " Successful Application of Oil-Based Drilling Fluids in Subsea Horizontal, Gravel-packed Wells in West Africa", SPE# 58743, presented at International symposium on Formation damage Control held in Lafayette, Louisiana 23-24 February 2000.

[28] **Helio Santos and J. Queiroz:** " How Effective is Underbalanced Drilling at Preventing Formation Damage?", SPE#58739, presented at International symposium on Formation damage Control held in Lafayette, Louisiana 23-24 February 2000.

[29] **M.T. Byrne, I.S.P. Spark, I.T.M Patey and A.J. Twynam**: " A Laboratory Drilling Formation Study Utilizing Cryogenic SEM Techniques", SPE#58738, presented at International symposium on Formation damage Control held in Lafayette, Louisiana 23-24 February 2000.

[30] **Ajay Suri and Mukul M. Sharma**: " Strategies for Sizing Particle Drilling and Completion Fluids" SPE# 68964 Prepared for presentation at the European Formation Damage Conference to be held in The Hague, The Netherland, from 21-22 May 2001.

[31] **M.A. Khan, S.Z. Jilani, H. Menouar and A.A. Al-Majed**: "A Non-Destructive Method for Mapping Formation Damage", Ultrasonics 39, pp. 321-328, 2001.

[32] **Di Jiao and M.M. Sharma**: " Formation Damage Due to Static and Dynamic Filtration of Water-Based Muds",SPE#23823, presented at the SPE Int'l Symposium on Formation Damage Control held in Lafayette, Louisiana, February 26-27,1992.

[33] **J.W. Dobson, P.D. Kayga, J.C. Harisson and R.A. Rose**: " Drill-In Fluid Particle Sizing; The Next Generation", Brineadd Inc.

[34] **Hands, N., Kowbel, K. Maikranz, S., and Nouris,R.**: 'Drill-in Fluid reduces Formation Damage, Increases Production Rates," Oil and Gas Journal, July 13,1998, 96:28

[35] **A.F. Van Everdingen**: " The Skin Effect and Its Influence on The Productivity Capacity of a Well", pp. 171 –176, AIME Vol. 198, 1953

[36] **Murray F. Hawkin**: " A NOTE on the SKIN EFFECT", PP 356-357, AIME, Vol. 207,July23, 1956.

[37] **Roland F. Krueger:** " An Overview of Formation Damage and Well Productivity in Oilfield Operation", SPE 10029, JPT, February 1986.

[38] **D. Brant Bennion, F. Brent Thomas and Douglas W. Bennion**: " Effective Laboratory Coreflood Tests To Evaluate and Minimize Formation Damage in Horizontal Well" presented in the 3rd Int'l Conference on horizontal well Technology, November 12-14, 1991, Houston, TX.

[39] **A. Hayadavoudi and A. Ghalambor**: " Controlling Formation Damage Caused by Kaolinite Clay Minerals: Part II", SPE#39464, presented at the 1998 SPE Int'l Symposium on Formation Damage Control held in Lafayette, Louisiana, 18-19 February,1998.

[40] **A. Hayadavoudi and A. Ghalambor**: " Controlling Formation Damage Caused by Kaolinite Clay Minerals: Part I", SPE#31118, presented at the 1996 SPE Int'l Symposium on Formation Damage Control held in Lafayette, Louisiana, 14-15 February,1996.

[41] **D.B. Bennion, F.B. Thomas, D.W. Bennion and R.F. Bietz**: " Fluid Design to Minimize Invasive Damage in Horizontal Wells", JCPT, November 1996.

[42] **T.P. Frick and M.J. Economides**: "Horizontal Well Damage Characterization and Removal" SPE# 21795,SPE Production and Facilities, February 1993.

[43] A Technical Index by Brine-Add Fluids Ltd, " Technical Information".

[44] **Jiao, D.; Sharma, M. M.**: " Mechanism of Cake Buildup in Crossflow Filtration of Colloidal Suspensions, J. Colloidal Sci. Vol. 162, No. 2, pp. 454-462, Feb. 1994.

[45] **Johannes K.F.**: " Polymers as Oilfield Chemicals: Fluid Loss Additives", An Online Magazine of the VDE/SPE Student Chapter, at the University of Leoben.

[46] SEM/EDS technique description by the Museum of Science and the Science Learning Network.

[47] **P. Permadi, W. Wibowo**: "Effects of Non-Uniform Skin Distribution on Horizontal Well Inflow Performance", SPE#68952, SPE Formation Damage Conference, The Hague, The Netherlands, 21-22 May 2001.

[48] **K. Leerloojier, C.A.T. Kuijvenhoven and P.A. Francis:** " Filtration control, Mud Design and Well Productivity", SPE 31079, SPE Formation Damage Control Symposium, Lafayette, LA,USA, 14-15 February 1996.

[49] **Kroell, E. and Spoeker, H.F.**: " Slimhole Completion and Production-What To Do After We Drilled The Well", paper IADC/SPE 35129, presented at the SPE/IADC Drilling Conference, New Orleans, March 12-15,1996.

[50] Manual for MICROSCAN II PARTICLE SYZE ANALYZER by QUANTACHROME CORPORATION.

[51] **William Hurst**: " Establishment of the Skin Effect and its impediment to fluidflow into a wellbore", The Petroleum Engineerting, October 1953.

[52] **D. Brant Bennion, F. Brent Thomas, Ronald F. Bietz:** " Formation Damage and Horizontal Wells- A Productivity Killer?", SPE 37138, 2nd International Conference on Horizontal well Technology, Calgary, Alberta, Canada, 18-20 November, 1996.

[53] **T. Beatty, D.B. Bennion, B. Hebner and R. Hiscock**: " Minimizing formation Damage in Horizontal Wells: Laboratory and Field Case Studies.", CIM 1993, Annual Technical Conference held in Calgary, 1993

[54] **R.A. Novey**: " Pressure Drop in Horizontal Wells: Can They Be Ignored?", 67th Annual Technical Conference and Exhibition, Washington DC, October 1992.

[55] **J.M. Peden, K.G. Arthur and Margarita:** " The Analysis of Filtration Under Dynamic and Static Conditions",SPE 12503, Formation Damage Control Symposium, Bakersfield, CA, 13-14 February 1984.

APPENDICES

APPENDIX A

FORMATION DAMAGE

A-1 COMPARISON OF FORMATION DAMAGE IN HORIZONTAL AND VERTICAL WELLS

Horizontal wells are much more susceptible to formation damage than their vertical counterparts for the following reasons:

1. Substantially longer contact time with the drilling fluid. In a vertical well, drilling may only be in the pay zone a matter of hours while in a horizontal well the time may be measured in weeks.
2. Most horizontal wells are not cased and perforated and are completed open-hole. Relatively shallow damage, which can be easily perforated on a standard vertical well, remains a major source of permeability reduction in many horizontal wells.
3. High drawdowns are difficult to obtain on horizontal wells due to the length of the well in the pay zone. This makes it much more difficult to clean up damage due to invaded fluid or solids.
4. Stimulation of horizontal wells is extremely difficult and expensive. Thus once formation damage occurs, it is usually permanent in nature and effect.

A-2 BASIC CAUSES OF FORMATION DAMAGE

Formation damage can potentially occur any time non-equilibrium or solid bearing fluids enter a reservoir, or when equilibria fluids are displaced at extreme velocities. [38,52,53] Thus, most processes used to drill, complete or stimulate reservoirs have the potential to cause formation damage. Krueger [37] indicated that almost every operation in the field is a potential source of damage to well productivity. Some of these processes that are potentially responsible for formation damage are:

1. Drilling
2. Cementing
3. Completions/stimulations
    a. Perforation
    b. Acidizing
    c. Fracturing
4. Workovers
    a. Kill fluids
    b. Hot oil treatments
5. Waterflooding or water disposal
6. Enhanced oil recovery
    a. Miscible flooding
    b. Chemical flooding
    c. Thermal flooding (in-situ combustion/steamflooding)
7. Excessive injection or production rates

A-3 Mechanisms OF Formation Damage

Formation damage falls into four broad categories based upon the mechanism of its origin.[38]

A-3.1 Mechanically Induced Formation Damage

i) Fines Migration

It has been long accepted that severe permeability impairment can occur when fluid velocities become large enough to physically shear interstitially bound particulates loose and move them to bridging/blocking locations at pore throats. Figure A-1 shows the effect of interstitial velocity on the permeability. Most reservoirs demonstrate a critical velocity at which fines migration occurs.

ii) Solids Entrainment

The injection of fluids that contains solid particulates (i.e. unfiltered injection waters or corrosion products from degenerating tubing strings or surface equipments) can cause gradual plugging and loss of permeability as illustrated in figure A-2.

iii) Relative Permeability (trapping) Effects

Deleterious relative permeability effects can also have a severely reducing effect on effective permeability, particularly in low permeability reservoirs. Figure A-3 shows a gas reservoir, which was initially saturated at Sw_i. The near wellbore is then resulting in much higher irreducible water saturation Sw_r (due to capillary trapping phenomenon) near the wellbore. It can be seen that effective permeability to the gas has been reduced substantially due to the increased trapping of the invaded aqueous phase.

A-3.2 Chemically Induced Damage

i) Clay Swelling

The phenomena of clay swelling, defined, as the direct substitution of water into hydratable clays such as smectite is the classic type of the formation damage. Expansion of swelling clays upon hydration can often cause severe reductions in formation permeability. Figure A-4 illustrates typical example for clay swelling problem.

ii) Clay Deflocculation

Deflocculation occurs when the delicate ionic charge balance that electronically binds clays and particulates together and to pore walls is disrupted resulting in migration and blockage of the clays, even though they may not classically be thought of as " swelling"

clays. This phenomenon commonly occurs when a system is subjected to a salinity reduction or "shock" as illustrated in figure A-5.

iii) Solids and Wax precipitation/deposition

Solids and wax precipitation is often a problem in production wells, particularly in miscible flooding projects.

iv) Incompatible Precipitates and scales

Other solids in the form of insoluble precipitates and scales can occur due to chemical incompatibility between formation and injected fluids. These include insoluble precipitates such as barium or calcium salphate, which can often cause severe long-term permeability impairment in injection and production wells.[38]

v) Acid Sludge

Many acids can also chemically precipitate insoluble acid "sludge" which can cause blocking and plugging of the pore system.

vi) Stable Emulsions

Acids and other aqueous fluids can cause the formation of extremely high viscosity oil external emulsions, which can become entrapped in the near welbore region and form a viscous and immobile " Emulsion Block".

vii) Chemical Adsorption and Wettability Alteration

The injection of various types of chemical additives, such as surfactants, scavengers, inhibitors, polymers, stabilizers can result in both wettability alteration, which can alter permeability, and also in physical adsorption, which can permanently impair permeability.

A-3.3 Biologically Induced Formation Damage

Entrainment of bacteria in injected fluid streams can be a source of severe formation damage and operational problems. Bacterial formation damage can occur both with and without oxygen present (aerobic and anaerobic).

A-3.4 Thermally Induced Formation Damage

This type of damage occurs almost exclusively at temperatures exceeding 150°C in hot water, steamflooding or in-situ combustion. Figure A-6 shows the effect of temperature of formation damage. The major sources of damage can be attributed to the

temperature induced transformation of inert clays such as kaolinite into swelling smectitic clay, the physical dissolution of portions of the rock matrix and release of encapsulated fines due to high temperature solubility effects and wettability alterations associated with steam-flooding. [38,40]

A-4 RECOMMENDED PROCEDURE FOR SPECIFIC RESERVOIR TYPES

Formation damage is extremely reservoir sensitive and it is impossible to definitively generalize if a particular damage mechanism will be predominant in one reservoir compared to another without laboratory and field studies. Table A-1 shows the potential formation damage mechanisms in different reservoir types.

A-5 CHARACTERIZING DAMAGE ZONE AROUND HORIZONTAL WELL

The distribution of damage surrounding a horizontal well is neither radial nor distributed evenly along the horizontal well. [38,47] Permeability anisotropy necessarily would generate an elliptical shape normal to the well. The time of exposure during drilling and completion would result in a truncated elliptical cone with the larger base near the heel section of the well and the minimum at the toe end.

The shape and distribution of damage around a horizontal well would reflect the vertical-to-horizontal permeability anisotropy, the time of exposure to the drilling and

completion fluids, the differential pressure, pump rate and the type of mud used. [49] Figure A-7 shows the damage distribution around horizontal wells schematically.

It is logical to expect the mud filtrate penetration to generate a truncated cone with the larger base near the vertical section of the well. Assuming a 1000ft horizontal well is to be drilled and that the rate of drilling is 100ft/day, then the first 100ft would be exposed to 10days of filtrate invasion, the next 100ft to 9days, and so on until the last 100ft section to only 1day of filtrate invasion. The base of this cone would be radial in case of permeability isotropy (i.e., $\beta=\sqrt{(K_H/K_V)}=1.0$) and elliptical in all other cases. If the vertical permeability were much smaller than the horizontal permeability (typical anisotropy), then the cone would be elliptical, with the larger axis of the ellipse being horizontal. In the rare case when the vertical permeability may be longer, then the larger axis of the ellipse would be vertical.

Table A-1. Potential Formation Damage Mechanism in different reservoir types [After Bennion et.al, 1996]

Damage Mechanism	Fluid-Fluid Compatibility	Rock-Fluid Compatibility	Solids Invasion	Phase Trapping	Chemical Adsorption	Fines Migration	Biological Damage	Effect of High OB
Homogeneous Sand-Clean	POSS	POSS	POSS	POSS	POSS	UNL	POSS	POSS
Homogeneous Sand-dirty	POSS	PROB	POSS	POSS	PROB	PROB	POSS	POSS
Laminated Sand-clean	POSS	POSS	POSS	POSS	POSS	UNL	POSS	POSS
Laminated Sand-dirty	POSS	PROB	POSS	POSS	PROB	PROB	POSS	POSS
Unconsolidated Sand	POSS	POSS	PROB	UNL	POSS	POSS	POSS	PROB
Fractured Sand, Permeable matrix	POSS	POSS	PROB	POSS	POSS	POSS	POSS	PROB
Fractured Sand, Low permeability matrix	POSS	UNL	PROB	POSS	POSS	UNL	POSS	PROB
Homogeneous Carbonate	PROB	UNL	POSS	PROB	POSS	UNL	POSS	POSS
Fractured Carbonate, Impermeable matrix	PROB	UNL	PROB	POSS	UNL	UNL	POSS	PROB
Fractured Carbonate, Permeable matrix	PROB	UNL	PROB	POSS	POSS	UNL	POSS	PROB
Vugular Carbonate	PROB	UNL	PROB	UNL	UNL	UNL	POSS	PROB

PROB: Probable damage mechanism under most conditions
POSS : Possible damage mechanism under specific conditions
UNL : Unlikely damage mechanism under majority conditions

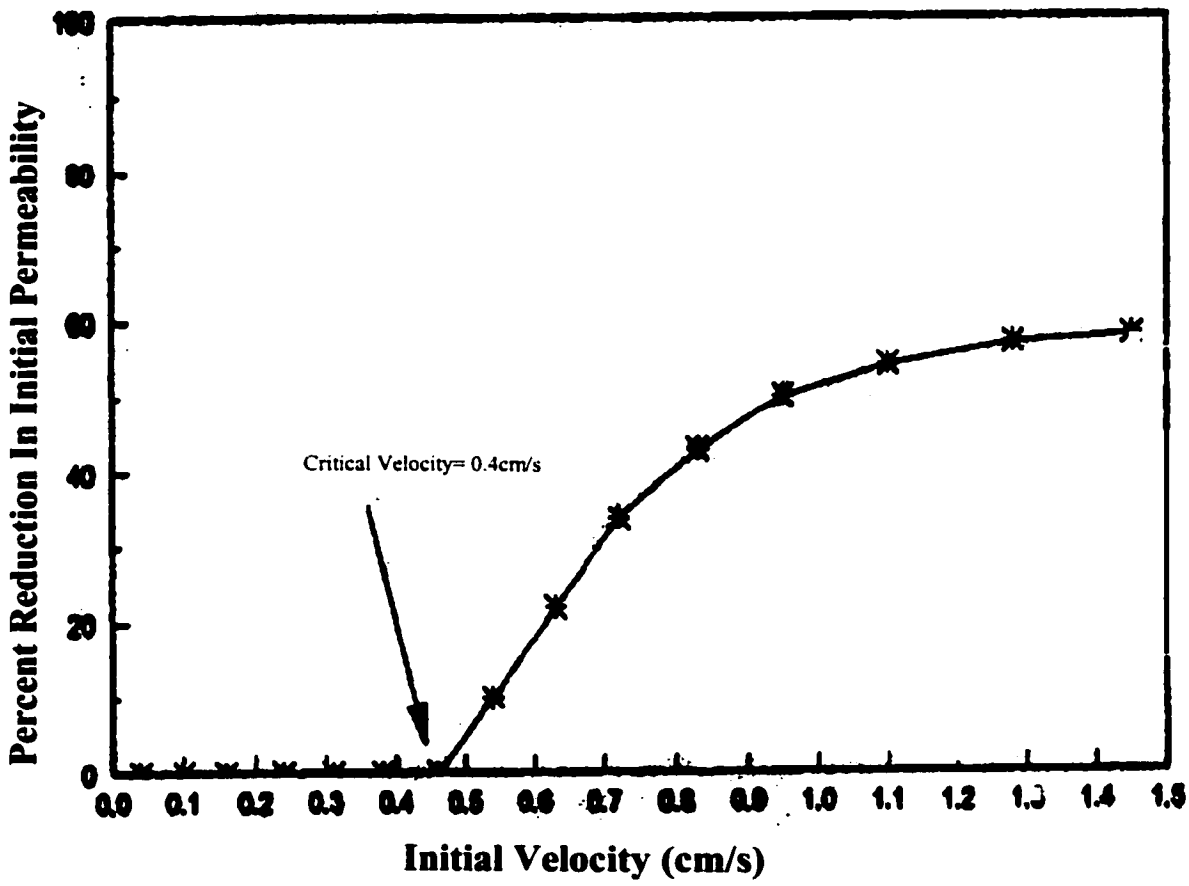

Figure A-1:Effect of Fines Migration on Return Permeability (After Bennion et.al. 1991)

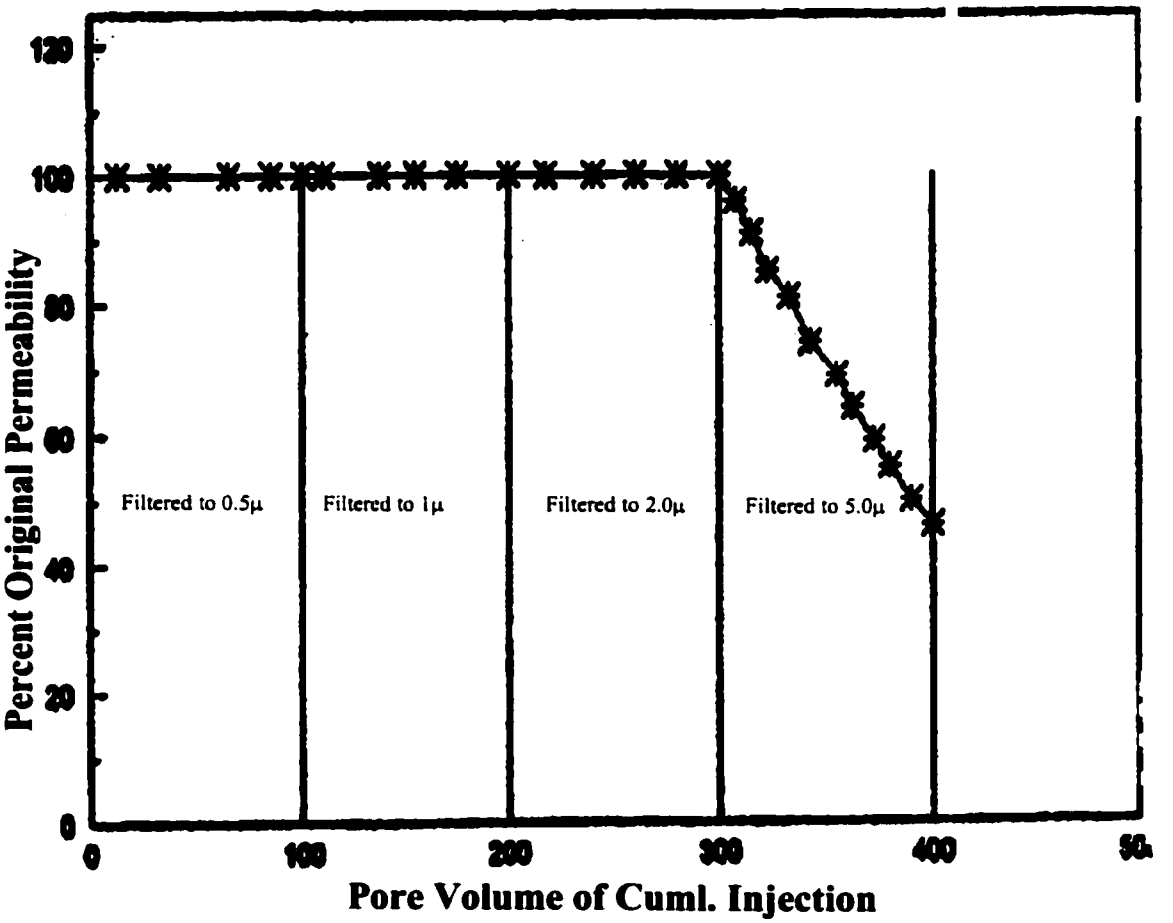

Figure A-2: Effect of Solid Entrainment on Return Permeability (After Bennion et.al.,1991)

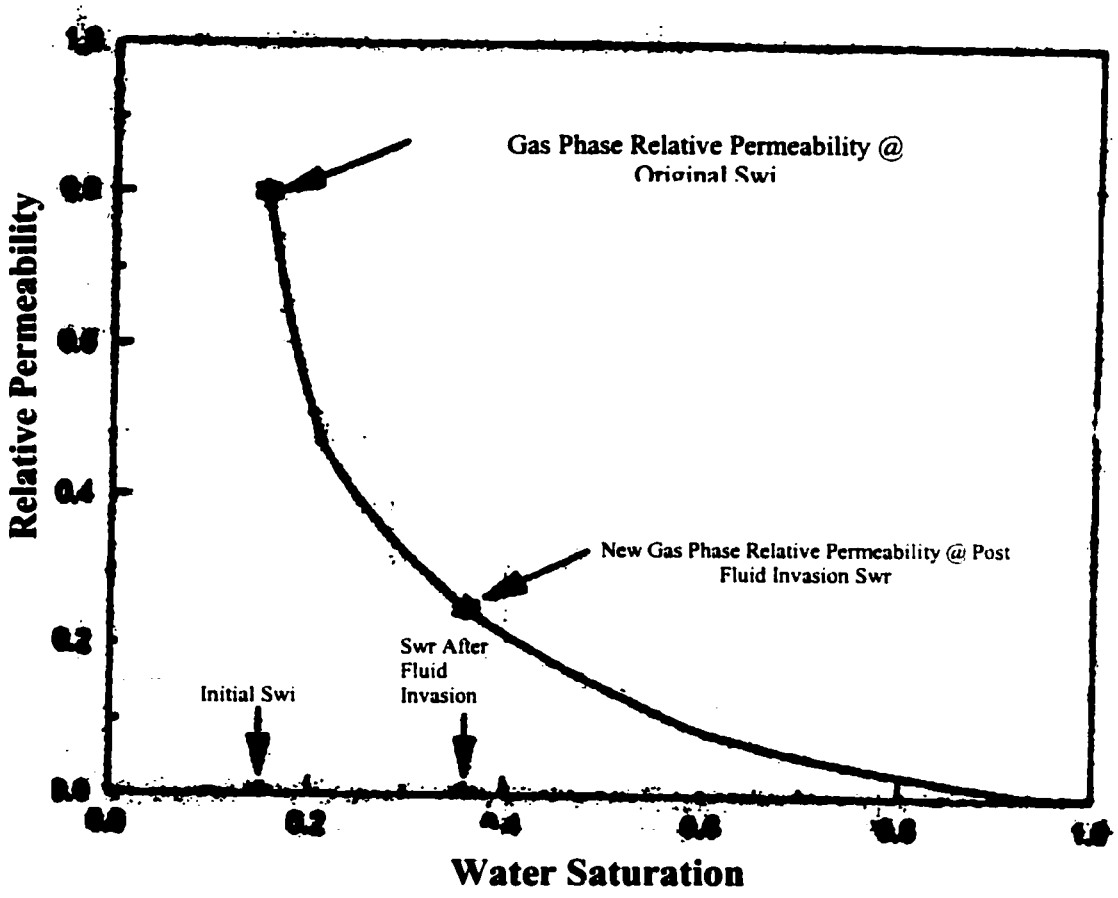

Figure A-3: Effect of Phase Trapping on Return Permeability (After Bennion et.al., 1991)

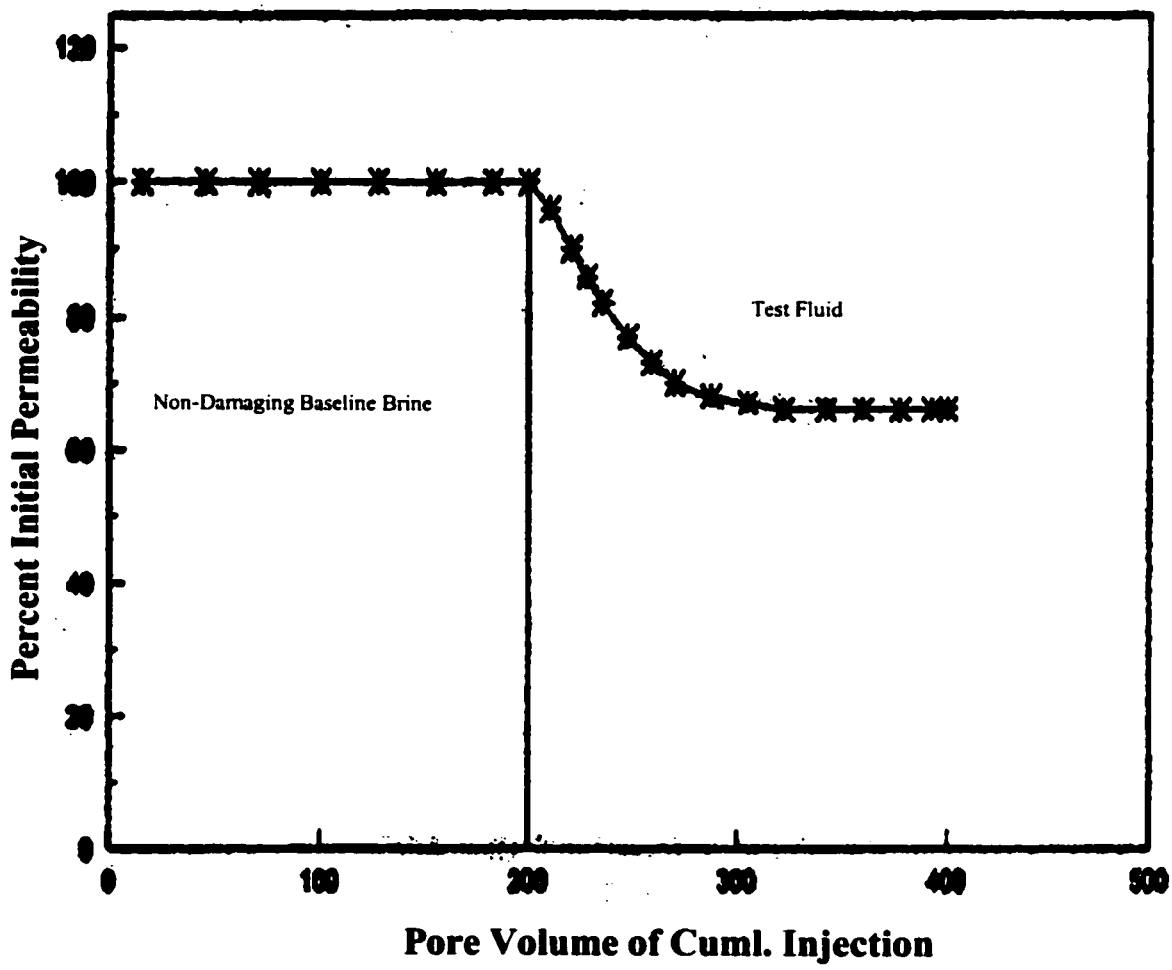

Figure A-4: Effect of Clay Swelling on Return Permeability (After Bennion et.al., 1991)

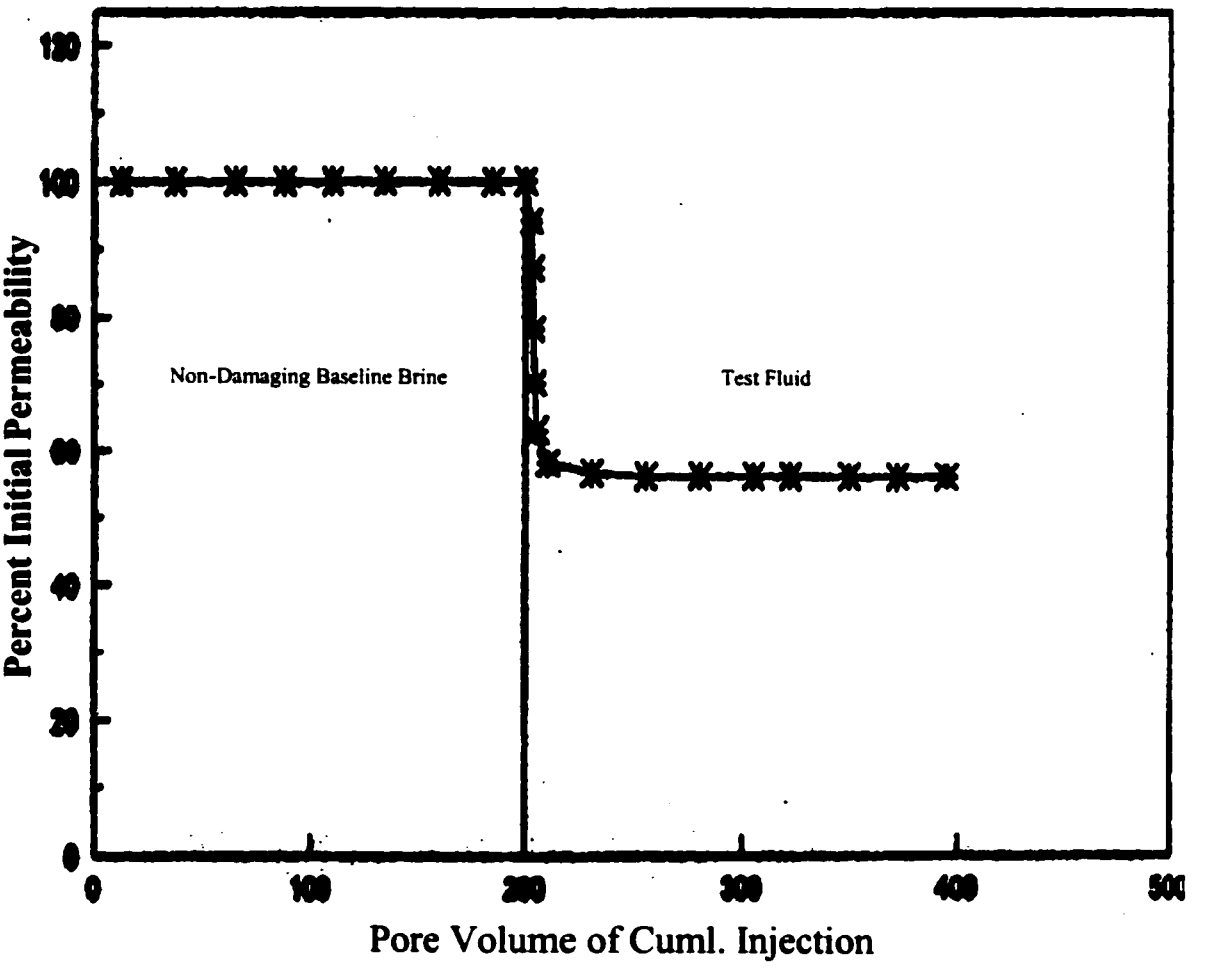

Figure A-5: Effect of Deflocculation of Clays on Return Permeability (After Bennion et.al., 1991)

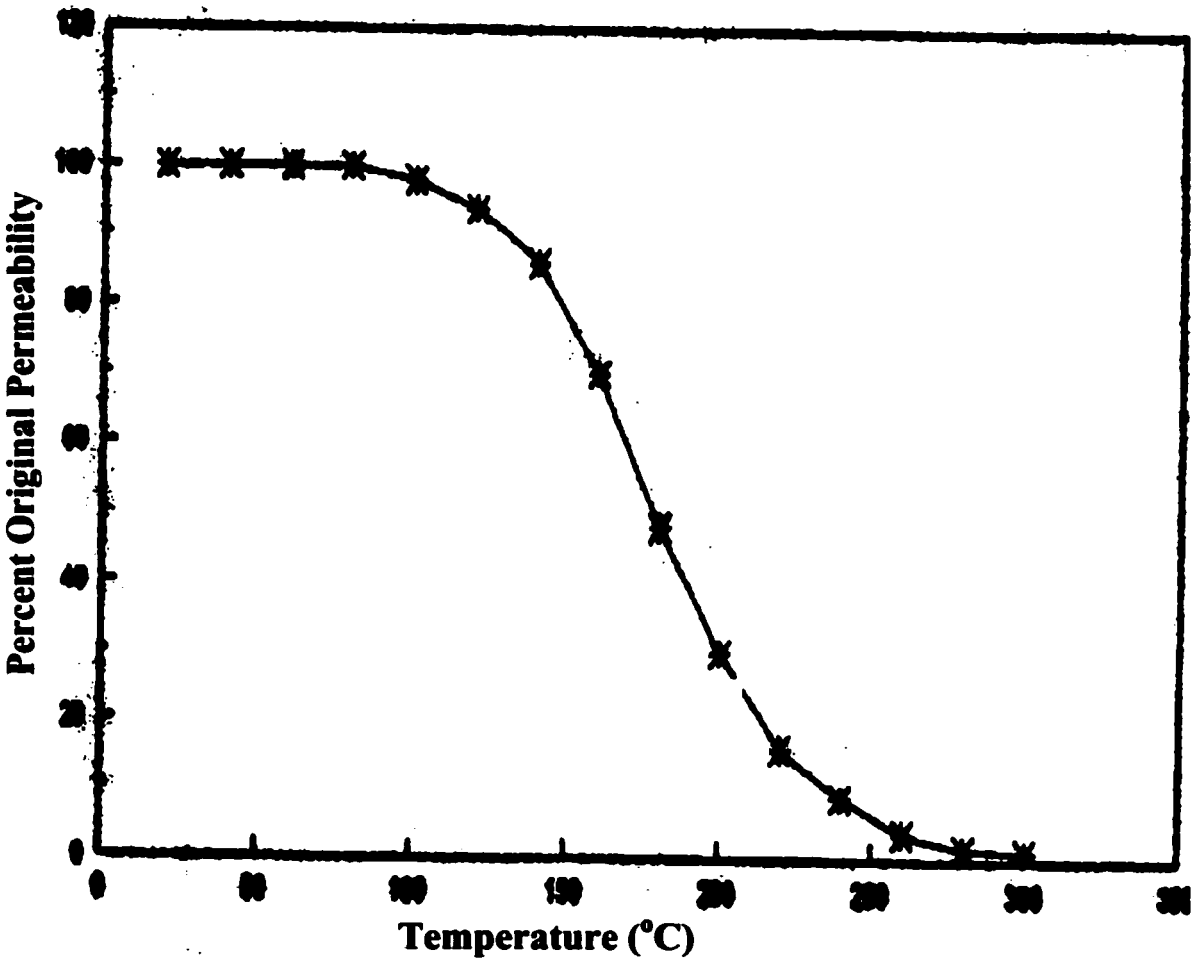

Figure A-6: Effect of Temperature on Return Permeability (After Bennion et.al.,1991)

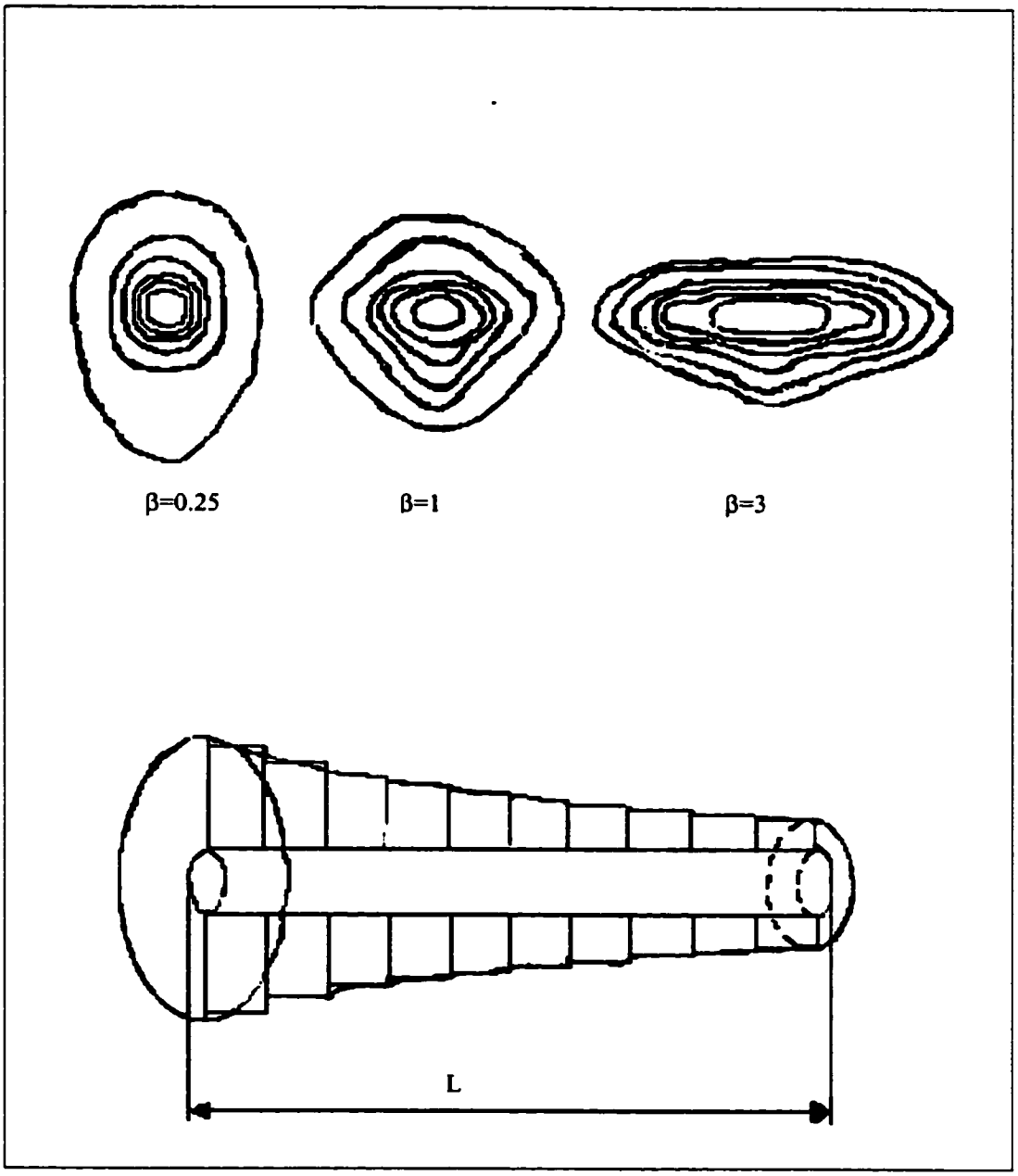

Figure A-7: Normal saturation profiles for three anisotropies and schematic of damage cone. (After Frick and Economides, 1993)

APPENDIX B

PARTICLE SIZING & BRIDGING PROCESS

B-1 DRILLING FLUID PARTICLE SIZING

Specially designed polymer, sized solids drill-in fluids are being effectively applied for drilling horizontal or highly deviated wells worldwide. Ideally, these systems should be compounded with inhibitive brine, shear thinning polymer additives and a minimal concentration of soluble bridging solids. The drilling fluid density is controlled by using soluble salt rather than by inert particulates to maintain an ultra-thin filter cake.

The design of drilling fluid stressed on proper filter cake development, formation protection and maximized return permeability. The absolute size of the $CaCO_3$ particle selected for bridging is based upon the formation pore opening to be sealed. Experience indicated that the largest particle, which should be used, is about one-half the diameter of the pore to be sealed, bridging occurring when a plurality of the carbonate particles attempted simultaneously enters the pore [33].

Bridging solids provide the basic structure for building a filter cake to prevent loss of fluid and solid particles into a permeable formation. Factors necessary to consider in the proper filter cake design are: particle size distribution, particle concentration and particle shape. Particle size distribution should be carefully controlled. The objective is to obtain a filter cake of maximum density; i.e. the closest possible packing. Close packing

reduces cake porosity and permeability thus reducing cake thickness and total solids required for effective bridging.

B-2 BRIDGING PROCESS

When fluid contacts the formation there is a spurt loss of whole fluid, which continues until solid bridging particles bridge the pore throats. A properly designed filter cake has three basic layers. Figure B-1 illustrates the fluid loss process as a filter cake is formed. The primary bridge is the formation of the initial bridge by the spurt loss to the formation. This bridge consists of the larger sized particles. The secondary bridge is formed as the smaller bridging solids mixed with colloidal particles layer over the top of the primary bridge. The final seal is basically a polymer film.

The development of a bridging film is a process significantly different from the formation of a drilling mud cake. Bridging films form very quickly and require a substantial fluid loss. This has been documented in the field by the very rapid stoppage of fluid loss when pills are spotted [33]. In the lab, fluid spurt loss from pill as a percentage of the total fluid volume is very small and the resulting films formed on sand faces have been observed to be persistent in adhering to the formation face [43].

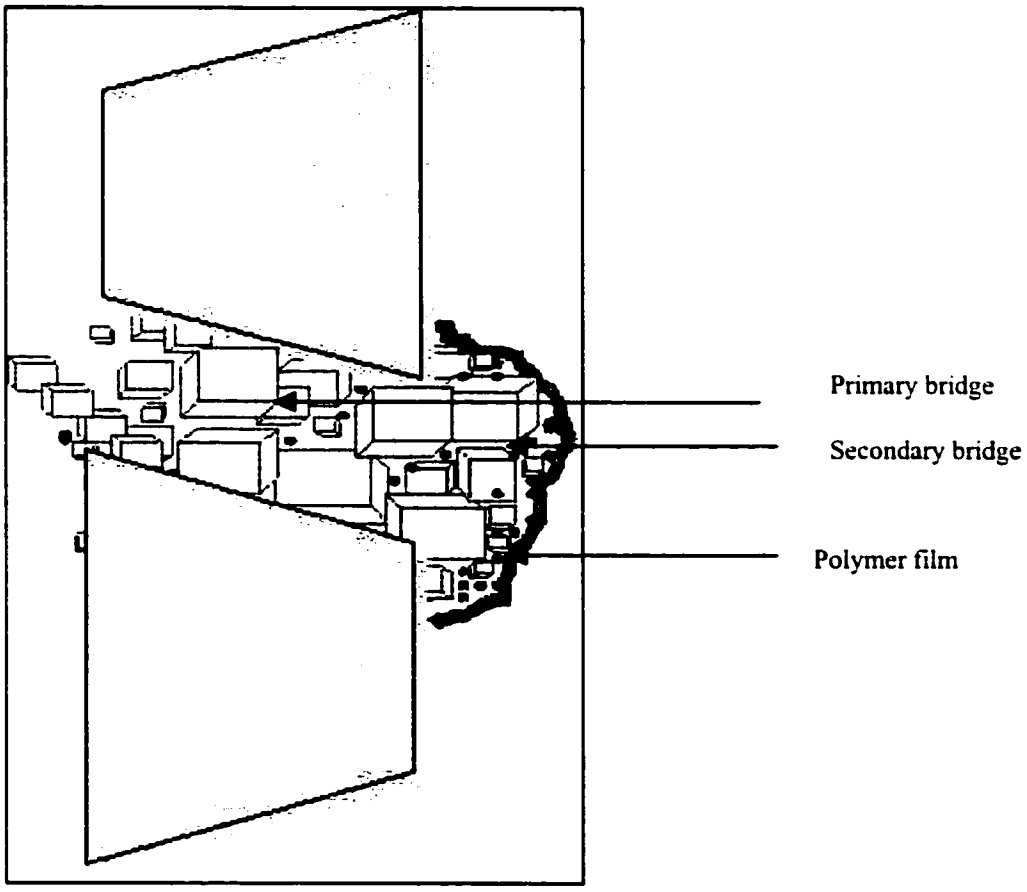

Figure B-1: Fluid loss and bridging process [From A Technical Index by Brine-Add Fluids Ltd, Online source]

B-3 ACTIONS OF FLUID LOSS AGENTS

One of the basic mechanisms of fluid loss agent is given in figure B-2. The fluid contains particles suspended. These particles move with the lateral flow out of the drill hole into the porous formation. The porous formation acts like a sieve for the suspended particles. So the particles will be captured near the surface and accumulated as a filter cake.

The hydrodynamic forces acting on the suspended colloids determine the rate of cake buildup and, therefore, the fluid loss rate. A simple model has been developed in the literature by Jiao et.al.[44] that predicts a power law relationship between the filtrate rate and the shear stress at the cake surface. The model shows that the cake formed will be inhomogeneous with smaller and smaller particles being deposited as filtration proceeds. An equilibrium cake thickness is achieved when no particles small enough to be deposited are available in the suspension. The cake thickness as a function of time can be computed from the model.

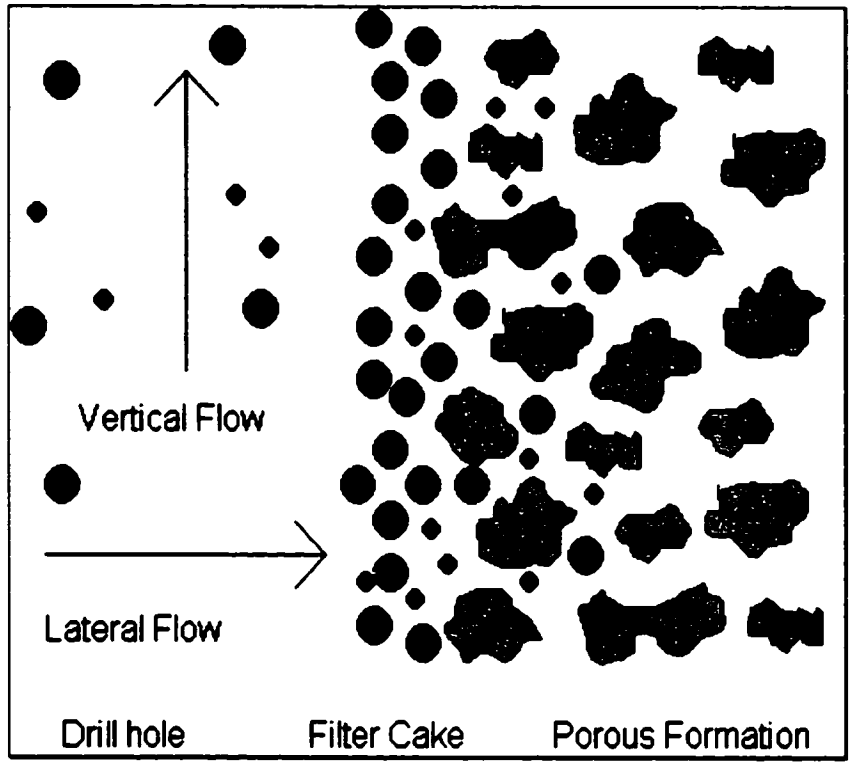

Figure B-2 : Formation of a Filter Cake in a Porous Formation from Suspended Particles in a Drilling Fluid. The Suspended Particles can Invade the Formation to some Extent.[After Johannes K.F., University of Leoben]

B-4 PARTICLE SIZE BY SCANNING ELECTRON MICROSCOPY(SEM)

Description of Techniques and Specimen Preparation

One of the most outstanding features of the SEM method is that it allows elemental analysis and observation from an ultra micro-area to a wide area on the specimen surface without destroying the specimen. SEM produces a detailed photograph that provides important information about the surface structure and morphology of almost any kind of sample. Figure B-3 shows the SEM equipment.

In SEM, electron beam is scanned across a sample's surface. When the electrons strike the sample, a verity of signals will be produced which shows sample's elemental composition. This SEM is a major tool for qualitative and quantitative analyses that are performed by bombarding a finely focused electron beam (electron probe) on the specimen, and measuring the intensities of the characteristic X-ray emitted.

Samples for SEM imaging and analysis consist of materials that are stable in a vacuum and under a high voltage electron beam. Specimens for analyses must be fine polished (or naturally have a flat surface). For SEM imaging we use a gold plating by SPI sputter coater in order to make the sample conductive.

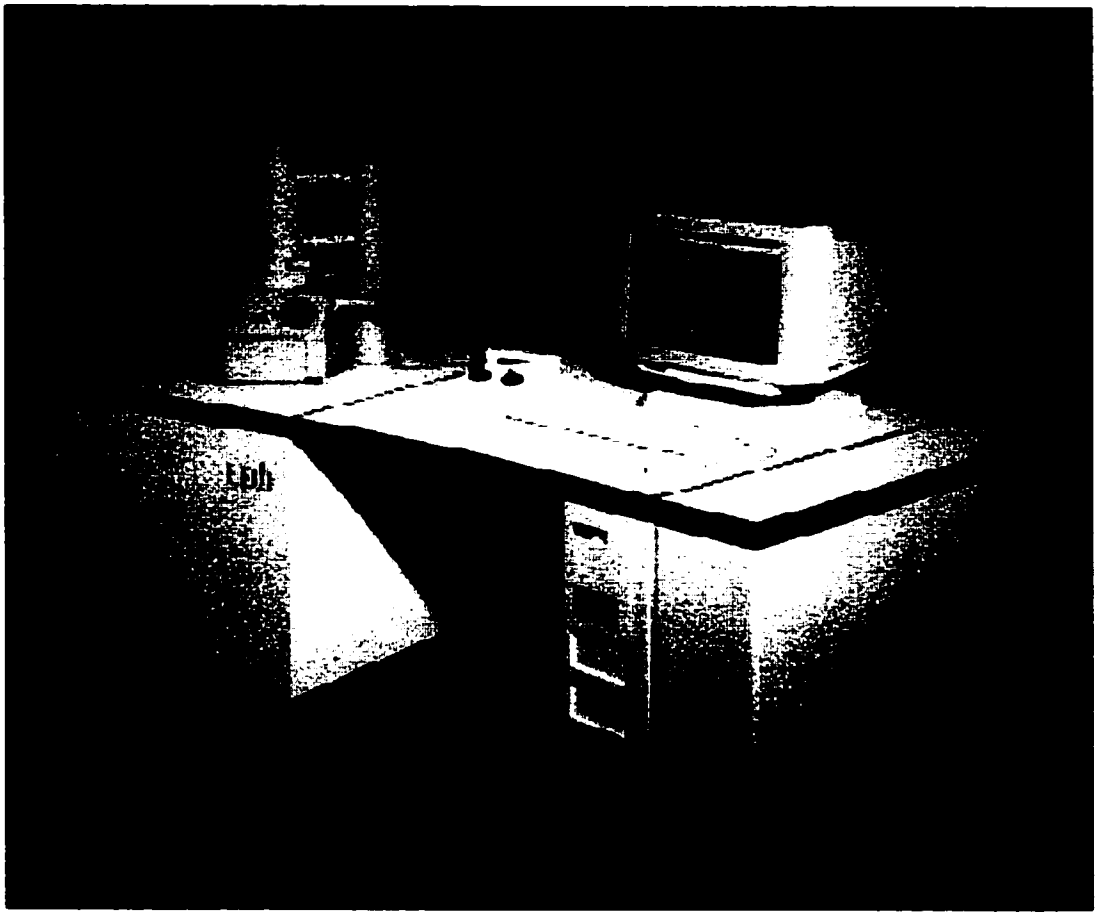

Figure B-3: The Scanning Electron Microscope(SEM) [After the Museum of science & Science network, online magazine]

Specimen mounts can be a common thin section, four-inch diameter rounds, cylinder or other appropriate mounts or irregular objects with maximal diameter of 90mm and 25mm thickness. The pictorial representation of the whole process of scanning electron microscopy is shown in figure B-4.

SEM Analysis and Procedure

The four $CaCO_3$ samples that are used as bridging additives in our polymeric Water-based mud formulations were mounted on holder with conductive copper tapes in order to hold them in place. And they were examined in a Scanning Electron Microscope (SEM). Imaging was performed in secondary Electron (SEI) mode.

The micrograph was taken at 200x and 300x magnifications. As it is evident in the micrographs, the particles sizes are different in each case as shown in figure B-5 through B-8. The general procedure for the analysis are given below:

1. SEM samples are coated with a very thin layer of gold by a machine called a sputter coater.
2. The sample is placed inside the microscope's vacuum column through an airtight door.
3. After the air is pumped out of the column, an electron gun (at the top) emits a beam of high-energy electrons. This beam travels downward through a series of magnetic lenses designed to focus the electrons to a very fine spot.

4. Near the bottom, a set of scanning coils moves the focused beam back and forth across the specimen, row by row.

5. As the electron beam hits each spot on the sample, secondary electrons are knocked loose from its surface. A detector counts these electrons and sends the signals to an amplifier.

6. The final image is built up from the number of electrons emitted from each spot on the sample, and will be displayed on the monitor. Figure B-4 shows pictorials of all the processes.

B-5 PARTICLE SIZE DISTRIBUTION

To measure the particle size distribution, MICROSCAN-II, by QUANTACHROME CORPORATION, equipment was used. MICROSCAN-II is equipment designed for particle size analysis. It can measure the particle size distribution both for powder and slurries.

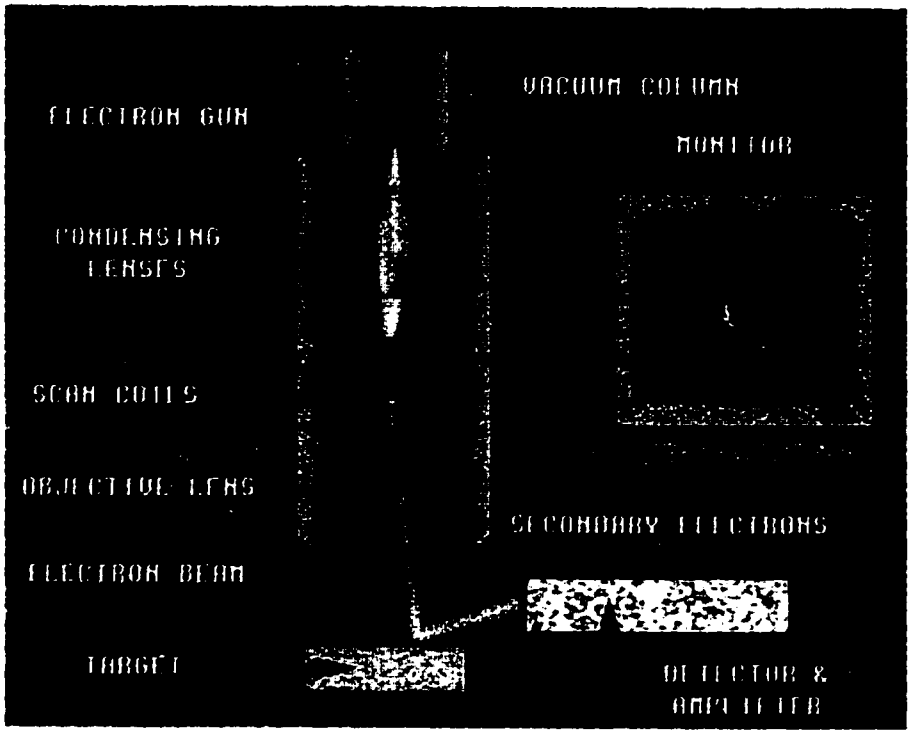

Figure B-4: **Pictorials of the whole process of the SEM system** [After the Museum of science & Science network, online magazine]

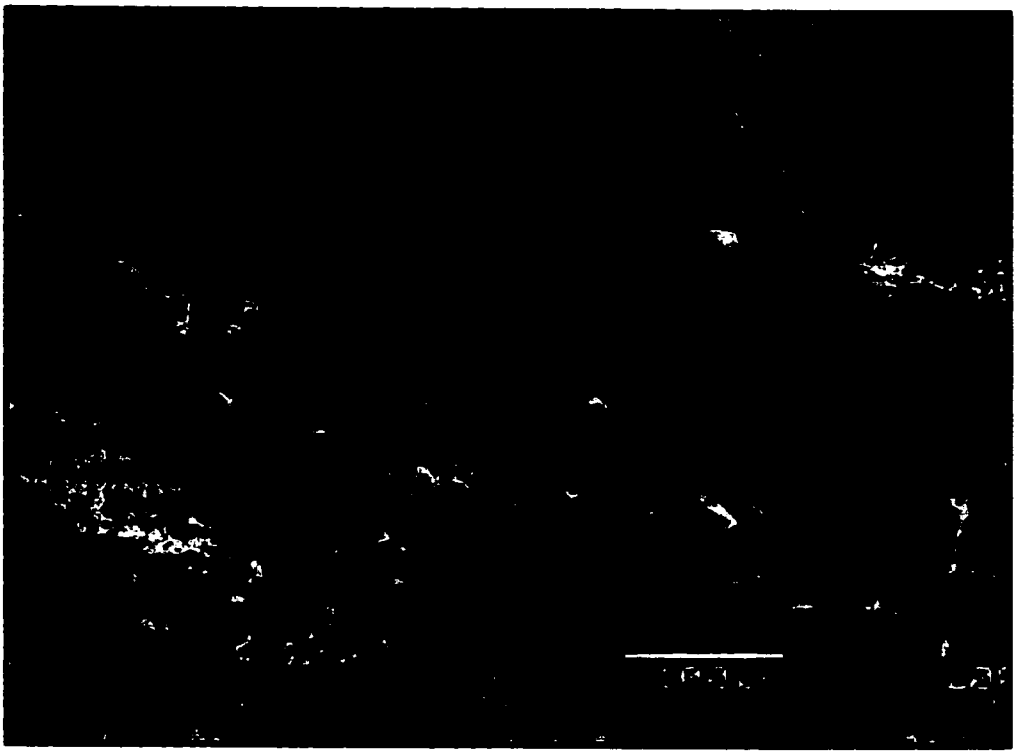

Sample A(200X)

Sample A(300X)

Figure B-5:SEM micrograph image of sized $CaCO_3$ sample A @ 200X and 300X magnification Respectively

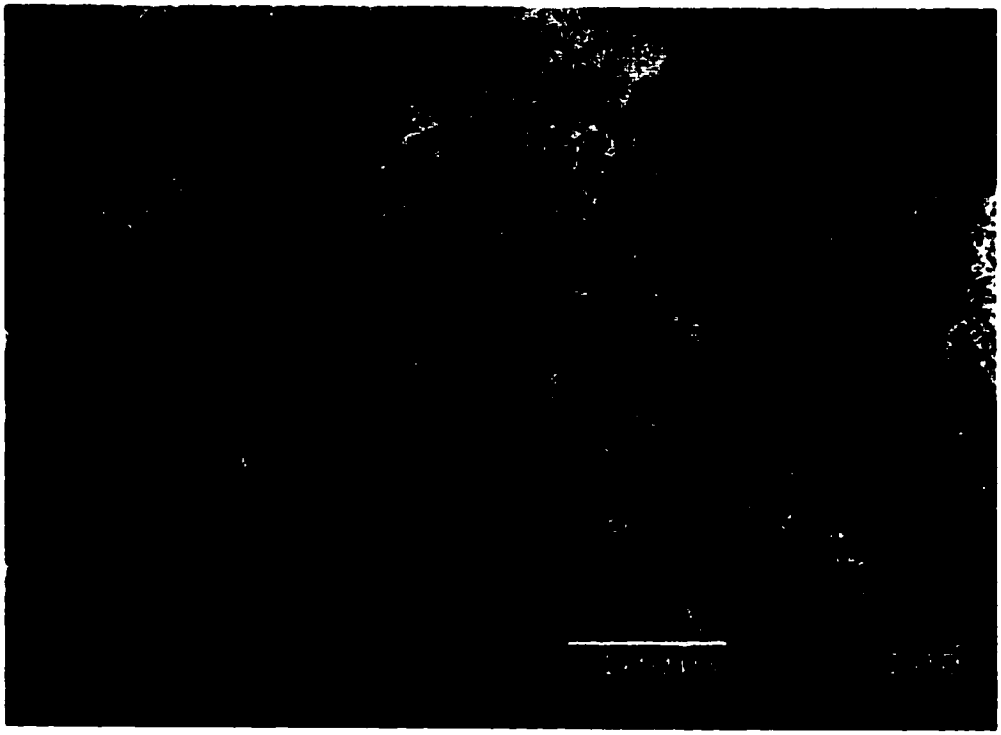

Sample B(X200)

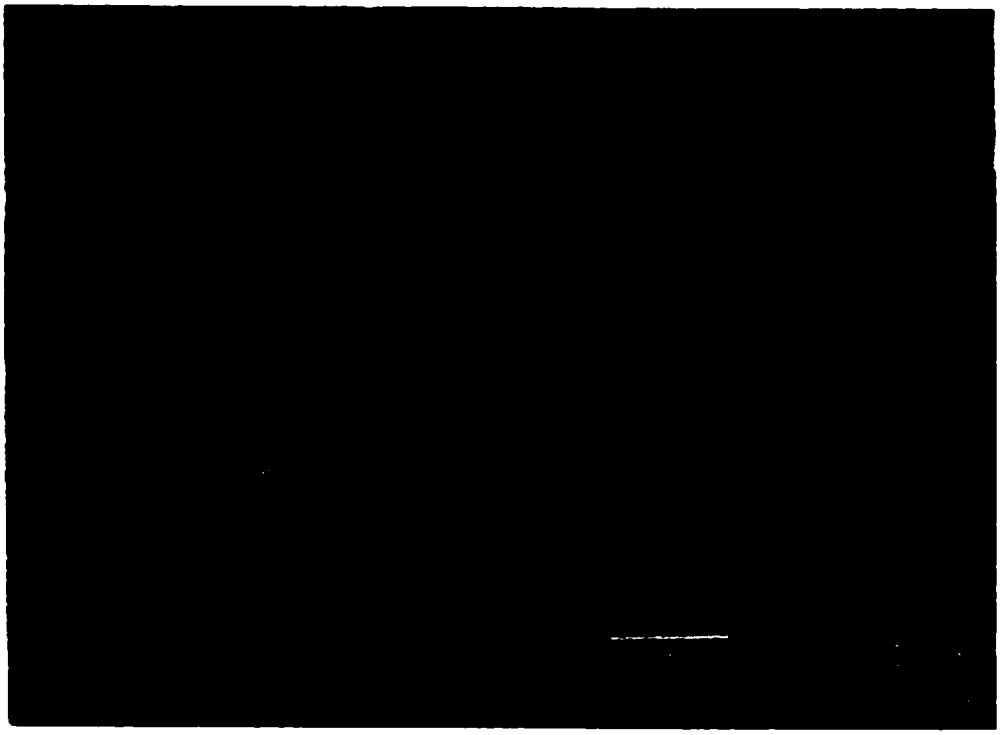

Sample B(X300)

Figure B-6:SEM micrograph image of sized $CaCO_3$ sample B @ 200X and 300X magnification Respectively

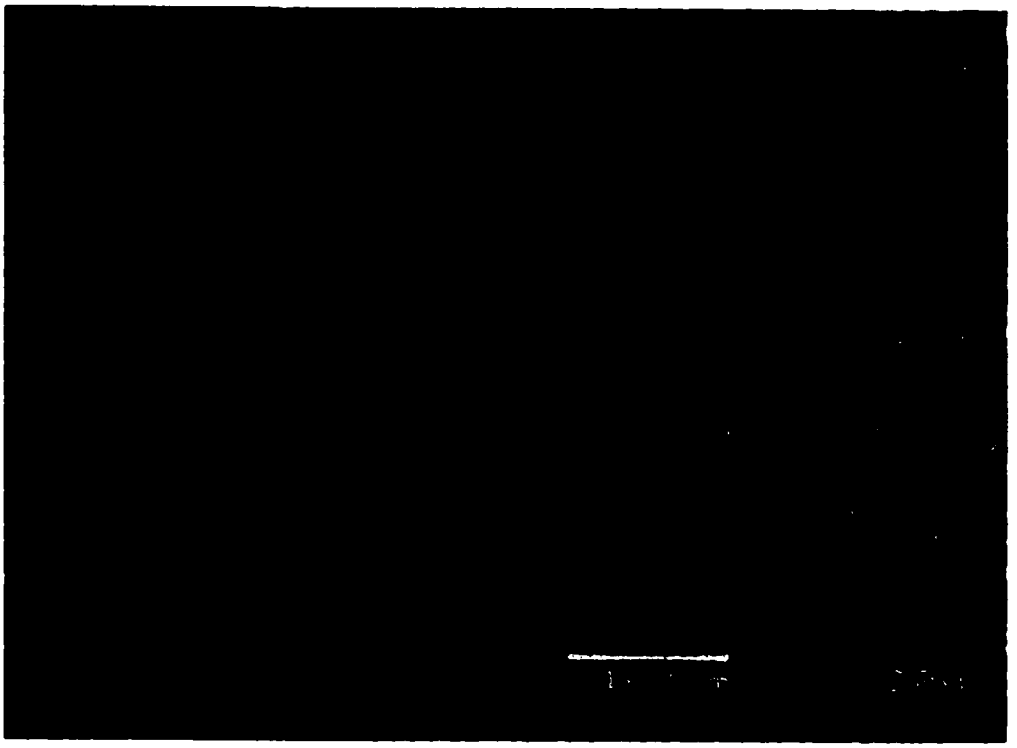

Sample C(200X)

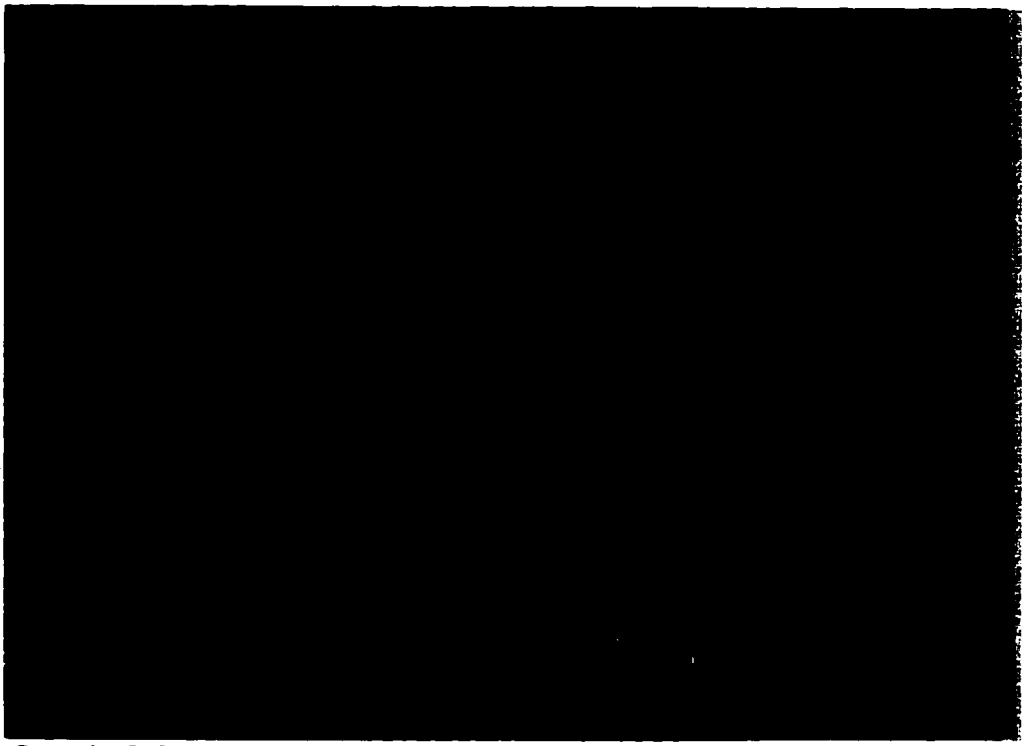

Sample C(300X)

Figure B-7:SEM micrograph image of sized $CaCO_3$ sample C @ 200X and 300X magnification Respectively

Sample D(200X)

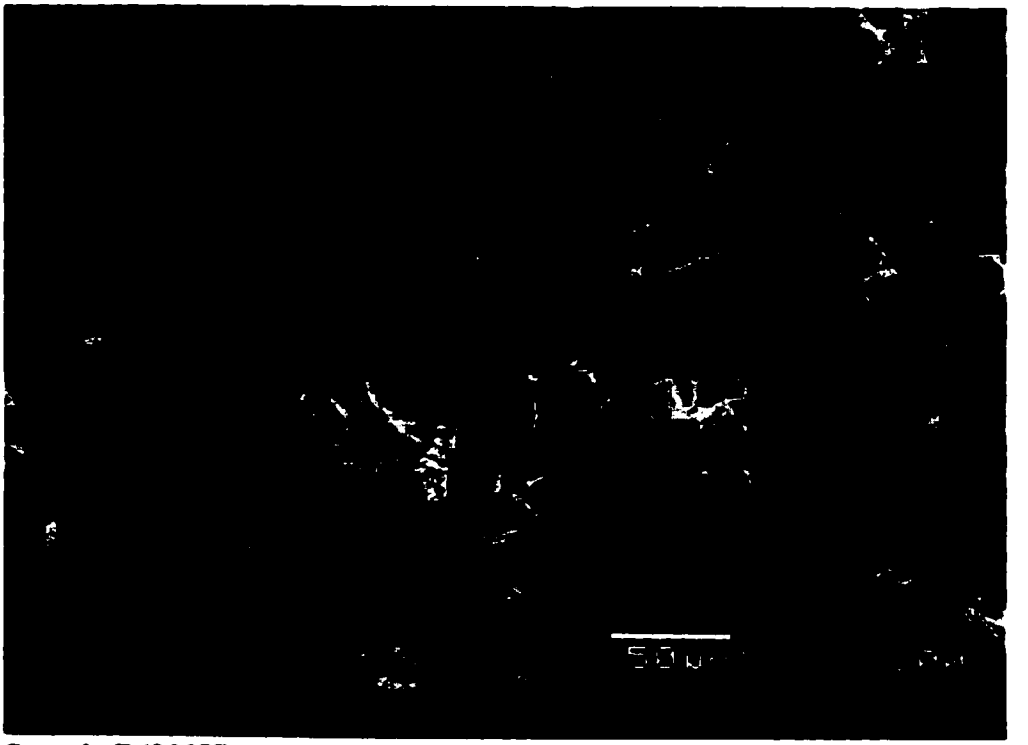

Sample D(300X)

Figure B-8: SEM micrograph image of sized $CaCO_3$ sample D @ 200X and 300X magnification Respectively

Equipment Description

The Microscan particle size analyzer employs soft X-rays generated from an X-ray tube to measure the particle concentration in a sedimentation cell. The X-rays are produced through a berillium window by an air-cooled tube having a tungsten target. The tube is operated at a voltage between 12.5 and 15kv with a power output of 15watts.

Sample Preparation and Analysis

The sample to be analyzed is dispersed in a fluid and passes for sedimentation process through the cell compartment before the analysis. The concentration of particles is determined by their attenuation of low energy x-rays, which scans the sedimentation vessel from bottom to the top at a rate determined by the analysis to be performed. The percentage of sedimented mass is correlated using Stokes law [50].

Stokes law

Three forces act upon a particle sedimenting in a viscous medium under the influence of gravity: force of gravity (F_g) directing downward, a buoyant force (F_b) and a drag force (F_d) both acting upwards. The resultant force acting to accelerate the particles is [50];

$$m\frac{dv}{dt} = F_g - (F_d + F_b) \qquad \text{B-1}$$

Or

$$m\frac{dv}{dt} = mg - m'g - F_d \qquad \text{B-2}$$

Where, m is the particle mass, g is the gravitational acceleration and m' is the mass of fluid displaced by the particles and therefore, has the volume equal to that of the particle. The term F_d is a function of particle velocity, v, and is zero when m is equal to m'. When a particle is less dense that the fluid, m<m', the particle will rise in the liquid medium and the drag force is directed downward. When m>m', the particle settles in the medium and drag force is directed upward. Stokes determined that the drag force F_d for spherical particles, is given by:

$$F_d = 3\pi\mu dDV \qquad \text{B-3}$$

Where μ is the fluid viscosity, V is the settling velocity and D is the particle diameter. Combining equation B-2 and B-3 yields;

$$m\frac{dv}{dt} = (m - m')g - 3\pi\mu D\frac{dh}{dt} \qquad \text{B-4}$$

Where h is the distance the particle has settled in time t.

By assuming that all particles are spherical, the mass term m and m' in equation B-4 can be replaced by $(\pi D^3\rho_s)/6$ and $(\pi D^3\rho_f)/6$ where ρ_f and ρ_s are fluid and particle specific densities respectively, thus

$$\left(\frac{\pi D^3 \rho_s}{6}\right)\frac{dv}{dt} = \frac{\pi}{6}(\rho_s - \rho_f) - 3\pi\mu D^3 \frac{dh}{dt} \qquad \text{B-5}$$

When particle reaches their terminal velocity, the term dv/dt vanishes leaving

$$\int_0^h dh = \frac{(\rho_s - \rho_f)D^2 g}{18\mu}\int_0^t dt \qquad \text{B-6}$$

Then,

$$D = \left[\frac{18\mu}{(\rho_s - \rho_f)g}\frac{h}{t}\right]^{1/2} \qquad \text{B-7}$$

Equation B-7 is the Stokes equation that is used in the particle size analysis by the MICROSCAN.

Particle Size Distributions

The microscan's primary measurement is the distribution of particle mass, presented as percent mass finer than the indicated particle size. If we consider a thin ($0.005cm^3$) element at depth h in the sample cell in a uniform suspension, through which the x-ray beam is transmitted. When sedimentation is initiated, those entering the element exactly compensate all particles leaving the thin volume element. Therefore, no concentration change occurs within the volume element until the largest particles located

at the top of the suspension have sedimented through the volume element. When no particles of size D are any longer above the volume element to replace those that leave, the concentration within the volume element starts to decrease and becomes equal to the concentration of particles smaller than diameter D. In this case, D represents the diameter of particles falling with velocity h/t.

When sedimentation commences, that is, at t=0, the suspension will contain a uniform concentration, given by,

$$C(h,0) = \frac{(m_0)_s}{V_s + V_f} \qquad \text{B-8}$$

Where $(m_0)_s$ is the mass of suspended solid at t=0, V_s and V_f are solid and liquid volumes respectively. At some later time t, the concentration at depth h is given by;

$$C(h,t) = \frac{m_s}{V_s' + V_f'} \qquad \text{B-9}$$

Where m_s and V_s' are the mass and volume of the solids in volume V_f' of the fluid measured at depth h from top of the fluid at time t. Knowing that the total volume of solids and fluids in the volume is necessarily constant,

$$\frac{C(h,t)}{C(h,0)} = \frac{m_s}{(m_0)_s} \qquad \text{B-10}$$

A plot of $\frac{C(h,t)}{C(h,0)}X100$ versus D yields a particle size distribution of the cumulative % under size by weight.

APPENDIX C:

ULTRASONIC VELOCITY FOR THE DRY, OIL SATURATED @ S_{WI} AND DAMAGED SAMPLE S

TABLE C-1: Ultrasonic Velocity for the Dry Sample

LONGITUDINAL DISTANCE (cm)	FLOODING TIME=4HOURS					12 HOURS			30 HOURS		
	PARTRICLE SIZE=8μ	12μ	21μ	41μ	78μ	8μ	12μ	21μ	8μ	12μ	21μ
1.4	2089.431	2089.431	2284.444	2284.444	2284.444	2089.431	2089.431	2089.431	2115.226	2031.621	2031.621
2.4	2097.959	2097.959	2294.643	2294.643	2294.643	2097.959	2097.959	2097.959	2123.967	2023.622	2023.622
3.4	2080.972	2080.972	2304.933	2304.933	2304.933	2080.972	2080.972	2080.972	2123.967	2023.622	2023.622
4.4	2080.972	2080.972	2284.444	2284.444	2284.444	2089.431	2089.431	2089.431	2123.967	2031.621	2031.621
5.4	2089.431	2089.431	2294.643	2294.643	2294.643	2089.431	2089.431	2089.431	-	2031.621	2031.621
6.4	2106.558	2106.557	2284.444	2284.444	2284.444	2047.809	2047.809	2047.809	-	2023.622	2023.622
7.4	2097.959	2097.959	2264.317	2264.317	2264.317	2047.809	2047.809	2047.809	-	2015.686	2015.686
8.4	2089.431	2089.431	2274.336	2274.336	2274.336	2039.683	2039.683	2039.683	-	2015.686	2015.686
9.4	2097.959	2097.959	-	-	-	2039.683	2039.683	-	-	2047.809	2047.809
10.4	-	-	-	-	-	-	-	-	-	2039.683	2039.683
11.4	-	-	-	-	-	-	-	-	-	2047.809	2047.809
12.4	-	-	-	-	-	-	-	-	-	2031.621	2031.621
13.4	-	-	-	-	-	-	-	-	-	2031.621	2031.621
14.4	-	-	-	-	-	-	-	-	-	2039.683	2039.683
15.4	-	-	-	-	-	-	-	-	-	2031.621	2031.621
16.4	-	-	-	-	-	-	-	-	-	2023.622	2023.622
17.4	-	-	-	-	-	-	-	-	-	2015.686	2015.686
18.4	-	-	-	-	-	-	-	-	-	2015.686	2015.686

TABLE C-2: Ultrasonic Velocity of the Oil saturated Berea Core Sample @ Swi

LONGITUDINAL DISTANCE (cm)	FLOODING TIME=4HOURS					12 HOURS			30 HOURS		
	PARTRICLE SIZE=8μ	12μ	21μ	41μ	78μ	8μ	12μ	21μ	8μ	12μ	21μ
1.4	2793.478261	2763.441	2855.556	2839.779	2763.441	2748.663	2763.441	2763.441	2677.083	2839.779	2778.378
2.4	2778.378378	2748.663	2839.779	2824.176	2748.663	2763.441	2793.478	2748.663	2691.099	2855.556	2793.478
3.4	2793.478261	2763.441	2839.779	2824.176	2748.663	2763.441	2778.378	2748.663	2705.263	2839.779	2793.478
4.4	2778.378378	2763.441	2839.779	2839.779	2748.663	2763.441	2778.378	2763.441	2705.263	2824.176	2793.478
5.4	2808.743169	2763.441	2839.779	2855.556	2748.663	2778.378	2778.378	2748.663	2705.263	2793.478	2778.378
6.4	2778.378378	2763.441	2824.176	2855.556	2763.441	2778.378	2778.378	2748.663	2705.263	2793.478	2824.176
7.4	2778.378378	2748.663	2824.176	2839.779	2763.441	2778.378	2763.441	2763.441	2705.263	2778.378	2808.743
8.4	2793.478261	2748.663	2824.176	2855.556	2778.378	2778.378	2763.441	2763.441	2705.263	2748.663	2778.378
9.4	2793.478261	2763.441	2824.176	-	2793.478	2793.478	2793.478	-	2691.099	2748.663	2793.478
10.4	-	-	-	-	-	-	-	-	2691.099	2763.441	2793.478
11.4	-	-	-	-	-	-	-	-	2705.263	2748.663	2808.743
12.4	-	-	-	-	-	-	-	-	2691.099	2763.441	2793.478
13.4	-	-	-	-	-	-	-	-	2705.263	2748.663	2793.478
14.4	-	-	-	-	-	-	-	-	2705.263	2748.663	2793.478
15.4	-	-	-	-	-	-	-	-	2705.263	2748.663	2793.478
16.4	-	-	-	-	-	-	-	-	2691.099	2748.663	2793.478
17.4	-	-	-	-	-	-	-	-	2691.099	2748.663	2793.478
18.4	-	-	-	-	-	-	-	-	2705.263	2793.478	2793.478
19.4	-	-	-	-	-	-	-	-	2691.099	-	-
20.4	-	-	-	-	-	-	-	-	2691.099	-	-
21.4	-	-	-	-	-	-	-	-	2691.099	-	-
22.4	-	-	-	-	-	-	-	-	2677.083	-	-
23.4	-	-	-	-	-	-	-	-	2677.083	-	-
24.4	-	-	-	-	-	-	-	-	2705.263	-	-

TABLE C-3: Ultrasonic Velocity for the Berea Core Samples After Damage

LONGITUDINAL DISTANCE (cm)	FLOODING TIME=4HOURS					12 HOURS			30 HOURS		
	PARTRICLE SIZE=8μ	12μ	21μ	41μ	78μ	8μ	12μ	21μ	8μ	12μ	21μ
1.4	2808.743169	2793.478	2793.478	2855.556	2778.378	2763.441	2793.478	2734.043	2677.083	2778.378	2808.743
1.9	2793.478261	2763.441	2808.743	2855.556	2763.441	2734.043	2763.441	2734.043	2691.099	2763.441	2839.779
2.4	2793.478261	2763.441	2839.779	2839.779	2763.441	2748.663	2763.441	2734.043	2691.099	2793.478	2839.779
2.9	2778.378378	2763.441	2839.779	2855.556	2763.441	2763.441	2734.043	2734.043	2691.099	2793.478	2839.779
3.4	2793.478261	2763.441	2839.779	2855.556	2748.663	2763.441	2763.441	2763.441	2705.263	2778.378	2839.779
3.9	2778.378378	2763.441	2824.176	2855.556	2748.663	2763.441	2763.441	2748.663	2705.263	2748.663	2855.556
4.4	2763.44086	2763.441	2839.779	2855.556	2763.441	2763.441	2748.663	2763.441	2705.263	2748.663	2839.779
4.9	2778.378378	2763.441	2839.779	2855.556	2748.663	2778.378	2763.441	2778.378	2705.263	2763.441	2839.779
5.4	2793.478261	2778.378	2839.779	2855.556	2748.663	2793.478	2808.743	2808.743	2705.263	2748.663	2808.743
5.9	2824.175824	2763.441	2839.779	2855.556	2778.378	2808.743	2808.743	2808.743	2705.263	2763.441	2808.743
6.4	2839.779006	2778.378	2839.779	2839.779	2778.378	2824.176	2808.743	2824.176	2705.263	2748.663	2824.176
6.9	2855.555556	2778.378	2855.556	2871.508	2808.743	2824.176	2839.779	2824.176	2719.577	2748.663	2824.176
7.4	2839.779006	2808.743	2855.556	2871.508	2824.176	2839.779	2839.779	2839.779	2705.263	2748.663	2808.743
7.9	2871.50838	2855.556	2871.508	2871.508	2824.176	2839.779	2839.779	2839.779	2719.577	2778.378	2824.176
8.4	2871.50838	2839.779	2903.955	2871.508	2839.779	2855.556	2824.176	2824.176	2719.577	2808.743	2824.176
8.9	2871.50838	2855.556	2937.143	2887.64	2855.556	2871.508	2824.176	2839.779	2719.577	2824.176	2808.743
9.4	2903.954802	2871.508	2937.143	2920.455	2903.955	2871.508	2839.779	2887.64	2719.577	2808.743	2808.743
9.9	-	-	-	-	-	-	-	-	2705.263	2808.743	2824.176
10.4	-	-	-	-	-	-	-	-	2705.263	2793.478	2808.743
10.9	-	-	-	-	-	-	-	-	2691.099	2808.743	2824.176
11.4	-	-	-		-	-	-	-	2691.099	2824.176	2824.176
11.9	-	-	-	-	-	-	-	-	2691.099	2824.176	2839.779
12.4	-	-	-	-	-	-	-	-	2705.263	2824.176	2839.779

TABLE C-3 CONTINUED

12.9	-	-	-	-	-	-	-	-	2719.577	2824.176	2855.556
13.4	-	-	-	-	-		-	-	2748.663	2839.779	2855.556
13.9	-	-	-	-	-	-	-	-	2763.441	2839.779	2855.556
14.4	-	-	-	-	-		-	-	2763.441	2839.779	2871.508
14.9	-	-	-	-	-	-	-	-	2763.441	2824.176	2871.508
15.4	-	-	-	-	-	-	-	--	2763.441	2824.176	2871.508
15.9	-	-	-	-	-	-	-	-	2793.478	2824.176	2871.508
16.4	-	-	-	-	-	-	-	-	2763.441	2839.779	2855.556
16.9	-	-	-	-	-	-	-	-	2763.441	2839.779	2871.508
17.4	-	-	-	-	-	-	-	-	2763.441	2839.779	2871.508
17.9	-	-	-	-	-	-	-	-	2778.378	2839.779	2887.64
18.4	-	-	-	-	-	-	-	-	2793.478	2839.779	2903.955
18.9	-	-	-	-	-	-	-	-	2763.441	2855.556	-
19.4	-	-	-	-	-	-	-	-	2778.378	-	-
19.9	-	-	-	-	-	-	-	-	2763.441	-	-
20.4	-	-	-	-	-	-	-	-	2778.378	-	-
20.9	-	-	-	-	-	-	-	-	2778.378	-	-
21.4	-	-	-	-		-	-	-	2763.441	-	-
21.9	-	-	-	-	-	-	-	-	2778.378	-	-
22.4	-	-	-	-	-	-	-	-	2793.478	-	-
22.9	-	-	-	-	-	-	-	-	2793.478	-	-
23.4	-	-	-	-	-	-	-	-	2793.478	-	-
23.9	-	-	-	-	-	-	-	-	2793.478	-	-